SEMICONDUCTOR THERMOELEMENTS and THERMOELECTRIC COOLING

A. F. IOFFE

(Director of the Institute for Semiconductors of the U.S.S.R. Academy of Sciences)

INFOSEARCH LIMITED
LONDON

Translated from Russian

A. F. IOFFE
Poluprovodnikovye Termoelementy, 103 pp., 1956

A. F. IOFFE, L. S. STIL'BANS, E. K. IORDANISHVILI, and T. S. STAVITSKAYA
Termoelektricheskoe Okhlazhdenie, 110 pp., 1956

Both books originally published by the Publishing House of the U.S.S.R. Academy of Sciences, Moscow-Leningrad. Revised and supplemented by Prof. A. F. Ioffe for the English edition. Translated by A. Gelbtuch. Edited by H. J. Goldsmid. Set on Vari-Typer by Brenda Marsh.

Printed in Great Britain by Tri-Litho Offset Ltd.

CONTENTS

Part 1
SEMICONDUCTOR THERMOELEMENTS

CONTENTS

Part 2
THERMOELECTRIC COOLING

Part 1

SEMICONDUCTOR THERMOELEMENTS

PREFACE

My book 'Semiconductor Thermoelements', published at the beginning of 1956, is a supplemented edition of 'Energetic Principles of Semiconductor Thermoelectric Batteries' published in 1949. This English translation naturally takes into account the advances reported in the world scientific literature since the publication of the book, as well as those achieved at the Institute for Semiconductors. We now have a better understanding of the mechanism of the appearance of thermal emf's and of the processes of thermal and electrical conduction in semiconductors, and of how to apply our knowledge to the achievement of practical results.

This book reflects the state of the problem as I understand it at present. In addition, I thought that readers of this translation would be interested in some devices which have already been constructed in the Soviet Union. The book is therefore supplemented with a brief description of certain instruments which have proved themselves in practice.

In principle, the application of semiconductor thermoelements extends over the entire field of power generation, refrigeration, and heating. The practical possibilities depend, however, on the characteristics of the available thermoelements, their efficiency, operating temperature limits, stability in operation, and cost.

The most important characteristic of the thermoelements is a quantity described in the text by the letter z, defined by the equation $z = \frac{\alpha^2\sigma}{\kappa}$, where α is the thermoelectric power, σ is the specific electrical conductivity, and κ is the specific thermal conductivity. When α is expressed in $V \times deg^{-1}$, σ in $ohm^{-1} \times cm^{-1}$ and κ in $W \times deg^{-1} \times cm^{-1}$, then z has the dimension of deg^{-1}. The value of z for our best thermoelements ranges from 1.5×10^{-3} to $3 \times 10^{-3}\,°K^{-1}$ depending on the operating temperature. This implies that the efficiency of thermoelectric generators is in the range 6-10%, the maximum temperature difference given by the Peltier effect across a single couple is 60-70°C, the coefficient of performance of a refrigerating unit is 0.4-0.7 at a temperature difference of 40°, whilst that of a heating unit is 1.5-1.8 for the same temperature difference.

These data define the practical possibilities at the beginning of 1957. Taking into account the fact that our level of knowledge of semiconductors

is still low and that the range of materials so far investigated is small, it may be expected that the characteristics listed above will be substantially improved and the applications of thermoelements will become more widespread.

I hope that this book will help to speed up progress towards this end. It has not been my aim to discuss the construction and technology of thermoelectric batteries for specific applications; these problems everyone will solve according to his needs. Everybody should, however, be guided by the general physical concepts which I have attempted to outline and explain here on the basis of our experience.

I hope that acquaintance with our experience and ideas underlying our work will prove useful to readers of the English translation.

A. F. Ioffe *March 1957*

FROM THE FOREWORD TO THE RUSSIAN EDITION

Although research into the problem of thermoelectricity is in progress in our country and although, e.g., thermoelectric generators utilising the waste heat from kerosene lamps for feeding radio receivers have been developed and are now produced on an industrial scale, it is obvious that the scale of this work does not bear any relation to the importance of the problem. The time has arrived to promote the advancement of applications of thermoelectricity and for taking thermoelements outside the walls of a few laboratories. The combined efforts of physicists and chemists, heat engineers and electrical engineers should be concentrated on the solution of this problem and, even at this early stage, it is necessary to secure the co-operation of our more advanced factories.

This book and the collective work by A. F. Ioffe, L. S. Stil'bans, T. S. Stavitskaya and E. K. Iordanishvili 'Thermoelectric Cooling' describe our experience in this field and are designed to furnish research and production workers with the necessary information.

The second chapter forms the core of the book. The first (introductory) chapter and the third (supplementary) chapter present, in an abbreviated form, previously published information facilitating understanding of the problem, or else describe new applications which have not yet been put into practice.

CHAPTER 1

INTRODUCTION

1.1 Discovery of thermoelectric phenomena. In 1822-1823 Seebeck described in the Reports of the Prussian Academy of Sciences a phenomenon which he named "the magnetic polarisation of metals and ores produced by a temperature difference". It is obvious from the description of his experiments that Seebeck discovered thermoelectric currents arising in a closed circuit made up of different conductors at different junction temperatures.

This was an epoch when the discovery by Oersted of the effect of an electrical current on a magnetic needle was followed by a series of investigations by Ampère, Biot, Savart, Laplace, and others who elucidated the interaction between electric currents and magnetic fields; Ampère's molecular current hypothesis reduced the source of magnetic phenomena to electrical currents. The science of electricity and magnetism grew from Monday to Monday (the day of the week on which the Paris Academy of Sciences used to sit); physicists, mathematicians and chemists played an active part in its development.

This scientific development spread from Paris to Switzerland and Germany, and then to England, where it was enriched by Faraday's discovery of electromagnetic induction.

When Seebeck's experiments are considered without prejudice there can be no doubt that the phenomena observed by him were caused by the electric current, (the disappearance of the magnetic effects whenever the current was cut off by the introduction of a non-conducting layer, the quantitative relationship between the magnetic field produced by the current and the observed deflections of the magnetic needle, etc.). However, Seebeck not only rejected this natural explanation of his results but fought actively against it for several years after, accusing the exponents of thermoelectric current theory of following a fashion started by Oersted's discovery.

An explanation of this dogmatic attitude of Seebeck towards his discovery may be found in the concluding part of his large treatise, in which he makes an attempt to relate the Earth's magnetism to the temperature difference between the equator or a range of southern volcanoes

and the polar ice cap. It appears that this hypothesis was closer to his heart than the discovery of a still further source of electric current. The value of Seebeck's paper does not, of course, lie in this hypothesis, (he himself showed that a temperature difference without a closed electrical circuit does not produce any magnetic effects), nor in the attempt to deny the existence of an electric current, but in the copious experimental material accumulated by him and covering a great variety of solid and liquid metals, their alloys, minerals, and semiconductors. Seebeck's mistake had a positive effect: in order to disprove the electrical origin of thermoelectric currents he compared, for a great variety of materials, the contact potential (Volta) effect with the effect of temperature difference on a magnetic needle, and demonstrated the difference between these phenomena.

The extensive thermoelectric series compiled by Seebeck is, even now, of interest. Using modern notation (α = thermoelectric power, and σ = specific electrical conductivity), the Seebeck series is in the order of magnitude of the product $\alpha\sigma$ and not the quantity $\alpha^2\sigma/\kappa$ (where κ is specific thermal conductivity) which, as will be seen later on, characterises the thermoelectric properties of materials. The thoroughness of Seebeck's investigations may be illustrated, for example, by the fact that in an article by Maria Telkes published in an American journal 125 years later the best couple was given as ZnSb and PbS, which were the first and the last members in Seebeck's series.

A comparison of the qualitative Seebeck series with modern measurements of the thermoelectric power of metals shows good agreement. The divergence between Seebeck's series and those of Justi and Meisner is not larger than the divergence between the latter two series. We are reproducing below the aforementioned thermoelectric series (the thermoelectric power in Justi's and Meisner's series is expressed in μV/deg).

Had Seebeck followed his discovery with an attempt to use a thermocouple to generate electrical energy, he could have obtained, using the first and last terms in his series, an efficiency of the order of 3%, i.e., as much as that of the best steam engines at that time.

It must also be noted that Seebeck did not fail to pay attention to phenomena caused by a temperature difference in homogeneous materials and that he estimated qualitatively thermoelectric relationships which were rediscovered 30 years later by W. Thomson, who proved their existence on the basis of a thermodynamic analysis of the thermoelectric processes.

Twelve years after Seebeck's discovery Peltier, a watchmaker, published in the French journal 'Annal. Phys. Chim.' for 1834 an article on temperature anomalies observed in the vicinity of the boundary between

Seebeck, 1822	Justi, 1948	Meisner, 1955			
		metals		semiconductors	
PbS	Bi −80	Bi	−70	MoS	−770
Bi	Co −21	Co	−17.5	ZnO	−714
Bi amalgam	Ni −20	Ni	−18	CuO	−696
Ni	K −14	K	−12	Fe_2O_3 (400°C)	−613
Co	Pd − 8	Pd	−6	FeO	−500
Pd	Na − 7	Na	−4.4	Fe_3O_4	−430
Pt No. 1	Pt − 5	Pt	−3.3	FeS_2	−200
U	Hg − 6	Hg	−3.4	MgO_3H_2	−200
Au No. 1	C −3.5			SnO	−139
Cu No. 1	Al −1.5	Al	−0.6	Fe_2O_3 (50°C)	−60
Rh	Mg −1.5	Mg	−0.4	CdO	−41
Au No. 2	Pb −1.0	Pb	−0.1	CuS	−7
Ag	Sn −1.0	Sn	+0.1	FeS	+26
Zn	Cs −0.5	Cs	+0.2	CdO	+30
C	Y −1.0	Y	+2.2	$GeTiO_3$	+140
Cu No. 3	Rh +1.0	Rh	+2.5	NiO	+240
Pt No. 4	Zn +1.5	Zn	+2.9	Mn_2O_3	+385
Cd	Ag +1.5	Ag	+2.4	Cu_2O	+474
Steel	Au +1.5	Au	+2.7	Cu_2O	+1000
Fe	Cu +2.0	Cu	+2.6	Cu_2O	+1120
As	W +2.5	W	+1.5	Cu_2O	+1150
Sb	Cd +3.5	Cd	+2.8		
SbZn	Mo +6.5	Mo	+5.9		
Fe	Fe +12.5	Fe	+16		
	Sb +42	Sb	+35		
	Si +44				
	Fe +49	Fe	+400		
	Se	Se	+1000		

two different conductors when a current was passing through them. The phenomenon first observed by Peltier, and therefore given the name of Peltier effect, consists in reality of the generation or absorption (depending on the direction of the current) of heat, at a rate Q, at the junction between two different conductors when a current I flows through them:

$$Q = \Pi I$$

where Π is the Peltier coefficient.

The Peltier effect is very closely related to the Seebeck effect, and the coefficient Π to the thermoelectric power α:

$$\Pi = \alpha T$$

where T is the absolute temperature of the junction. A temperature difference produces an electric current in a closed circuit made of different materials, whilst, in turn, a current flowing through such a circuit produces a temperature difference. It is interesting that Peltier did not notice this connection in spite of the fact that he carried out his experiments using a thermoelectric circuit. In these experiments, the Seebeck effect was used solely for secondary purposes, namely as a source of weak currents.

The anomalies discovered by Peltier were found to be the more pronounced the larger the thermoelectric powers of the metals involved; they were particularly conspicuous at the junction of bismuth with antimony. Peltier was, however, looking for, and finding, in his experiments the confirmation of a preconceived idea that the universal law of heat generation by current, viz the Joule-Lenz law, is only valid for strong currents. Peltier thought that in the case of weak currents produced by a thermocouple the individual properties of the metals began to have an effect. He did not find a confirmation of this hypothesis in the bulk properties of the conductors, but the anomalies at the junctions were affected by the nature of the metal (in reality by its thermoelectric properties). Peltier did not notice this and sought an explanation in the hardness or softness of the metal or its electrical conductivity, and when the facts did not come up to his expectations, for example in the case of bismuth, the thermal anomalies of which were attributed by Peltier to high electrical conductivity, he refused to believe the measurements.

A few more years passed, during which Becquerel and other investigators tried to explain the true nature of the Peltier phenomenon, until in 1838 the St. Petersburg Academician Lenz put an end to all doubts with a simple experiment. Lenz placed a droplet of water in a dent at the junction of bismuth and antimony rods. The droplet turned into ice when the current was reversed. It is known that to freeze 1 gm of water it is necessary to remove 80 cal, whilst in melting 1 gm of ice the same amount must be supplied. It thus became obvious that, depending on its direction, an electric current generates or absorbs heat at the junction of two conductors.

Thermoelectric phenomena did not attract attention amongst physicists. They were obscured by the striking phenomena of electromagnetism which led Faraday to the discovery of electromagnetic induction. Physics was moving towards the generalising laws of Maxwell's theory, and engineering towards electrical machinery. Thirty years had passed since Seebeck's discovery when, owing to the evolution of thermodynamics, all types of energy conversion became of interest, including the conversion of thermal and electrical energy in the Seebeck and Peltier effects.

This, in fact, was the approach adopted by W. Thomson, one of the founders of thermodynamics. Thermodynamic analysis of the Seebeck and

Peltier effects led him not only to the establishment of the relationship between these two processes, which has already been mentioned above, but also to the discovery of a third phenomenon, the Thomson effect, consisting of the generation or absorption of heat q by the passage of a current I through a homogeneous conductor in which there is a temperature gradient $\frac{\partial T}{\partial x}$:

$$q = \tau I \frac{\partial T}{\partial x} ;$$

τ became known as the Thomson coefficient; as will be seen later it is related to the coefficients α and Π.

It should be remembered that the Thomson effect was earlier experimentally observed and investigated by Seebeck.

In 1857 Thomson published his theory of the thermoelectric phenomena in anisotropic crystals; however, only in the 20th century was it shown by Bridgman that a change of the direction of the current in a crystal is connected with the absorption or generation of heat, as in the case of the Peltier effect. Such an internal Peltier effect was called the Bridgman effect.

In 1920–21, almost one hundred years after Seebeck's discovery, Benedicks reported the discovery of two more thermoelectric effects depending on the value of the temperature gradient and not on the temperature difference between the ends of the conductors. When the ends of a conductor are at the same temperature, but if there is a warmer or cooler portion in between them, then, according to Benedicks, a potential difference will appear between the ends of the conductor when the warm (or cool) portion is not symmetrically placed, i.e. is closer to one of the ends. A careful check of the Benedicks effect by other investigators did not confirm its existence. It may be presumed that even if this effect exists it is negligible.

The phenomena enumerated above exhaust the field of thermoelectricity, if phenomena arising in a magnetic field, generally referred to as thermomagnetic phenomena, are not included.

Thermocouples have been used for temperature measurement for a long time, but the problem of their power application became of importance only with the growing demand for sources of electrical energy.

In 1885 Rayleigh considered the problem of the efficiency of a thermoelectric generator and calculated it, though somewhat inaccurately. The problem of a thermoelectric electrical energy generator was again taken up in 1909 by Altenkirch, this time, on the whole, correctly. In 1910 Altenkirch investigated the problem of thermoelectric cooling and heating. However, since the only conductors technically known at that time were metals, such devices were found to be uneconomical. It is true that a few

thermoelectric generators (by Gülcher, Coblentz, and others) made their appearance, but they did not find wide application since their efficiency did not exceed 0.6% and sometimes not even 0.1%. Therefore thermoelectricity again moved to a back place in the advance of physics, together with luminescence, photoelectricity, and piezoelectricity.

The position on the electrical engineering front (and, therefore, also the subjects of physical investigations) underwent a radical change with the advent of semiconductors. It is very characteristic of the present degree of relationship between physics and engineering that all these phenomena have again begun to attract considerable attention among physicists and are playing an important role in semiconductor production engineering. The thermoelectric aspects will be discussed in detail in this book. As far as other fields are concerned, it is enough to mention fluorescent lamps, ceramic piezoelectric materials, and solid and vacuum photocells, developed both in the Soviet Union and abroad.

The prospects of attaining appreciable efficiencies in thermoelectric generators became more favourable. In conjunction with the problems of industrialisation of the Soviet Union at the beginning of the first five-year plan, I outlined in 1929 the advantages of thermoelectric generators made of semiconductors and calculated that their efficiency could reach 2.5-4% with prospects of an appreciable increase in the future. In fact, in 1940 Yu. P. Maslakovets described a thermoelement, made of lead sulphide with an excess of lead and sulphur, with an efficiency of the order of 3%.

It seems to us that all the energetic applications of thermoelectricity: 1) thermoelectric generators, 2) thermoelectric refrigerators, and 3) thermoelectric industrial and domestic heating devices, are not only of great theoretical interest, but present real prospects of practical application on the basis of the modern science of semiconductors. Moreover, some previously unforeseen applications have arisen, such as the construction of thermoelectric sound and ultrasonic generators, vacuum thermoelements, etc.

1.2 **Thomson's thermodynamic relationships.** Three thermoelectric effects have been established experimentally: 1) the appearance of a thermoelectric voltage dE in an open circuit consisting of two different conductors when there is a temperature difference dT between their ends:

$$dE = \alpha_{1-2}\, dT \tag{1}$$

(α_{1-2} is known as the thermal emf coefficient or sometimes simply as the thermal emf, or thermoelectric power, between the given conductors; α may depend also on temperature); 2) the generation of heat, dQ watts, at the boundary between two conductors when a current, dI amperes, flows through them:

$$dQ = \Pi_{1-2}\, dI \tag{2}$$

(change of direction of the current leads to a change from the generation of heat to the absorption of heat and vice versa); 3) generation of heat, dq watts, by a current dI in a portion of the conductor with a length dx in the presence of a temperature gradient $\frac{\partial T}{\partial x}$:

$$dq = r dI \frac{\partial T}{\partial x} dx. \tag{3}$$

The relationship between α_{1-2}, Π_{1-2} and r follows from the laws of thermodynamics.

We shall consider a closed circuit made up of two conductors with a temperature difference dT between the junctions. According to the law of conservation of energy we can equate the algebraic sum of all types of energy generated in the circuit in a unit time to zero under steady-state conditions.

The Peltier heat in watts generated at one junction will be denoted by $\Pi_{1-2} dI$, whilst the heat absorbed at the other junction will be denoted by $\Pi_{2-1} dI$; we have $\Pi_{2-1} = \Pi_{1-2} + \frac{\partial \Pi_{1-2}}{\partial T} dT$.

The Thomson heat generated in one second in one conductor is $r_1\, dI\, dT$, whilst that absorbed in the other conductor is $r_2\, dI\, dT$. The electrical power consumed in the circuit is $\alpha\, dT\, dI$.

Consequently, the equation of conservation of energy in the circuit can be written down in the form

$$\frac{\partial \Pi_{1-2}}{\partial T} dT\, dI + (r_1 - r_2)\, dI\, dT = \alpha_{1-2}\, dT\, dI$$

or

$$\frac{\partial \Pi_{1-2}}{\partial T} + r_1 - r_2 = \alpha_{1-2}. \tag{4}$$

Another relationship between the coefficients α, Π, and r may be derived from the equation of the second law of thermodynamics, which is, however, only applicable to reversible processes.

All three thermoelectric phenomena ought to be regarded as reversible; their sign changes both with a change of the sign of the temperature difference dT and with a change in the direction of the current dI.

However, the irreversible phenomena of heat conduction and Joule heat generation will also inevitably take place. Whilst the Joule heat, as we shall see later, may be neglected for extremely small currents, the heat transferred by thermal conduction is of the same order as the Peltier heat and sometimes much greater.

Thomson assumed that the thermoelectric phenomena are not basically related to the heat conduction process and the generation of heat by the current. The thermal conductivity of a given material and its resistivity, which govern the irreversible processes in thermocouples, do not determine the Seebeck, Thomson, and Peltier effects. These last three phenomena may be considered in isolation, assuming that the thermal conductivity and the resistivity are arbitrarily low and neglecting irreversible processes as incidental.

These considerations cannot be regarded as a convincing proof. More recently Onsager stated the conditions under which such a division of processes into reversible and irreversible is permissible. It appears that Onsager's conditions are satisfied both by metals and semiconductors. This cannot, however, be regarded even yet as definitely established.

Following Thomson, we shall assume, however, that the reversible part of thermoelectric processes may be considered separately from the irreversible processes and shall then check the resulting conclusions. Agreement between these conclusions and experimental results may be regarded as some confirmation of the underlying assumptions. Since we shall consider below only the theoretical conclusions, the theory will be regarded here merely as a way of deriving these results.

Thus, we shall apply the second law of thermodynamics to thermoelectric processes in a thermocouple with hot and cold junction temperatures T_1 and T_0 respectively. The hot junction receives an amount of heat $\Pi_1 I$, and the cold junction gives up an amount of heat $\Pi_0 I$; at the same time an amount of heat $rI dT$ is generated at a temperature T in each portion of the conductors in which there is a temperature difference dT.

Reversibility of the processes leads to the condition that the total change of entropy of all the processes is equal to zero:

$$\frac{\Pi_1}{T_1} I - \frac{\Pi_0}{T} I + I \int_T^{T_1} \frac{r_2 - r_1}{T} dT = 0 .$$

Dividing this equation by I and differentiating it with respect to T, we obtain

$$\frac{d\dfrac{\Pi}{T}}{dT} + \frac{r_2 - r_1}{T} = 0, \qquad \frac{T\dfrac{d\Pi}{dT} - \Pi}{T^2} = \frac{r_1 - r_2}{T},$$

whence

$$\frac{d\Pi}{dT} - \frac{\Pi}{T} = r_1 - r_2 . \tag{5}$$

Equation (5) together with equation (4) gives

$$\alpha = \frac{\Pi}{T} . \tag{6}$$

Each of the quantities in expression (6) may be separately measured, thus making it possible to check this expression, obtained by separating reversible from irreversible processes in the thermocouple. Experimental material so far accumulated has always confirmed equation (6) within the the limits of experimental accuracy. We shall, therefore, use equation (6), regarding it as an experimental fact. This equation gives

$$\frac{d\alpha}{dT} = \frac{T\dfrac{\partial \Pi}{\partial T} - \Pi}{T^2} = \frac{1}{T} \times \frac{\partial \Pi}{\partial T} - \frac{\Pi}{T^2} = \frac{1}{T}\left(\frac{\partial \Pi}{\partial T} - \frac{\Pi}{T}\right).$$

According to equation (5) the expression in brackets is equal to $(r_1 - r_2)$. We have therefore

$$\frac{d\alpha_{1-2}}{dT} = \frac{1}{T}(r_1 - r_2) . \tag{7}$$

On the left hand side of equation (7) is a quantity relating to the boundary between the two conductors, and on the right hand side a difference between two terms, each of which depends on the properties of only one conductor.

A question can, therefore, be posed as to whether α_{1-2} may be regarded as a difference between two quantities, α_1 describing the first conductor and α_2 describing the second conductor. Integrating equation (7) we obtain $\alpha_{1-2} = \int_0^T \frac{r_2}{T} dT - \int_0^T \frac{r_1}{T} dT$, where the lower limit of the integral corresponds to the temperature of absolute zero, at which both α_{1-2} and $\frac{d\alpha_{1-2}}{dT}$ are equal to zero. It is natural to regard

$$\alpha_{1-2} = \alpha_2 - \alpha_1 = \int_0^T \frac{r_2}{T} dT - \int_0^T \frac{r_1}{T} dT ,$$

$$\alpha_2 = \int_0^T \frac{r_2}{T} dT , \quad \alpha_1 = \int_0^T \frac{r_1}{T} dT . \tag{7a}$$

In order to determine a_1 and a_2 in practice it would be necessary to know $r(T)$ from the absolute zero to the specified temperature. Experimental measurement of Thomson heat over such a wide temperature range is difficult and so far has only been accomplished for the normal silver alloy. The difference $a_2 - a_1$ and its temperature dependence have been determined frequently for a wide variety of materials.

It can be readily shown that by measuring, at a certain temperature T_0, a_{1-2}, a_{2-3}, a_{3-4}, $\ldots$, $a_{(n-1)-n}$, we shall obtain $a_{1-2} + a_{2-3} + a_{3-4} + \ldots + a_{(n-1)-n} = a_{1-n}$. In fact, since all the junctions 1–2, 2–3, 3–4 ...are at the same temperature T_0, any change of the emf of the couple 1,n by connecting into the circuit intermediate conductors 2,3,... would require the conversion of heat from the surroundings into electrical energy without any compensation, which contradicts the second law of thermodynamics. The independence of the value of $a_{i,n}$ from the effect of the intermediate conductors forms the basis for setting up a thermoelectric series. Experiment has always confirmed this relationship.

If we could ascribe to some substance a definite value $a = a_0$ we would then be able to determine the absolute as well as the relative values of the thermal emf coefficient of all substances. Equation (7a) makes this possible once $\int_0^T \frac{r}{T}\,dT$ has been measured for one substance only; the accuracy of such a measurement is, however, low, although numerous investigators (Borelius, Keesom, and others) have made attempts to determine $r(T)$ close to the absolute zero. Consideration of the mechanism of thermoelectricity affords another method for determining the absolute values of a and this will be considered in the following paragraph.

Equation (6) has been checked many times for different materials and found to hold in all cases. Using equations (6) and (7) it is possible to express the Peltier coefficient Π and the Thomson coefficient r through a and $\frac{da}{dT}$. In particular, when $\frac{da}{dT} = 0$, $r_1 = r_2$ and therefore the quantities of Thomson heat generated in the two branches of the thermocouple are equal and opposite in sign. The Thomson heat generated in a closed circuit is

$$q = (r_1 - r_2) I (T_1 - T_2),$$

and the Peltier heat is

$$Q = a I T.$$

The higher $(T_1 - T_2)$ as compared with T, the greater is the relative part played by Thomson heat.

It would appear that purely thermodynamic considerations make possible not only the establishment of a relationship between Π, r, and a, but also the determination of the actual value of a. In fact, let us consider a junction between two electronic conductors through which passes 1 coulomb of electricity, at an infinitesimally slow rate, so that the current I is infinitesimally small; the temperature of the whole circuit is assumed to be constant and equal to T. In such a circuit there is no heat conduction or Joule heat loss and the whole circuit may be regarded as a system in equilibrium in which all processes change their sign with the change of the sign of I.

Equilibrium of two conductors implies an equilibrium of their chemical potentials μ. We shall regard μ as referring to one electron and equate it to free energy $U - TS$:

$$\mu = U_1 - TS_1 = U_2 - TS_2 = U - TS$$

On the other hand, the average energies U of electrons in two conductors in contact are different and their entropies S are also different, viz

$$S_1 - S_2 = \frac{U_1 - U_2}{T}$$

When an electron passes through the boundary its energy changes by an average of $U_1 - U_2$; it is this energy that is generated in the form of of Peltier heat Π_{1-2}. Hence

$$S_1 - S_2 = \frac{\Pi_{1-2}}{T} = a_{1-2}. \qquad (8)$$

It might have been expected that the thermal emf a at the boundary between two electronic conductors could be determined as a difference of entropies of 1 coulomb of electricity in the two conductors. This assumption is, however, not entirely correct: in the equilibrium state the electron velocity distribution follows a certain statistical law. In a stream of electrons the velocity distribution changes; for example, fast electrons pass from one conductor into another in a larger number than slow electrons. Electrons which remain in the first conductor restore the statistical equilibrium which brings about a further change of entropy. Therefore the entropy flux from one substance into another is not equal to the difference of the entropies in each of the substances before the exchange of the electrons. Equation (8) may only be regarded as an approximation. Calculation of the exact value of a_{1-2} is, therefore, only possible starting with the consideration of the mechanism of electron transfer.

Let j denote the current of electrons through the boundary between two substances; this current consists of currents of electrons with all values of kinetic energy ϵ:

$$j \propto \int_0^\infty j(\epsilon)\, d\epsilon .$$

The average value of the energy of electrons in the current is

$$\bar{\epsilon} = \frac{\int_0^\infty \epsilon\, j(\epsilon)\, d\epsilon}{\int_0^\infty j(\epsilon)\, d\epsilon} .$$

Let $f_0(\epsilon)$ denote the equilibrium energy distribution function of the electrons and $l(\epsilon)$ the free path length of an electron with an energy ϵ; the current j can then be represented in the form

$$j = C \int_0^\infty \frac{df_0(\epsilon)}{d\epsilon}\, l(\epsilon)\, \epsilon\, d\epsilon .$$

This expression is equally true for a current of gaseous molecules. Substituting it into the equation for $\bar{\epsilon}$ we obtain

$$\bar{\epsilon} = \frac{\int_0^\infty \frac{df_0(\epsilon)}{d\epsilon}\, l(\epsilon)\, \epsilon^2 d\epsilon}{\int_0^\infty \frac{df_0(\epsilon)}{d\epsilon}\, l(\epsilon)\, \epsilon\, d\epsilon} .$$

If S is the flow of entropy with the passage of one electron, then the flow of entropy $\frac{S}{e}$ corresponding to 1 coulomb of electrical charge, on which the value of α depends, will be described by the expression

$$\alpha = \frac{S}{e} = \frac{1}{e}\left(\frac{\bar{\epsilon}}{T} - \frac{\mu}{T}\right) = \frac{k}{e}\left(\frac{\bar{\epsilon}}{kT} - \frac{\mu}{kT}\right) .$$

Using the notation $\frac{\epsilon}{kT} = \epsilon^*$ and $\frac{\mu}{kT} = \mu^*$, we have

$$\alpha = \frac{k}{e}\left[\frac{\int_0^\infty \frac{df_0(\epsilon^*)}{d\epsilon^*}\, l(\epsilon^*)\, \epsilon^{*2} d\epsilon^*}{\int_0^\infty \frac{df_0(\epsilon^*)}{d\epsilon^*}\, l(\epsilon^*)\, \epsilon^* d\epsilon^*} - \mu^*\right] . \qquad (8a)$$

The Peltier heat $\Pi = \alpha T = \frac{1}{e}(\bar{\epsilon} - \mu)$.

These are the most general expressions for the thermal emf and the Peltier coefficient which are valid both for degenerate and non-degenerate semiconductors and metals.

1.3 Statistical theory. At the beginning of this century, the theory of metals was based on the concept of the presence in each metal of a certain concentration of free electrons n, different for differing metals, moving at random within the metal in a similar way to gas molecules. According to these theories (Rieke, Drude, Lorentz and Debye) electrons were governed by the same Boltzmann statistics as gaseous molecules. As in a gas their average translation energies were regarded as equal to $\frac{3}{2}kT$ where k is the Boltzmann constant and T the absolute temperature.

The thermal emf V in an open circuit consisting of two metals, calculated according to this theory, was

$$V = \frac{k}{e}\int_{T_1}^{T_2} \log\frac{n_2}{n_1}\, dT .$$

It can be readily calculated that, e.g., when $\frac{n_2}{n_1} = 2.7$, $V = 86\times10^{-6}(T_2 - T_1)$ volts, and $\alpha = 86\ \mu V/\text{deg}$, which is much higher than the experimentally observed value of α in cases where one would expect that $\frac{n_2}{n_1} > 2.7$.

For the majority of metals α does not exceed a few μV/deg.

The quantum theory of metals developed in 1927–1928 by Ya. I. Frenkel' in one form and by A. Sommerfeld in another form eliminated this discrepancy as well as many others.

According to the theory of Sommerfeld who applied Fermi-Dirac quantum statistics to electrons in metals, the thermal emf between two metals is to a first approximation (taking into account only linear terms) equal to zero. Only the next approximation leads to a certain finite, although very small, value of α. All this is not surprising. Let us consider a metallic rod, the ends of which are at different temperatures. Since the temperature does not change the concentration of electrons n in the metal but brings about only a slight redistribution of their thermal agitation velocities, it is obvious that a large thermal emf cannot arise in such a metal.

The state of semiconductors in the quantum theory is similar to that of the classical metal considered at the beginning of the 20th century. Some of the electrons in semiconductors are found to be free. The concentration of free electrons in semiconductors varies but is usually so much smaller than in metals that the Boltzmann classical statistics are applicable. A rise of temperature leads to a change in both the concentration of free electrons and their kinetic energy which, as in the case

of gas molecules, may be equated to $\frac{3}{2}kT$. Let us consider a rod of semiconductor in which there is a temperature gradient $\frac{dT}{dx}$. At the hot end of the rod both the concentration and the velocities of the electrons are higher than at the cold end. Therefore more electrons will start to diffuse in the direction of the temperature gradient than in the opposite direction. The diffusion flux, carrying the negative charge away from the hot end and transferring it to the cold end, sets up a potential difference between the ends.

The diffusion process is increasingly retarded by the electrical field in the interior of the semiconductor until the flux of electrons caused by diffusion is equal to the reverse flux caused by the potential difference which has arisen. Under these conditions a dynamic electron equilibrium in the semiconductor will be established, under which the temperature difference between the ends of the rods will maintain a corresponding potential difference.

The number of electrons passing through any cross-section of the conductor in a unit time in both directions is equal. However, the velocities of electrons proceeding from the hot end are higher than the velocities of electrons passing through the given section from the cold end. This difference ensures that there is a continuous transfer of heat energy in the direction of the temperature gradient without any actual charge transfer.

The heat transfer mechanism is substantially different when negative (electrons) and positive (holes) charge carriers participate simultaneously in the current. Simultaneous transfer of equal numbers of holes and electrons does not lead to an accumulation of the charge and an increase of the potential. Simultaneous diffusion of electrons and holes from the hot end to the cold end is caused not only by the difference in the carrier velocities but also by their concentration gradient.

In the case of such a bipolar diffusion a thermal emf can also arise due to the following two factors:

1) When the concentration of one type of carrier (e.g. negative) exceeds the concentration of the opposite type of carrier the flux of the first type of carrier will carry towards the cold end predominantly a charge which will retard their motion and, conversely, accelerate the carriers of the opposite sign until the fluxes of both carriers are equal; an electric field governed by the temperature gradient will thus be established.

2) The difference of charge carrier mobilities forms the second source of thermal emf's. The mobility u is related to the diffusion coefficient D by the universal relationship established by Einstein:

$$\frac{u}{D} = \frac{e}{kT}.$$

Under the effect of the concentration gradient set up by the temperature gradient, the carriers characterised by higher values of u and D would have moved forward had they not created a space charge on becoming separated from the carriers of opposite sign. The corresponding electric field E retards their motion and accelerates the slower carriers of the opposite sign. The electric field E equalises the velocities of both types of carrier enabling them to diffuse as a single body.

Therefore, even when thermal agitation creates an equal number of current carriers of each sign, their diffusion produces an electric field in the conductor depending on the difference in carrier mobilities. The expression for this electric field E will be similar to that for the diffusion of ions in an electrolyte, namely

$$E = E_0 \frac{u_1 - u_2}{u_1 + u_2},$$

where E_0 is the electric field which would have existed in the presence of current carriers of one sign only, and u_1 and u_2 are the mobilities of positive and negative charges.

The advantage of semiconductors when used as materials for thermoelements is due to their higher values of thermal emf. We shall try to explain the reasons for this property of semiconductors.

In metals the concentration of free charge carriers is high (of the order of 10^{22} cm^{-3}) and does not depend on temperature; the kinetic energy of the highly degenerate electrons is virtually independent of temperature, and the same applies to the contact potential of the metal at its boundaries. Under such conditions thermal emf's as a rule do not exceed a few μV per °C.

In semiconductors, however, temperature has a pronounced effect on the concentration n and kinetic energy ϵ of free charge carriers, whilst the absolute value of the concentration is smaller by a few orders of magnitude (10^{14} to 10^{20} cm^{-3}). The contact potential ϕ of semiconductors with respect to metals and the corresponding chemical potential μ are also functions of temperature. Thermal emf's amount in this case to hundreds of μV/°C.

What part does each of the above enumerated factors (low concentration, and the temperature dependence of the concentration, kinetic energy and contact potential) play in the appearance of high thermal emf's?

In the volume of a semiconductor the temperature gradient sets up a diffusion flux due to the concentration gradient $\frac{dn}{dx}$ and the gradient of the mean kinetic energy of free charge carriers $\frac{d\epsilon}{dx}$. When the charge

carriers are of one sign, the diffusion flux which transports them sets up an electric field E counteracting the diffusion. In the equilibrium state the electrical current produced by the field E balances the diffusion flux.

We shall consider separately the phenomena occurring in the bulk of the semiconductor and at its boundaries.

A temperature gradient may produce a unidirectional diffusion flux in two ways: 1) because of a concentration gradient of free carriers $\frac{\partial n}{\partial x}$, when $n = f(T)$; and 2) because of variation of the coefficient of diffusion D with temperature. Variation of D with temperature may in turn stem from two causes: a) D may depend on the temperature T of the medium in which the carriers move; and b) D may vary depending on the velocity v or kinetic energy ϵ of electrons transported by diffusion.

It will readily be seen that thermal agitation in the medium and its temperature T cannot by themselves produce a unidirectional flow of charge carriers, whilst in each portion of the solid an equilibrium thermal agitation is established corresponding to temperature T_m. Therefore $\frac{\partial D}{\partial T_m}$ does not lead to the appearance of a thermal emf.

On the other hand, dependence of the coefficient of diffusion on the kinetic energy of electrons $\frac{\partial D}{\partial \epsilon}$ may give rise to a unidirectional flow of carriers, even at a constant concentration n, when in addition to the temperature gradient $\frac{dT}{dx}$ there exists also a kinetic energy gradient $\frac{d\epsilon}{dx}$. In fact, when the coefficient of diffusion of the carriers (electrons and holes) increases with rising temperature, i.e. when $\frac{\partial D}{\partial \epsilon} > 0$, more carriers will pass through each cross-section in the direction from the hot end to the cold end than in the reverse direction. The carriers will accumulate at the cold end, setting up an electric field E_D which will balance the diffusion flux. Conversely, when $\frac{\partial D}{\partial \epsilon} < 0$, the diffusion flux directed from the cold end to the hot end will predominate; charge carriers will accumulate at the hot end and the sign of the field E_D, and therefore also of the corresponding part of thermal emf α_D, will be opposite.

Therefore the equilibrium condition for carriers in an insulated specimen with free non-degenerate carriers of one sign may be expressed in the form

$$E u n = D \frac{dn}{dx} + n \frac{dD}{dx}$$

where u is the mobility of free carriers.

1. We shall first consider a special case of a semiconductor in which $n = \text{const}$ and $D = f(T) = F(\epsilon)$. Let E_D be the electric field in this case and α_D the corresponding thermal emf.

The equilibrium condition becomes:

$$E_D u n = n \frac{dD}{dx} = n \frac{\partial D}{\partial \epsilon} \frac{d\epsilon}{dx}.$$

Using Einstein's relationship

$$\frac{u}{D} = \frac{e}{kT}$$

we obtain

$$E_D \frac{dx}{d\epsilon} = \frac{k}{e} T \frac{1}{D} \frac{\partial D}{\partial \epsilon}.$$

In order to express the dependence of D on T we shall use the familiar properties of mobility u which is interrelated with D. The mobility of electrons is proportional to the time τ required by the electrons to cover the mean free path, and

$$\tau = \frac{\overline{l}}{v} \propto \frac{\overline{l}}{\sqrt{\epsilon}}$$

where $\overline{l}$ is the mean free path length.

The relationship between $\overline{l}$ and ϵ depends on the conditions of scattering of free charge carriers; it varies depending on the nature of the chemical binding forces, lattice defects, and impurities, and is usually expressed in the form

$$\overline{l} \propto \epsilon^r.$$

We have therefore

$$u(\epsilon) \propto \tau \propto \epsilon^{(r-\frac{1}{2})}$$

and since $T \propto \epsilon$,

$$D \propto uT \propto \epsilon^{(r+\frac{1}{2})}$$

$$\frac{1}{D} \frac{\partial D}{\partial \epsilon} = \frac{1}{\epsilon} (r + \tfrac{1}{2}).$$

Substituting this value in the equilibrium condition, we obtain

$$\alpha_D = E_D \frac{dx}{dT} = \frac{k}{e}(r + 1/2)$$

2. Let us now put D = const and $n = f(T)$; the corresponding component of thermal emf will be denoted by α_n. We then have

$$E_{un} = \frac{D\partial n}{\partial x} = D\frac{\partial n}{\partial T}\frac{\partial T}{\partial x}$$

$$\alpha_n = E\frac{dx}{dT} = \frac{k}{e}T\frac{\partial \ln n}{\partial T}$$

3. Finally, let us consider the effect of the temperature dependence of the contact potential ϕ on the thermal emf α_ϕ; this dependence is determined by the temperature dependence of the chemical potential μ since

$$\frac{\partial(\phi e)}{\partial T} = -\frac{\partial \mu}{\partial T}$$

where

$$\mu = kT \ln\left\{\frac{n h^3}{2(2\Pi m kT)^{3/2}}\right\}$$

$$\frac{\partial \mu}{\partial T} = -k\left(\frac{3}{2} + \frac{\mu}{kT} - T\frac{\partial \ln n}{\partial T}\right)$$

$$\alpha_\phi = \frac{\partial \phi}{\partial T} = +\frac{k}{e}\left(\frac{3}{2} + \frac{\mu}{kT} - T\frac{\partial \ln n}{\partial T}\right).$$

It will be seen that the expressions α_n and α_ϕ contain the term $T\frac{\partial \ln n}{\partial T}$ which is governed by the temperature dependence of concentration. However, in the expression for the total thermal emf

$$\alpha = \alpha_D + \alpha_n + \alpha_\phi = \frac{k}{e}\left(r + 2 + \frac{\mu}{kT}\right)$$

this term cancels out. The potential difference produced by the concentration gradient in the bulk of the semiconductor is balanced by the difference of the contact potential at its boundaries. The experimentally

observed thermal emf is not related to the temperature dependence of the concentration of the current carriers $\frac{\partial n}{\partial T}$. On the other hand, the absolute value of the concentration n appears in the expression for α, through the chemical potential, in the form $\ln n$. In the subsequent considerations we shall frequently employ the dependence of α on $\ln n$ and plots using as coordinates $\alpha = f(\log n)$, and n.

All this is confirmed by the example of semiconductors in which the concentration of electrons (small in comparison with that in metals) remains constant in a wide temperature range. Semiconductors of this type include, for example, lead sulphide and lead telluride containing an excess of lead. Despite the constant concentration, the thermal emf is of the order of hundreds μV/deg, i.e. of the same order as in semiconductors with a pronounced temperature dependence of concentration.

The difference in electron velocities at the hot and cold ends of the semiconductor leads, however, to the appearance of a potential difference between the two ends. The higher the electron concentration in the semiconductor, the lower is the electric field E required for transferring the same number of electrons as that which diffuses owing to the difference in the velocities at the hot and cold ends of the rod.

The thermal emf α per 1°C may be regarded as an entropy flux of 1 coulomb of electrical charge. As we have seen, the value of α depends not only on the entropy difference between two substances or two portions of a single conductor at different temperatures, but also on the conditions of the motion of the electrons. These conditions may, in turn, depend on the nature of the semiconductor, and on the mechanism of electron scattering in the transfer of electrons from one portion of the semiconductor to another. Therefore, the value of α is closely related to the mobility u which is governed by the same scattering mechanism.

On the other hand, the scattering mechanism, and therefore also the values of u and α in anisotropic crystals (with the exception of crystals with cubic symmetry), depend on the direction. Therefore, a thermal emf appears between two rods cut out from the same crystal in different crystallographic directions, and Peltier heat is generated when current is passed through such a couple. When the current lines within a homogeneous crystal are bent, Peltier heat is generated everywhere where the current lines have a curvature. This is the so-called Bridgman effect.

The most important factor for all applications of thermoelectricity is the experimental fact that there are semiconductors with current carriers of opposite sign. Experience shows that when one end of a semiconductor rod is heated and the other end cooled there will appear in some substances an electric field directed from the hot end to the cold end, whilst

in other substances the field will have an opposite direction, as if, in the first case, negative electrons diffused from the hot end to the cold end, and, in the second case, the diffusion of positive carriers took place. This effect is explained by the quantum theory as a result of the incomplete saturation by electrons of all the normal quantum states. Vacant quantum states behave in the same way as free electrons possessing a positive charge. They have been named 'holes'.

The term 'free' as applied to electrons and holes should not be considered in the literal sense. Their movements in the crystal lattice only resemble the movements of charges in an air-free space. The powerful electric fields set up by atoms, ions, and dipoles in the crystal lattice affect, however, the laws of motion. The band theory of semiconductors leads to the conclusion that in two cases: 1) when the electrons in the conduction band occupy a small number of quantum states, and 2) when only a small number of vacant states (holes) remains in the valence band - the average velocities of electrons and holes obey the same laws of electrodynamics as free charges in vacuo, although with the distinction that these charges should be credited with a different mass from that of a free electron (9.1×10^{-28} gm). The charge of electrons and holes, e, in the bulk of the crystal should be taken as -1.6×10^{-19} coulombs for electrons and $+1.6 \times 10^{-19}$ coulombs for holes. Thus, for example, the acceleration a produced by the electrical force Ee is not equal to $\frac{Ee}{m}$ where m is the free electron mass. The acceleration $\bar{a}$ for the mean velocity of motion extending over a number of crystalline cells may, however, be regarded as proportional to the applied force:

$$\bar{a} = Ee\frac{1}{m^*}.$$

The value of m^* is not equal to m but is called the 'effective mass'. The ratio m^*/m depends on the structure of the crystal and its dielectric constant and, in anisotropic crystals, also on the direction of motion.

This should not, however, be interpreted in the sense that inside a crystal lattice the electron possesses a different real mass, a different weight, or a different zero energy $U = m^*c^2$. Neither the inertia nor the weight of electrons in metals are different from the inertia and weight of free electrons, and it is these quantities that determine the real mass of any given body. The presence in a semiconductor of electrons with a very high effective mass does not lead to any increase of its weight.

Similarly, the movement of positive holes does not mean that there are free positive charges in the body. When a body is made to rotate very quickly it is found that the free charges in it possess inertia. These charges are found, however, to be negative electrons with the

same charge-to-mass ratio $\frac{e}{m} = 1.76 \times 10^8$ coul/gm as that for free electrons, even in the case of conductors with a purely hole-type mechanism of conductivity.

Therefore the concepts 'hole' and 'effective mass' should be regarded as convenient auxiliary means of simplifying complicated statistical calculations of the behaviour of a large number of electrons in the periodic lattice field. All departures from periodicity, due either to the thermal agitation of atoms, geometrical defects, or extraneous impurities, affect the uniform and, on the average, rectilinear motion of an electron in a crystal which is subjected to an external electric field. All such imperfections introduce a certain probability of deviation of the electron path from the direction of the electron before meeting the given distortion of the periodicity.

Therefore, distortions are found to act as electron scattering centres. The greatest distortions of the regular lattice structure produce very pronounced scattering, following which all electron velocity directions become equally probable, regardless of the direction of the electron motion before encountering the distortion. Weaker non-homogeneities produce probabilities of deflections through smaller angles, but after a few such collisions the initial direction of motion ceases to have any preference. The aggregate of distortions satisfying this last condition may be summed up by the concept of the 'scattering centre'.

The path of a carrier from one scattering centre to another or to a distortion at which it loses its kinetic energy, giving it up to the crystal lattice, is called 'the free path length' of the electron or hole. Both the effective mass and the free path length in one and the same crystal are different for an electron and for a hole.

When a closed thermocouple circuit is composed of semiconductors with the same (electronic- or hole-) type conductivity mechanism, the emf's produced by the temperature difference are directed in both arms of the thermocouple from the hot to the cold junction or vice versa. Therefore, they oppose each other in the circuit, and the thermoelectric voltage is equal to their difference:

$$E = (\alpha_1 - \alpha_2)(T_1 - T_2).$$

On the other hand, when the thermoelectric circuit consists of an electronic and a hole type conductor, their thermal emf's are additive:

$$E = (\alpha_1 + \alpha_2)(T_1 - T_2).$$

It is evident that such a combination of conductors possesses substantial advantages.

Electronic and hole type conductors exist not only among semiconductors but also among metals, but the physical meaning of 'holes' in metal is more difficult to fit into a band scheme. According to this scheme, in the valence band of the metal there should remain only a small number of quantum states unoccupied by electrons, whilst, in fact, metals represent substances in which the valence band is only partly filled. Nevertheless, one has to consider that metals such as tungsten, molybdenum, zinc, etc. exhibit purely hole type conductivity, whilst lead and tin exhibit a mixed hole and electronic conductivity.

The type of current mechanism in a given conductor may be determined not only on the basis of the sign of the thermal emf but also from the direction in which the current carriers are deflected by a magnetic field perpendicular to the direction of the current. The laws of electromagnetism (e.g. the rule of the three fingers of the left hand interrelating the directions of deflection, magnetic field, and current) govern the direction in which the magnetic field deflects the carriers, regardless of whether the current is due to the flow of electrons from left to right or of holes from right to left. When the current carriers are electrons, the portion of the conductor towards which the current is deflected by the field becomes negatively charged with respect to the opposite side; when the current is produced by the holes, the side towards which the current is deflected is charged positively.

This phenomenon is known as the Hall effect. Experiment shows that measurements of the thermal emf and the Hall effect always yield the same current carrier signs, provided the current consists of charges of one sign only.

In conductors with mixed conductivity both the thermal emf's of holes and electrons, and potential differences produced by them in a magnetic field oppose each other and are therefore small. The quantitative rules of such a subtraction differ somewhat for the two phenomena. Thus, denoting by n_+ and n_- the concentrations of holes and electrons and by u_+ and u_- their mobilities, i.e. their average drift velocities in an electric field of 1 V/cm, we obtain for the Seebeck effect

$$a \propto \frac{n_+u_+ - n_-u_-}{n_+u_+ + n_-u_-}.$$

On the other hand the emf produced by the Hall effect is given by the expression

$$E_H \propto \frac{u_+^2 n - u_-^2 n}{(u_+n_+ + u_-n_-)^2}.$$

In the special case where $n_+ = n_-$ and $u_+ = u_-$ both a and E_H become equal to zero. The converse deduction that when $E_H = 0$, then also $a = 0$ cannot be regarded with confidence. In metals, however, it is possible to consider with sufficient accuracy that $u_+ = u_-$ and therefore to assume that when $E_H = 0$ then, also, $n_+ = n_-$, i.e. to expect that $a = 0$.

We meet with this state of affairs in the case of metals Pb and Sn for which E_H is extremely small and changes sign when going over from Pb to Sn. This allows us to assume that the case $a = 0$ is somewhere between a_{Pb} and a_{Sn} which differ only by 0.2 μV/deg. The values of thermal emf's referred to this zero value may be regarded as the absolute values of the thermal emf coefficients.

The difference between the absolute values of a determined from $a = \int_0^T \frac{r}{T}\,dT$ for the normal silver alloy and from the assumption that the mean value between a_{Pb} and a_{Sn} can be regarded as $a = 0$ amounts to about 1 μV/deg, as follows from the comparison of Justi's table which was based on first definition, with Meisner's table which was calculated on the basis of the second definition.

Even in metals the value of a is very sensitive to the presence of the smallest amounts of impurities and therefore the two series do not fully coincide, both as far as the absolute value of a is concerned, and also with regard to the order of metals in the thermoelectric series (e.g. the positions of Cu, Pt, Au, Nos. 1-4, see p. 3).

In semiconductors impurities play a decisive role as may be seen from Meisner's second series reproduced on page 3 in which quite different values are given for one and the same compound. Thus, for example, the values listed for Cu_2O are 474, 1000, 1120 and 1150 μV/deg and for Fe_2O_3 –613 and –60 μV/deg.

As we shall see later, the introduction of impurities into semiconductors opens up a way for the improvement of their thermoelectric properties.

1.4 Calculation formulae. In this paragraph we are giving formulae for the calculation of the thermal emf per 1°C, a, without giving any proofs. Detailed information on this subject will be found: 1) in part II of the article by A. G. Samoilovich and L. L. Korenblit (Uspekhi Fizicheskikh Nauk, 1953, *49*, No. 2-3); 2) in part I of the article by V. I. Davydov and I. M. Shmushkevich (ibid, 1940, *24*, No. 1); and 3) in the book by A. F. Ioffe "The Physics of Semiconductors", published by the Academy of Sciences in 1957.*

The other thermoelectric coefficients, namely the Peltier coefficient

* English translation, Infosearch, London, 1958.

Π and the Thomson coefficient τ may, as we have seen earlier, be derived from the expression for α.

For metals, in particular monovalent metals, the quantum theory yields the following relationship

$$\alpha = \frac{1}{3e}\pi^2 k^2 T\left[\frac{1}{\mu} + \left(\frac{1}{l}\times\frac{dl}{d\epsilon}\right)\right]. \tag{9}$$

Here μ is the chemical potential of electrons, which in the case of metals is equal to the Fermi level energy, and l is the free path length of electrons with a kinetic energy ϵ. For metals one may assume that

$$l \propto \epsilon^2, \tag{10}$$

and since the electrons contributing to the current have predominantly $\epsilon \approx \mu$, we have

$$\frac{1}{\mu} + \frac{1}{l}\times\frac{dl}{d\epsilon} = \frac{3}{\mu},$$

whence

$$\alpha = \frac{1}{e}\pi^2 k^2 T\frac{1}{\mu} = \pi^2\frac{k}{e}\times\frac{kT}{\mu}. \tag{11}$$

The value of μ is almost independent of temperature and therefore in monovalent metals α is proportional to the absolute temperature T:

$$\alpha \propto T. \tag{12}$$

Expression (11) gives an order of magnitude of

$$\alpha \approx 10.86\,\frac{3\times10^{-2}}{5} = 5.2\ \mu\text{V/deg}$$

which is in good agreement with experimental data.

An exception here is lithium for which $\alpha = 41\,\mu$V/deg. A. G. Samoilovich and F. Serova have shown that in this case there takes place, in addition to the diffusion of electrons, a dragging of current carriers by thermal waves (phonons) from the hot to the cold end of the conductor and the term $\frac{1}{l}\times\frac{dl}{d\epsilon}$ acquires the value $-\frac{2.8}{\epsilon}$ as compared with $+\frac{2}{\epsilon}$ for the majority of metals. The possibility of dragging of electrons by phonons was first pointed out by L. E. Gurevich.

In semiconductors one has to take into account the possibility of the existence of both free electrons with a concentration n_- and holes

with a concentration n_+. The thermal emf's produced by the electrons and the holes have opposite signs and therefore one is subtracted from the other. In this case the thermal emf is given by the following expression

$$\alpha = \frac{1}{T\sigma}\left[u_- n_-(2kT - \mu) - u_+ n_+(2kT - \mu + \Delta E)\right],$$

where σ is the specific electrical conductivity, u the mobility and ΔE the width of the forbidden energy band.

N. L. Pisarenko derived an expression for α which is more convenient for computation purposes

$$\alpha = \frac{k}{\sigma}\left\{u_- n_-\left[A + \ln\frac{2(2\pi m_-^* kT)^{3/2}}{h^3 n_-}\right] - u_+ n_+\left[A + \ln\frac{2(2\pi m_+^* kT)^{3/2}}{h^3 n_+}\right]\right\}. \tag{13}$$

The value of the constant A depends on the electron scattering mechanism, and in particular on the value of $\frac{1}{l}\times\frac{dl}{d\epsilon}$. The latter is in turn governed by the character of scattering centres.

In crystals with an atomic lattice with covalent binding the thermal vibration spectrum consists of acoustic vibrations, the frequencies of which are initially (at the low frequencies and long wavelengths which play the main rôle in the interaction with slow electrons) proportional to their momentum. For such crystals

$$\frac{dl}{d\epsilon} = 0, \quad l = \text{const}. \tag{14}$$

In crystals with an ionic lattice the electrons are principally scattered by electromagnetic polar vibrations in which positive and negative ions move in opposite directions. The most important of these 'optical' vibrations are the longitudinal vibrations producing an accumulation of charges in some parts and a reduced density of charges in other parts. This leads to the appearance of most powerful electric fields deflecting the moving electrons.

In ionic crystals it is necessary to consider two temperature ranges:

1) temperatures at which the average kinetic energy of electrons $\frac{3}{2}kT$ is much lower than the energy of natural vibrations of the ions $h\nu_0$ (these vibrations correspond to the residual rays); at these temperatures, which are below the Debye temperature θ, we have at $kT \ll h\nu_0$

$$l = l_0 \sqrt{\frac{\epsilon}{h\nu_0}}\, e^{\frac{h\nu_0}{kT}}; \tag{15}$$

2) on the other hand, at high temperatures when $kT >> h\nu_0$

$$l \propto \epsilon. \tag{15a}$$

At temperatures above the Debye temperature, when $kT >> h\nu_0$, the electrons in many crystals interact with vibrations of a frequency which changes little with the increase of the momentum of the atoms, so that

$$l \propto \epsilon^{-1}. \tag{16}$$

Electron scattering centres need not only result from the thermal vibrations, i.e. the interaction of electrons with phonons; any other distortions of the crystalline lattice may form scattering centres. Of these it is the presence of ionised impurity atoms that is of the greatest importance. In this case, we have as in metals

$$l \propto \epsilon^2. \tag{17}$$

Scattering on neutral atoms is usually small; it corresponds to

$$l \propto \epsilon^{1/2}. \tag{18}$$

Shear strains in deformed crystals and geometrical defects also produce electron scattering. However, the number of affected places is usually too small to produce a noticeable effect in comparison with other sources of scattering.

When various scattering sources are present in a crystal lattice they can be replaced with sufficient accuracy by scattering with a path length L satisfying the following equation

$$\frac{1}{L} = \sum \frac{1}{l}. \tag{19}$$

The constant A in expression (13) acquires, depending on the type of relationship between l and ϵ or between mobility u and temperature T, the following values.

For atomic lattices

$$l \propto \epsilon^0, \quad u \propto \frac{1}{T^{3/2}}, \quad A = 2. \tag{20a}$$

For ionic lattices at $kT << h\nu_0$:

$$l = l_0 \sqrt{\frac{\epsilon}{h\nu_0}}\, e^{\frac{h\nu_0}{kT}}, \quad u \propto e^{\frac{h\nu_0}{kT}}, \quad A = 2.5. \tag{20b}$$

For ionic lattices at $kT >> h\nu_0$:

$$l \propto \epsilon, \quad u \propto \frac{1}{T^{1/2}}, \quad A = 3.0. \tag{20c}$$

For scattering by vibrations of constant frequency

$$\left.\begin{aligned} & l \propto \epsilon^{-1}, \quad u \propto \frac{1}{T^{5/2}}, \quad A = 1.0 \\ \text{or} \quad & l \propto \epsilon^{-3/2}, \quad u \propto \frac{1}{T^3}, \quad A = 0.5. \end{aligned}\right\} \tag{20d}$$

For scattering on impurity ions

$$l \propto \epsilon^2, \quad u \propto T^{3/2}, \quad A = 4.0. \tag{20e}$$

In general when $l \propto e^r$, $u \propto T^{r-3/2}$ and $A = r + 2$, when the scattering takes place on thermal fluctuations. When lattice defects which do not depend on temperature form the scattering centres, $u \propto T^{r-1/2}$.

The character of the binding forces which governs the dependence of l on ϵ is difficult to determine. Therefore the value of r has to be estimated from the temperature dependence of mobility.

In practical applications of thermoelectric phenomena, the simultaneous presence of holes and electrons is undesirable if the hole and electron mobilities u_+ and u_- do not differ much from each other. For these purposes it is also desirable to use semiconductors with high electrical conductivity. Both requirements are satisfied by the introduction of impurities into the semiconductor, creating either free electrons or holes.

For a semiconductor with current carriers of one type only, expression (13) may be simplified and replaced by the formula

$$\alpha = \frac{k}{e}\left(A + \ln \frac{2(2\pi m^* kT)^{3/2}}{h^3 n}\right). \tag{21}$$

Expressions for α may also be written down in a different form. For atomic lattices with current carriers of one type

$$\alpha = \frac{k}{e}\left(2 - \frac{\mu}{kT}\right) \tag{22a}$$

or, denoting by ΔE the distance of the impurity level from the corresponding band edge, we have at $\Delta E >> kT$

$$\alpha \approx \frac{k}{e} \times \frac{\Delta E}{2kT}. \tag{22b}$$

The last expression requires that the value of α should decrease with increasing temperature proportionally to $\frac{1}{T}$ and tend to infinity as the temperature tends to absolute zero. This conclusion not only disagrees with experimental data, but is also at variance with the principles of thermodynamics according to which not only $\alpha(T)_{T=0} = 0$, but also $\left(\frac{d\alpha}{dT}\right)_{T=0} = 0$.

This contradiction indicates that the approximations made in the derivation of expressions (21), (22a) and (22b) are inadequate and that some properties which manifest themselves at low temperatures have been neglected.

For ionic semiconductors

$$\alpha = \frac{k}{e}\left(3 - \frac{\mu}{kT}\right). \tag{23}$$

The polaron model of ionic semiconductors evolved by S. I. Pekar leads to more complex functions $l(\epsilon)$ and therefore somewhat different formulae for α. Pekar's theory is found to be well substantiated in the case of ionic semiconductors, when the electrons diffuse simultaneously with the polarisation of the surrounding medium. For a constant temperature T one can put according to Pekar

$$l_{\text{pol}} \propto \epsilon^2.$$

For practical purposes it is convenient to write expression (21) as a relationship between α and σ both of which can be readily measured. By introducing an impurity or an excess of one of the components of the

compound it is possible to vary the concentration n within wide limits without appreciably affecting the mobility u. Therefore the expression for α may be rewritten in the form

$$\alpha = \frac{k}{e}\left[A + \ln \frac{2(2\pi m^* kT)^{3/2} eu}{h^3}\right] - \frac{k}{e}\ln(neu)$$

or

$$\alpha = C - 86 \times 10^{-6} \ln\sigma = C - 2 \times 10^{-4} \log\sigma. \tag{24}$$

There is a large group of semiconductors with high electrical conductivity in which the concentration n does not vary with temperature. The effective mass m^* is also independent of temperature. According to expression (21) the temperature dependence of α for these materials takes the form

$$\alpha = \frac{k}{e}\left[A + \ln \frac{2(2\pi m^* k)^{3/2}}{h^3 n}\right] + \frac{3}{2} \times \frac{k}{e} \ln T. \tag{25}$$

In such cases expressions (24) and (25) are well substantiated by experiment. In the plot $\alpha = f(\log\sigma)$ α is represented by a straight line with a slope of approximately 2×10^{-4} (see figs. 8 and 9, pp. 52 and 54). The temperature dependence of α at a given constant concentration n also corresponds to a slow logarithmic rise of α with T.

With the increase of free electron concentration the system gradually changes into the degenerate state when it is no longer possible to apply the limiting case of Boltzmann statistics in place of Fermi-Dirac statistics, which in general govern the electrons.

These more general formulae yield for the concentration

$$n = \frac{4\pi(2m^* kT)^{3/2}}{h^3} F_{1/2}\left(\frac{\mu}{kT}\right). \tag{25a}$$

The most general expression for α for a given current carrier concentration n of one sign has the form

$$\alpha = \pm\frac{k}{e}\left[\frac{r+2}{r+1} \times \frac{F_{r+1}\left(\frac{\mu}{kT}\right)}{F_r\left(\frac{\mu}{kT}\right)} - \frac{\mu}{kT}\right] \tag{26}$$

In particular, for atomic lattices, in which $r = 0$

$$\alpha = \pm \frac{k}{e}\left[2\frac{F_1\left(\frac{\mu}{kT}\right)}{F_0\left(\frac{\mu}{kT}\right)} - \frac{\mu}{kT}\right]. \qquad (26a)$$

$F_{1/2}\left(\frac{\mu}{kT}\right)$, $F_r\left(\frac{\mu}{kT}\right)$ and $F_{r+1}\left(\frac{\mu}{kT}\right)$ in expressions (25a), (26) and (26a) denote Fermi integrals

$$F_r\left(\frac{\mu}{kT}\right) = \int_0^\infty \frac{x^r dx}{e^{x-\frac{\mu}{kT}} + 1}$$

where x is reduced energy of the electrons $x = \frac{\epsilon}{kT}$.

The values of the function F_r for a range of values of r, and expressions for κ, σ, and α are listed on pages 90–92.

Having studied the conditions of transition from Boltzmann statistics to Fermi statistics, K. S. Shifrin found that the effect of degeneracy becomes noticeable when $\frac{\mu}{kT} > -2$ and when $\frac{\mu}{kT} > 2$ the state of electrons must be regarded as strongly degenerate.

T. A. Kontorova has, however, shown that Pisarenko's expression (21) is of such a form that it does not lead to large errors up to values of $\frac{\mu}{kT} \approx 1$.

All the foregoing considerations and formulae are based on the assumption that in a temperature gradient it is possible to regard the state of each small portion of material, containing a large number of atoms and electrons, as an equilibrium state, each portion only being described by different parameters. L. E. Gurevich showed in 1945 that this is not always true. The flux of phonons proceeding from the hot end to the cold end drags a larger number of electrons than that which follows from conditions of normal diffusion and an electric field. This factor may bring about an increase of the thermal emf.

In fact, soon afterwards, F. A. Serova and L. G. Samoilovich showed that the abnormally high thermal emf of lithium is due to the drag effect.

Elementary calculation of the possible drag effect in semiconductors, carried out in 1951 by G. E. Pikus, indicated that its influence on the thermal emf is negligible.

Experimental data for germanium and silicon have shown, against expectations, that the phonon drag effect is very high at low temperatures.

The disagreement with Pikus's calculations is attributed to the fact that electrons do not interact with all the thermal vibration phonons but only a few phonons, the wavelengths of which are not less than the wavelength of the electrons, or, more precisely, the wavelength vector G of such a phonon should be less than double the wavelength vector K of the electron.

Phonons satisfying this requirement possess a much larger free path length and a much longer relaxation time than the bulk of the phonons in the solid. Moreover, these phonons possess the most marked directional properties along the temperature gradient. Therefore, the effect of dragging of electrons by such phonons is particularly large.

At extremely low temperatures the drag effect is small since the free path length of both phonons and electrons depends on the dimensions of the crystals from which the solid is composed. At higher temperatures only the longwave phonons still retain a free path length of the order of the crystal dimensions. At still higher temperatures, the free path length of all phonons is smaller than the external dimensions, but the free path length of longwave phonons exceeds by many times its average value which governs the thermal conductivity of the solid. With a still further rise of temperature this difference becomes less pronounced and at a sufficiently high temperature, for which Pikus's calculations are valid, it no longer has any effect.

Accordingly, the increase of thermal emf, above that given by the formulae listed above, becomes particularly pronounced in a certain temperature range - usually below room temperature - for germanium around 30°K and for silicon around 100°K; in the case of silicon α reaches the value of 50,000 μV/°C. A complete theory of these phenomena has been given by C. Herring.

1.5 **Experimental facts.** A systematic study of thermal emf's of various semiconductors has been carried out by B. M. Gokhberg and M. S. Sominskii. Among the materials investigated by them there was only one substance, namely WO_3, which satisfied equation (22b): in the temperature range from liquid air temperature (90°K) to 400°K the thermal emf was found to be inversely proportional to the absolute temperature.

In V_2O_5 the relationship given by equation (22b) was only observed above –30°C (240°K); below this temperature α was proportional to the absolute temperature. The temperature dependence of α may be plotted in the form of two intersecting straight lines by plotting α vs. T up to 240°K and vs. $\frac{1}{T}$ above 240°K. It is remarkable, however, that despite

the abrupt change in the temperature dependence of α the temperature dependence of resistivity does not undergo a noticeable change at 240°K. The function $\log \rho = f\left(\frac{1}{T}\right)$ represents a straight line in the entire range from liquid air temperature (90°K) to 500°K.

In Cu_2O α is found to be independent of temperature from 90° to 355°C (or 630°K), whilst above 630°K it is inversely proportional to temperature. Andersen has shown that in this case the sudden change of slope from a straight line for α against $\frac{1}{T}$ at 630°K coincides with a change of slope in the graph $\log \rho = f\left(\frac{1}{T}\right)$. The constancy of α below 630°K is at variance with theoretical predictions since here one would expect impurity conduction obeying expression (22b).

For tin sulphide (SnS) α is proportional to T at low temperatures; then α becomes constant, and at high temperatures it is proportional to $\frac{1}{T}$.

The temperature dependence of α is even more complex in the case of Tl_2S: at low temperatures α increases with an increase of T, then it decreases, then it again increases, and at high temperatures it again decreases.

The aforementioned semiconductors possess relatively high resistivities and a wide forbidden band. Data are also available for several other semiconductors of this type.

Expression (22b), according to which α is proportional to $\frac{1}{T}$, is found to be valid only at elevated temperatures (above 600°K in Cu_2O, above 700°K in BaO, and above 700°K in NiO). On the other hand, at low temperatures α is proportional to T, which is contrary to expression (22b) but in full agreement with the requirements of quantum thermodynamics. Such a temperature dependence of α was found to hold for SiC below 200°K, CdO below 700°K, SbS below 190°K, and Ge below 30°K, and also in SnS, TiO_2 and certain other materials.

At intermediate temperatures there is often a range over which α is nearly constant; as has been mentioned earlier, this is true of Cu_2O in the range 90 to 630°K. α was found to be constant in MoS_2 from 300 to 500°K, in Bi_2S_3 from 110 to 450°K, in SiC from 100 to 300°K, and in PbS from 30 to 750°K. In this temperature range the two tendencies - α proportional to T at low temperatures and α proportional to $\frac{1}{T}$ at high temperatures - appear to be balancing each other.

Modern theory of thermoelectric phenomena indicates that the thermal emf in impurity semiconductors with a non-degenerate system of electrons

can only decrease with rise of temperature. According to this theory α can be proportional to temperature only in substances with degenerate electrons. In two cases (Ge and CdO), when such a temperature dependence of α was observed in semiconductors it was possible to demonstrate that the electrons were, as in metals, in a degenerate state.

There is, however, no reason to expect that in all semiconductors the electrons become degenerate as the absolute zero is approached. Incidentally, close to the absolute zero α and even $\frac{d\alpha}{dT}$ should tend to zero, since when T tends to 0°K, the entropy according to Nernst's theorem tends to zero, and, therefore, α also tends to zero.

Experimental data are in good agreement with such an extrapolation of the function $\alpha = f(T)$, but so far no theoretical foundations for this behaviour are available. General empirical formulae describing thermoelectric properties of semiconductors over a wide temperature range are also non-existent. It is only possible to state a qualitative rule according to which the thermal emf α of a semiconductor starting with $\alpha = 0$ at $T = 0$ is at first proportional to T, then rises less steeply with T often remaining constant in a certain temperature range, and then it begins to decrease approaching the theoretical expression (22a).

All the semiconductors discussed above are materials with a high resistivity ($\rho > 1$ ohm × cm) which are unsuitable for use in high efficiency thermoelements. Data on semiconductors with low resistivity ($\rho < 10^{-2}$ ohm × cm) are reported in the section dealing with thermoelectric cooling and are discussed further on in this section (see pp. 41–72).

Since in order to calculate α it is necessary to know the effective mass of current carriers m^* and the scattering law, it is not possible to calculate α independently. The value of m^* may be estimated on the basis of several other properties of semiconductors: from the activation energy of impurities, the mobility, and magnetic and optical phenomena. The nature of the carrier scattering governs the temperature dependence of mobility.

The values of α for specific semiconductors calculated on the basis of such information are found to be close to the results of direct measurements. A detailed analysis is given in the section on thermoelectric cooling.

Within the temperature limits with which we have been dealing so far the thermal emf theory outlined above may serve as a basis for calculations. All the calculated values of α are found to agree within experimental accuracy with the observed values.

CHAPTER 2

THERMOELECTRIC GENERATORS

2.1 Energetic principles of thermoelectric batteries. Let us consider a thermoelement (fig. 1), consisting of p-type (1) and n-type (2) semiconductor rods joined by a metallic bridge (3). An external resistance R is connected in the circuit across the cold ends of the thermoelement; this resistance acts as a load for the electrical energy generated. When the potential difference across the cold ends of the circuit is denoted by U volts, the power delivered by the thermoelement will be $W = \frac{U^2}{R}$, whilst the current $I = \frac{U}{R}$.

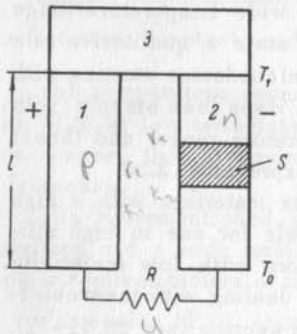

Fig. 1

We shall denote the thermal emf, which is in this case equal to the sum of the thermal emf's of the two branches, by α V/deg; $\alpha = |\alpha_1| + |\alpha_2|$.

The hot ends, joined by the bridge, are maintained at a temperature T_1, receiving heat energy from a source with a slightly higher temperature. The cold ends are at a temperature T_0, slightly above the temperature of the surroundings or of the heat exchange medium.

We shall denote the internal resistances of the two branches by r_1 and r_2 and their thermal conductivities by K_1 and K_2. Denoting the resistivities by ρ, the specific thermal conductivities by κ, and assuming that the lengths of both rods are equal to l, and their cross-section areas are S_1 and S_2, we have

$$r = r_1 + r_2 = \left(\frac{\rho_1}{S_1} + \frac{\rho_2}{S_2}\right) l,$$

$$K = K_1 + K_2 = (\kappa_1 S_1 + \kappa_2 S_2)\,\frac{1}{l}.$$

On the basis of the general laws of thermoelectric phenomena we can calculate the Peltier heat generated and absorbed by the thermoelement

at its two ends, the Thomson heat generated or absorbed inside the rods, the heat transferred by conduction from the hot to the cold ends, the Joule heat generated by the current in the rods, and the useful electrical energy delivered by the thermoelement. We shall refer to energy per second and express the power in watts. These units will also be used for purely thermal quantities; e.g. specific thermal conductivity will be expressed in W/deg × cm and not in cal/deg × cm × sec.

$$1 \text{ cal/deg} \times \text{cm} \times \text{sec} = 4.19 \text{ W/deg} \times \text{cm}$$

The amount of heat energy Q_1 received by the hot junctions, due to the Peltier effect, is

$$Q_1 = \alpha_1 I T_1 .$$

The power Q_0 delivered at the cold junction is

$$Q_0 = -\alpha_0 I T_0 .$$

The Thomson heat Q generated in each rod is, according to equation (7),

$$Q = \pm \int_{T_0}^{T_1} T \frac{d\alpha}{dT} I dT .$$

In the special case, when α at both ends has the same value, $Q = 0$.

The heat flux Q_h transferred from the hot junction to the cold junction through the two rods is

$$Q_h = K(T_1 - T_0).$$

The Joule heat generated in the two rods is $Q_J = I^2 r$. The useful power W delivered by the thermoelement is $W = I^2 R$; the current is

$$I = \frac{\alpha(T_1 - T_0)}{R + r}$$

Putting

$$\frac{R}{r} = m, \qquad (27)$$

we have

$$Q_1 = \alpha_1^2 T_1 (T_1 - T_0) \frac{1}{r(m+1)},$$

$$W = \alpha^2 (T_1 - T_0)^2 \frac{m}{r(m+1)^2}.$$

For the time being we shall neglect the Thomson heat, regarding it as small in comparison with the other terms and shall assume $\alpha_1 = \alpha_0 = \alpha$. When $\alpha_1 \neq \alpha_0$ the Thomson heat is accounted for in the determination of the efficiency by substituting for α the mean value for the two ends $\bar{\alpha} = \frac{\alpha_1 + \alpha_0}{2}$.

Of the total Joule heat $I^2 r$ generated in the thermoelement, half passes to the hot junction, returning the power $\frac{1}{2} I^2 r$ and the rest is transferred to the cold junction.

The efficiency η will be defined as the ratio of the useful electrical energy $I^2 R$ delivered to the external circuit to the energy consumed from the heat source. The latter consists of the Peltier heat Q_1, and the heat Q_h transferred by conduction to the cold junction, from which it is necessary to deduct the electrical energy $\frac{1}{2} I^2 r$ returned to the heat source.

$$\eta = \frac{W}{Q_1 + Q_h - \frac{1}{2} I^2 r} =$$

$$= \frac{\alpha^2 (T_1 - T_0)^2 \frac{1}{r} \times \frac{m}{(m+1)^2}}{\alpha^2 T_1 (T_1 - T_0) \frac{1}{r} \times \frac{1}{(m+1)} + K(T_1 - T_0) - \frac{1}{2} \times \frac{\alpha^2 (T_1 - T_0)^2}{r(m+1)^2}} =$$

$$= \frac{T_1 - T_0}{T_1} \times \frac{\frac{m}{m+1}}{1 + \frac{Kr}{\alpha^2} \times \frac{m+1}{T_1} - \frac{1}{2} (T_1 - T_0) \frac{1}{m+1}}$$

Thus the efficiency of the thermoelement is fully determined by a) the hot and cold junction temperatures; b) the quantity $\frac{Kr}{\alpha^2}$ which depends on the properties of the materials used in the thermoelement and which will be denoted by $\frac{1}{z}$, so that

$$z = \frac{\alpha^2}{Kr} \tag{28}$$

and, finally, c) the selected ratio $m = \frac{R}{r}$.

In order to achieve as high an efficiency as possible in thermoelements at given values of α, κ, and ρ and an arbitrary ratio $\frac{R}{r} = m$, it is necessary to find the optimum cross-section areas S_1 and S_2, so that at given values of κ and ρ the product Kr is minimum. To find the condition for a minimum of Kr we shall differentiate

$$Kr = (\kappa_1 S_1 + \kappa_2 S_2) \left(\frac{\rho_1}{S_1} + \frac{\rho_2}{S_2} \right) = \kappa_1 \rho_1 + \kappa_2 \rho_2 + \kappa_1 \rho_2 \frac{S_1}{S_2} + \kappa_2 \rho_1 \frac{S_2}{S_1}$$

with respect to $d\left(\frac{S_1}{S_2}\right)$ and equate the derivative to zero. This gives

$$\frac{\rho_1}{\kappa_1} \times \frac{\kappa_2}{\rho_2} = \left(\frac{S_1}{S_2} \right)^2. \tag{29}$$

At this value of $\frac{S_1}{S_2}$

$$Kr = \left(\sqrt{\kappa_1 \rho_1} + \sqrt{\kappa_2 \rho_2} \right)^2,$$

$$z = \frac{\alpha^2}{Kr} = \frac{\alpha^2}{\left(\sqrt{\kappa_1 \rho_1} + \sqrt{\kappa_2 \rho_2} \right)^2} \text{ deg}^{-1}. \tag{30}$$

This expression contains only the properties of the materials of the two branches of the thermoelement, but not their dimensions.

We shall now find the ratio $\frac{R}{r} = m$ giving the highest efficiency. The condition for delivering the maximum power to the load leads, in the case of a thermoelement as with other current sources, to the requirement $R = r$, i.e. $m = 1$, and

$$\eta = \frac{1}{2} \frac{T_1 - T_0}{T_1 + \frac{2}{z} - \frac{1}{4} (T_1 - T_0)}.$$

We shall find the condition for the maximum efficiency by putting $\frac{\partial \eta}{\partial m} = 0$; straightforward calculations give

$$\left(\frac{R}{r}\right)_{opt} = M = \sqrt{1 + \frac{1}{2}z(T_1 + T_0)}, \qquad (31)$$

where $(T_1 z)$ and M are dimensionless numbers.

Substituting this optimum value of m, denoted here by M, into the expression for η we find

$$\eta = \frac{T_1 - T_0}{T_1} \times \frac{M - 1}{M + \frac{T_0}{T_1}}. \qquad (32)$$

Henceforward η will refer only to this maximum efficiency.

The first factor represents the thermodynamic efficiency of a reversible engine, and the second describes the reduction of this efficiency as a result of irreversible losses due to heat conduction (κ) and Joule heat (ρ) entering into the expression for z.

The greater is M in comparison with unity, i.e. the larger the values of z and $T_1 + T_0$, the smaller is the reduction of the efficiency due to irreversible losses. Therefore an increase of the hot junction temperature T_1 increases η not only by increasing the value of the efficiency of a reversible engine $\frac{T_1 - T_0}{T_1}$ but also because of the simultaneous increase of M at a given z.

This equation also shows clearly that in order to achieve the maximum efficiency the material has to satisfy only one condition, namely the maximum value of z compatible with the maximum temperature T_1 of the heat source, or more precisely the maximum product $z\frac{T_1 + T_0}{2}$ attainable for the given material.

Neglecting the quantity $\frac{1}{2}I^2 r$ in the expression for the efficiency, assuming it to be small in comparison with $Q_1 + Q_h$, we obtain

$$M' = \sqrt{1 + T_1 z}, \qquad (33)$$

$$\eta' = \frac{T_1 - T_0}{T_1} \times \frac{M' - 1}{M' + 1} \qquad (34)$$

The value of η' differs little from η as long as η itself is small. For example, in the special case when $T_1 = 600°K$, $T_0 = 300°K$ and $z = 2 \times 10^{-3}$, we have $M = 1.38$, $M' = 1.48$, $\eta = 0.101$, $\eta' = 0.097$.

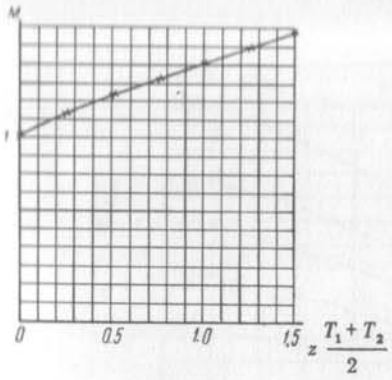

Fig. 2

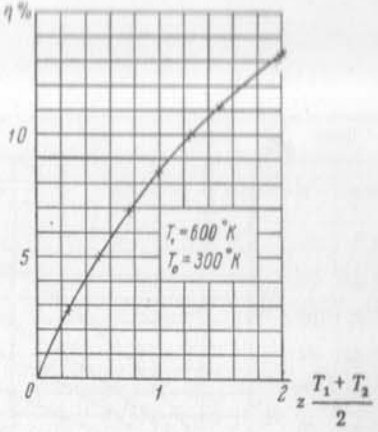

Fig. 3

The dependence of M and η on the product $\frac{1}{2}z(T_1 + T_0)$ is shown in figs. 2 and 3 and in table 1 for $T_1 = 600°K$, $T_0 = 300°K$ and $\frac{T_1 - T_0}{T_1} = 0.5$.

TABLE 1

$\frac{1}{2}z(T_1+T_0)$	M	$\frac{M-1}{M+\frac{T_1}{T_0}}$	η %
0.25	1.12	0.074	3.7
0.50	1.23	0.133	6.6
0.75	1.32	0.176	8.8
1.0	1.41	0.215	10.8
1.25	1.50	0.250	12.5
1.50	1.58	0.280	14.0
2.0	1.73	0.330	16.5

Assuming $T_0 = 300°K$, we show in table 2 and fig. 4 the values of the efficiency η and M as functions of z at different values of T_1 and in fig. 4a the dependence of η on T_1 for different values of z.

2.2 Materials for semiconductor thermoelements. We shall now consider the selection of the most suitable materials for thermoelements.

First of all, it should be noted that semiconductors, owing to their much higher values of α, are definitely preferable to metals. In fact, for

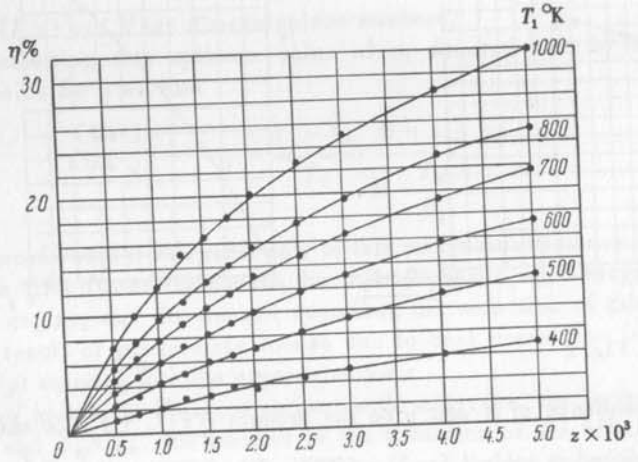

Fig. 4

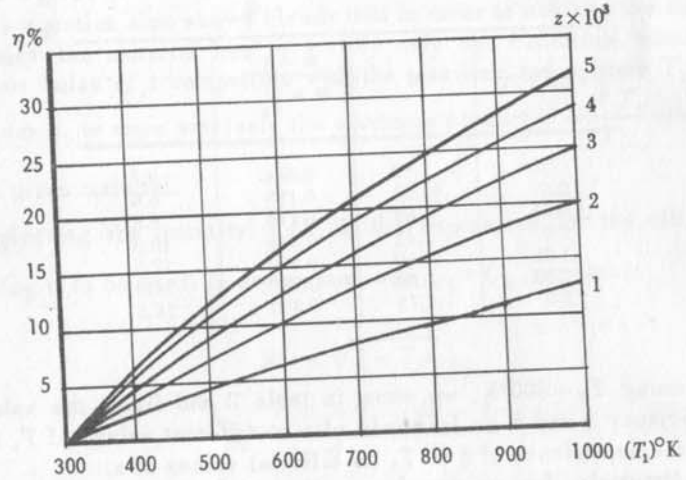

Fig. 4a

TABLE 2

T_1 °K	400		500		600		700		800		1000	
$z \times 10^3$	M	η %	M	η %	M	η %	M	η %	M	η %	M	η %
0.5	1.085	1.15	1.095	2.25	1.111	3.45	1.12	4.4	1.13	5.4	1.15	7.2
0.75	1.13	1.5	1.14	3.2	1.155	4.7	1.17	6.1	1.19	7.6	1.22	10.0
1.0	1.162	2.13	1.185	4.15	1.20	5.9	1.225	7.8	1.25	9.6	1.285	12.5
1.25	1.20	2.65	1.225	5.0	1.25	7.2	1.275	9.2	1.30	11.1	1.35	15.0
1.5	1.24	3.0	1.27	5.8	1.295	8.2	1.325	10.5	1.35	12.7	1.40	16.5
1.75	1.27	3.35	1.30	6.3	1.325	9.2	1.37	11.8	1.40	14.0	1.46	18.0
2.0	1.31	3.75	1.345	7.1	1.375	10.1	1.42	13.0	1.45	15.5	1.52	20.0
2.5	1.38	4.4	1.41	8.2	1.46	11.7	1.50	14.8	1.55	17.5	1.62	22.6
3.0	1.43	4.9	1.48	9.2	1.53	13.0	1.85	16.5	1.63	19.5	1.72	25.0
4.0	1.55	6.0	1.62	11.1	1.675	15.5	1.73	19.2	1.88	23.0	1.90	28.5
5.0	1.66	6.8	1.73	12.5	1.80	17.2	1.87	21.5	1.94	25.0	2.08	32.0

most metals $\alpha < 10 \times 10^{-6}$ V/deg. The ratio of electrical conductivity $\sigma = 1/\rho$ to thermal conductivity κ for all metals is close to the theoretical value predicted by quantum mechanics

$$\frac{\kappa}{\sigma} = \frac{\pi^2}{3}\left(\frac{k}{e}\right)^2 T = 2.44 \times 10^{-8}\, T .$$

At an average temperature $T = 500°K$

$$z = 8.2 \times 10^{-6}$$

and at $T_1 = 700°K$ and $T_0 = 300°K$

$$\eta = 8.5 \times 10^{-4} = 0.085\% .$$

For the best pair of metals Bi-Sb we can put: $\alpha = 100 \times 10^{-6}$, $\kappa\rho = 9 \times 10^{-6}$, $z = 1.1 \times 10^{-3}$, $T_1 < 450°K$, $T_0 = 300°K$ and $\eta = 3.1\%$.

In several semiconductors z reaches, and sometimes exceeds, the value of 1×10^{-3}, and η approaches 10%. Furthermore, several semiconductors possess a high melting point, thus permitting operation at high

values of T_1. Therefore, efficiencies of the order of 10–15% and more cannot be regarded as unattainable with the use of semiconductors. Values of η equal to 3.3 and even 7% have been reported in literature.

The higher the value of $z = \frac{\alpha^2}{\kappa\rho}$ for the individual branches of the thermoelement, the higher is the value of $z = \frac{(\alpha_1 + \alpha_2)^2}{(\sqrt{\kappa_1\rho_1} + \sqrt{\kappa_2\rho_2})^2}$ which determines the efficiency of the entire thermoelement. However, the relationship between the z of the thermoelement and the values of z_1 and z_2 for the individual branches cannot be stated in a general form. In individual cases, when $z_1 = z_2$, then $z = z_1 = z_2$; when $\kappa_1\rho_1 = \kappa_2\rho_2$, then $z = \frac{1}{4}(z_1 + z_2) + \frac{1}{2}\sqrt{z_1 z_2}$. If $\alpha_1 = \alpha_2 = 172\ \mu$V/deg, as is required for the best utilisation of semiconductor materials (see below), then

$$z = \frac{4}{\left(\frac{1}{\sqrt{z_1}} + \frac{1}{\sqrt{z_2}}\right)^2} = \frac{4z_1 z_2}{(\sqrt{z_1} + \sqrt{z_2})^2}.$$

Starting with equation (21) for semiconductors it is possible to establish the relationship between α and $\sigma = 1/\rho$. Assuming the temperature to be constant and the mobility to be practically independent of concentration n, one would expect a linear relationship between α and $\ln\sigma$:

$$\alpha = C - 86 \times 10^{-6} \ln\sigma = C - 2 \times 10^{-4} \log\sigma. \qquad (35)$$

The value of C depends on temperature T, mobility, and the character of the chemical bonds in the semiconductor.

In addition, σ is related to κ. The thermal conductivity of the semiconductor κ is composed of the electronic thermal conductivity κ_{el} and the thermal conductivity due to thermal vibrations and the propagation of heat waves (denoted here as phonon thermal conductivity κ_{ph}):

$$\kappa = \kappa_{el} + \kappa_{ph}. \qquad (36)$$

The former is related to electrical conductivity σ by the Wiedemann-Franz law. However, the coefficient of proportionality has a value equal to that for metals

$$\frac{\kappa_{el}}{\sigma} = \frac{\pi^2}{3}\left(\frac{k}{e}\right)^2 T \qquad (37)$$

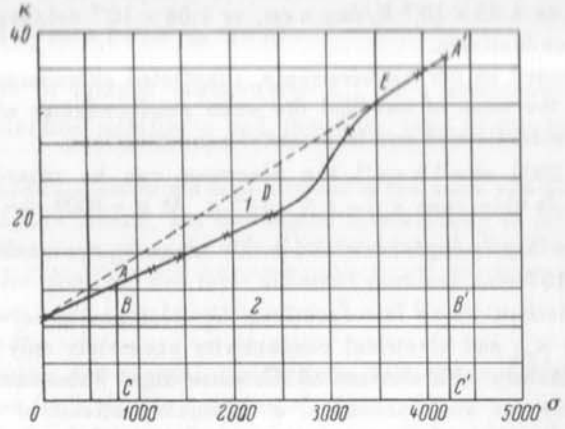

Fig. 5. Dependence of thermal conductivity of a semiconductor on its electrical conductivity.

1 - $\kappa = \kappa_{el} + \kappa_{ph}$; *2* - κ_{ph}; *AB* and *A'B'* - κ_{el}; *D* - start of degeneracy; *E* - complete degeneracy.

only at very high concentrations of free electrons (more than 2.5×10^{19} cm^{-3}) when the latter must be regarded as degenerate.

At lower concentrations usually prevailing in semiconductors

$$\frac{\kappa_{el}}{\sigma} = 2\left(\frac{k}{e}\right)^2 T = 1.48 \times 10^{-8}\ T\ \text{V}^2/\text{deg.}, \qquad (38)$$

which gives, at room temperature ($T = 293°$K),

$$\frac{\kappa_{el}}{\sigma} = 4.35 \times 10^{-6}\ \text{V}^2/\text{deg.}*$$

* In the general case the Wiedemann-Franz law for semiconductors has the following form

$$\frac{\kappa_{el}}{\sigma} = (r + 2)\left(\frac{k}{e}\right)^2 T, \qquad (38a)$$

which for atomic lattices with $r = 0$ reduces to equation (38). r is the exponent in the formula giving the electron free path length l as a function of kinetic energy ($l \propto \varepsilon^r$).

In other words, every 1000 $ohm^{-1} \times cm^{-1}$ of electrical conductivity corresponds to 4.35×10^{-3} W/deg × cm, or 1.04×10^{-3} cal/deg × cm × sec of thermal conductivity.

Fig. 5, based on our measurements, illustrates expressions (36), (37) and (38) in the case of one and the same semiconductor with different electrical conductivities and free carrier concentrations.

At $\sigma < 2500$ $ohm^{-1} \times cm^{-1}$ the electrons can be regarded as non-degenerate. In this case $\kappa_{el} = 4.5 \times 10^{-6} \sigma$. At $\sigma = 4000$ $ohm^{-1} \times cm^{-1}$ the electrons are largely degenerate and in this range κ_{el} approaches the value $\kappa_{el} = 7.3 \times 10^{-6} \sigma$.

The Wiedemann-Franz law describes the relationship between thermal conductivity κ_{el} and electrical conductivity accurately only in the case of semiconductors with carriers of the same sign. When carriers of both signs are present simultaneously, a continuous stream of charges can flow in the direction of the temperature gradient and the thermal conductivity κ_{el} increases appreciably.

On the way from the hot to the cold junction the concentration of the holes and electrons decreases, the recombining pairs of charges liberating an energy ΔE_0.

We shall denote the current transported by the holes by I_1 and that transported by the electrons by I_2. In an electric field E, $I_1 = E\sigma_1$ and $I_2 = E\sigma_2$. Further, we shall write down $\kappa_{el}/\sigma = LT$.

The thermal conductivity due to the diffusion of carriers can then be expressed as

$$\kappa_{el} = L(\sigma_1 + \sigma_2)T + 2LT\,\frac{\sigma_1 - \sigma_2}{\sigma_1 + \sigma_2}\left(\frac{\Delta E_0}{2kT} + r + 2\right)^2.$$

In addition to the recombination of charges, heat may also be conducted from the hot end to the cold end by the transfer of other types of excitation energy. All such processes increase the thermal conductivity of semiconductors when the latter are heated above a certain temperature. They reduce, therefore, the efficiency of the thermoelements at these temperatures.

By analogy with diffusion and thermal conduction in gases, the phonon part of thermal conductivity κ_{ph} can be expressed as

$$\kappa_{ph} = \frac{1}{3} c v \bar{\lambda}, \qquad (39)$$

where c is specific heat (J/cm^3), v is sound velocity (cm/sec) and $\bar{\lambda}$ is the mean phonon free path length (cm).

In the case of the majority of semiconductors $c = 1.2$ to 1.6, $v = 2 \times 10^5$ to 5×10^5, and $\frac{1}{3} cv = 1 \times 10^5$ to 3×10^5.

The value of thermal conductivity κ_{ph} of a semiconductor is also related to electron mobility u and, therefore, also to electrical conductivity.

Both phonons and electrons are scattered by the same non-homogeneities of the crystalline lattice, but the degree of scattering is different owing to their different wavelengths (7×10^{-7} for electrons and approximately 5×10^{-8} cm for phonons) and their different physical nature. There should however exist some correlation between $\bar{\lambda}$ and the mean free path length of electrons $\bar{l}$.

In comparing the thermal conductivity and the mobility of various materials one finds that in a series of substances with similar structure the thermal conductivity decreases, whilst the mobility increases, with increasing atomic weight. Thus, in the series: diamond, silicon, germanium, κ_{ph} decreases from 2 to 1 and 0.6 W/deg × cm, whilst the electron mobility increases from 900 to 1400 and 3600 $cm^2/V \times sec$. Thus, as has been pointed out by H. J. Goldsmid, the ratio u/κ_{ph}, governing the value of z of thermocouples, increases with increasing atomic weight.

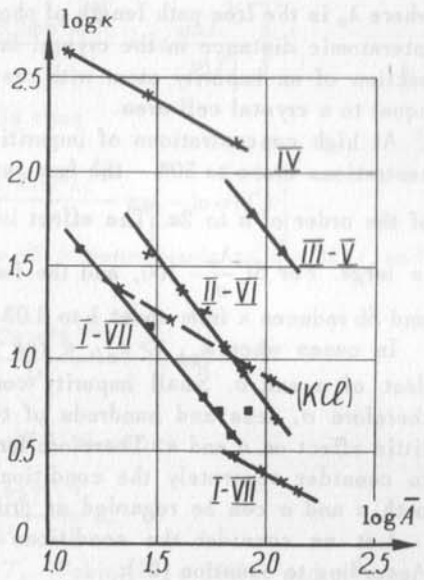

Fig. 6

The factors affecting the value of thermal conductivity κ_{ph} are clearly seen in the diagram in fig. 6. The thermal conductivity decreases, not only with increasing average atomic weight, but also in going over from purely valence type to ionic compounds, i.e. from elements in group IV of the periodic system towards the compounds of groups III with V, II with VI, and I with VII.

Elements and atomic compounds in the first and second rows of the periodic system (B, C, Si, SiC) have a thermal conductivity of 1 to 2 W/cm × deg. Valence compounds and elements in the next two rows, e.g. GaSb and InSb, have thermal conductivities of the order of tenths of W/cm × deg, and, for materials in the last rows, κ_{ph} does not exceed a few hundredths of W/cm × deg. A similar behaviour is exhibited by elements of group IV (C, Si, Ge), alkali halide compounds (from LiF to RbBr), oxides of elements in group II (from BeO to HgO), and titanates of group II elements.

Of major importance for thermoelements is the effect of impurities on the thermal conductivity. When N impurity atoms are dissolved in a crystal containing N_0 atoms, the initial thermal conductivity κ_0 drops to a value κ described, at low concentrations, by the expression

$$\frac{\kappa_0}{\kappa} = 1 + \frac{N}{N_0} \times \frac{\lambda_0}{a} S,$$

where λ_0 is the free path length of phonons in the pure substance; a is the interatomic distance in the crystal lattice and S is the scattering cross-section of an impurity atom with respect to phonons expressed in units equal to a crystal cell area.

At high concentrations of impurities within the solid solution – concentrations close to 50% – the free path length of phonons drops to values of the order of a to $2a$. The effect is largest in substances for which $\frac{\lambda_0}{a}$ is large. For Si $\frac{\lambda_0}{a} \approx 100$, and the formation of a solid solution with Ge and Sb reduces κ from about 1 to 0.03 W/deg × cm.

In cases when $\kappa_{ph} >> \kappa_{el}$, κ can be regarded as practically independent of a and σ. Small impurity concentrations which increase n, and therefore σ, tens and hundreds of times have, under these conditions, little effect on u and κ. Therefore for such semiconductors it is possible to consider separately the conditions of the maximum of $a^2\sigma$, in which both a and σ can be regarded as primarily functions of concentration n.

Let us consider the conditions at which $a^2\sigma$ reaches a maximum. According to equation (21):

$$a = \frac{k}{e}\left[A + \ln \frac{2(2\pi m^* k)^{3/2}}{h^3} + \ln euT^{3/2} - \ln\sigma\right] = \frac{k}{e}(S - \ln\sigma),$$

$$a^2\sigma = \left(\frac{k}{e}\right)^2 \sigma\,[S^2 - 2S\ln\sigma + (\ln\sigma)^2],$$

$$\frac{\partial(a^2\sigma)}{\partial\sigma} = \left(\frac{k}{e}\right)^2 [(\ln\sigma)^2 - 2(S-1)\ln\sigma + S(S-2)].$$

The condition $\frac{\partial(a^2\sigma)}{\partial\sigma} = 0$ gives

$$\ln\sigma = S - 1 \pm 1.$$

When the sign is positive, $\ln\sigma = S$ and $a = 0$, and, therefore, also $a^2\sigma = 0$. When the sign is negative, $\ln\sigma = S - 2$ and

$$a = 2\frac{k}{e} = 172 \times 10^{-6}\ \text{V/deg}, \tag{40}$$

$$(a^2\sigma)_{max} = 3 \times 10^{-8}\sigma. \tag{41}$$

Condition (40) for the maximum of $a^2\sigma$ is valid at all temperatures, and at all values of the coefficient A in Pisarenko's formula. Therefore $(a^2\sigma)_{max}$ is determined under these conditions by the value of σ. The temperature dependence of $a^2\sigma$ will have the following form

$$a^2\sigma = \left(\frac{k}{e}\right)^2 \sigma(T)\left[A + \ln\frac{2(2\pi m^* k)^{3/2}}{h^3} + \ln\frac{euT^{3/2}}{\sigma(T)}\right]^2.$$

In atomic lattices $u = u_0 T^{-3/2}$. In this case

$$a^2\sigma = \left(\frac{k}{e}\right)^2 \sigma(T)\left[A + \ln\frac{2(2\pi m^* k)^{3/2}}{h^3} eu_0 - \ln\sigma(T)\right]^2.$$

$a^2\sigma$ has a maximum when the value of σ corresponds to $a = 2k/e$, and therefore

$$\ln\sigma = (A-2) + \ln\frac{2(2\pi m^* k)^{3/2}}{h^3} + \ln euT^{3/2}.$$

For atomic lattices $A = 2$ and $uT^{3/2} = u_0 T_0^{3/2}$, therefore

$$\sigma_{opt} = \frac{2e(2\pi m^* k T_0)^{3/2}}{h^3} u_0$$

where u_0 is mobility at temperature T_0. Taking $T_0 = 300°\text{K}$ and $m^* = m_0$ we have

$$\frac{2(2\pi m_0 k T_0)^{3/2}}{h^3} = 2.5 \times 10^{19},$$

$$\sigma_{opt} = 2.5 \times 10^{19} \times 1.6 \times 10^{-19} u_0 \approx 4u_0 \tag{42}$$

for all temperatures.

In many semiconductor materials which may find application in thermoelectric batteries $n = \text{const}$ and $u \propto T^{-3/2}$, or $uT^{3/2} = u_0 T_0^{3/2}$, $uT^{3/2} = u_0 T_0^{3/2} \frac{1}{T}$ and $A = 1$. For such materials

$$\sigma_{opt} = \frac{1}{2.7} \times \frac{2e(2\pi m^* k T_0)^{3/2}}{h^3} u_0 \frac{T_0}{T}.$$

At $m^* = m_0$

$$\sigma_{opt} = 1.44 u_0 \frac{T_0}{T} \text{ ohm}^{-1} \times \text{cm}^{-1}. \tag{43}$$

In these two cases the optimum values of z are:
for atomic lattices with $A = 2$

$$z_{opt} = \frac{\alpha^2 \sigma}{\kappa} = 1.16 \times 10^{-7} \frac{u_0}{\kappa}, \tag{44}$$

and for lattices in which $A = 1$

$$z_{opt} = 4.3 \times 10^{-8} \frac{u_0}{\kappa} \times \frac{T_0}{T} \text{ deg}^{-1}. \tag{45}$$

When $\kappa \approx \kappa_{ph}$, then $\kappa T \approx \text{const} = \kappa_0 T_0$ and

$$z_{opt} = 4.3 \times 10^{-8} \frac{u_0}{\kappa_0} \text{ deg}^{-1}.$$

If $u_0 = 1000$ cm²/sec × V, and $\kappa_0 = 5 \times 10^{-3}$ cal/deg × cm × sec = 2.1×10^{-2} W/deg × cm

$$z_{opt} = 2.05 \times 10^{-3} \text{ deg}^{-1}.$$

The minimum value of $\alpha = 0$, $\alpha^2\sigma = 0$ and $z = 0$ occurs for an atomic lattice when

$$\sigma_{min} = 29 u_0 \text{ ohm}^{-1} \times \text{cm}^{-1},$$

and for a lattice with $A = 1$ when

$$\sigma_{min} = 10.7 \, u_0 \frac{T_0}{T}.$$

Fig. 7 shows $(\alpha^2\sigma)/(\alpha^2\sigma)_{max}$ as a function of $\ln(\sigma/u_0)$.

It follows from expressions (42) and (43) that the optimum free electron concentration n at 300°K is equal, for an atomic lattice with $A = 2$, to

$$n_{opt} = \frac{\sigma_{opt}}{eu} = \frac{4u}{eu} = 2.5 \times 10^{19} \text{ cm}^{-3}. \tag{46}$$

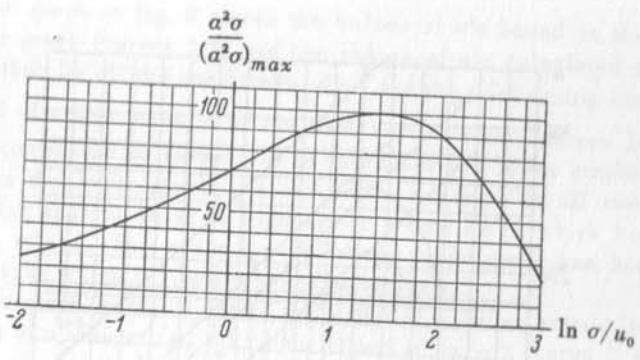

Fig. 7

This condition corresponds to $n = \frac{2(2\pi m_0 kT)^{3/2}}{h^3}$ and $\alpha = \frac{k}{e}(2 + 0) = 2\frac{k}{e}$.

For a lattice with $A = 1$ we have, at $T = T_0 = 300$°K,

$$n_{opt} = 9 \times 10^{18} \text{ cm}^{-3}. \tag{47}$$

Pisarenko's formula gives for this value of n_{opt}

$$\alpha = \frac{k}{e}(1 + \ln 2.7) = 2\frac{k}{e}.$$

These concentrations are close to the onset of electron degeneracy.

Fig. 8 shows the results of measurements on PbSe with hole conductivity and PbTe with hole and electronic conductivity containing different free charge concentrations.

On the basis of the temperature dependence of mobility, which in Pisarenko's formula has the form $uT^3 = \text{const}$ or $uT^{5/2} = \text{const}$, the constant A for these substances ought to have the value $A = \frac{1}{2}$ or $A = 1$ (assuming $m^*/m_0 = 1$). The experimental points down to $n = 4 \times 10^{18}$ fall on to straight lines in good agreement with Pisarenko's equation. When it is assumed that $m^*/m_0 = 1$ these lines correspond to values $A = 1.2$ for p-type PbTe, $A = 1$ for p-type PbSe and $A = \frac{1}{2}$ for n-type PbTe.

Alternatively, it could be assumed that all these compounds with an analogous chemical structure are covered by a single law $uT^{5/2} = \text{const}$

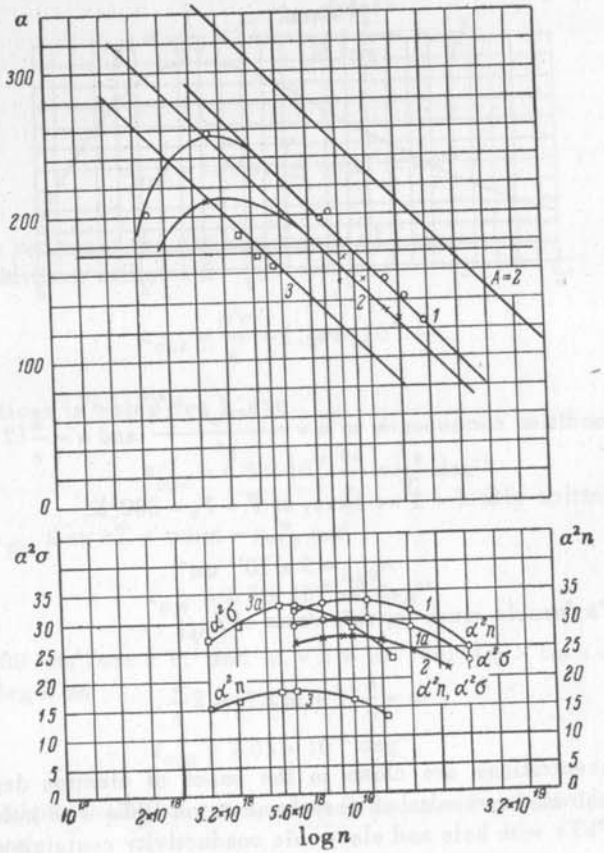

Fig. 8. Comparison of experimental results with Pisarenko's formula.

- ○ *p*-type PbTe ($A = 1.2$, $m^*/m_0 = 1$; or $A = 1$, $m^*/m_0 = 1.13$)
- □ *n*-type PbTe ($A = 0.5$, $m^*/m_0 = 1$; or $A = 1$, $m^*/m_0 = 0.7$)
- × *p*-type PbSe ($A = 1$, $m^*/m_0 = 1$)

and $A = 1$. In this case their effective masses would be different: $m^*/m_0 = 1.13$ for *p*-type PbTe, $m^*/m_0 = 1$ for *p*-type PbSe and $m^*/m_0 = 0.7$ for *n*-type PbTe.

The lower graph in fig. 8 shows the values of $\alpha^2 n$ based on the data in the upper graph (curves 1-3) and the values of $\alpha^2\sigma$ calculated on the assumption that for all the specimens $A = 1$ and the relationship between mobility and effective mass is of the form $um^{*5/2} = \text{const}$ (curves 1a and 3a, which correspond to curves 1-3 in the upper and lower graphs). As is seen from the lower graph, $\alpha^2\sigma$ reaches a maximum in all cases at $\alpha = 172\,\mu\text{V/deg}$ and its value is highest for *n*-type PbTe which has the lowest ratio m^*/m_0. The scale for $\alpha^2\sigma$ in the lower graph has been so selected that, at $m^*/m_0 = 1$, $\alpha^2 n$ coincides with $\alpha^2\sigma$.

The upper graph in fig. 9 shows the value of α for an atomic lattice as a function of n with $m^*/m_0 = 1$ (curve 1) and $m^*/m_0 = 1/4$ (curve 2, which apparently corresponds to electrons in germanium). The lower graph in fig. 9 shows the variation of $\alpha^2 n$ for both cases (curves 1 and 2); for the lattice with $m^*/m_0 = 1/4$ (curve 2) the scale has been increased ten times. In semiconductors, the lower the effective mass and, therefore, the lower the corresponding $(\alpha^2 n)_{max}$, the larger is the value of $(\alpha^2\sigma)_{max}$.

In addition to curves 1 and 2 representing $\alpha^2 n$, the lower graph in fig. 9 also shows the values of $\alpha^2\sigma$ (curves 1a and 2a) plotted, this time, on the same scale.

The values of σ can be obtained from the corresponding values of n by multiplying the latter by the mobility u, which is in turn determined by the value of m*. For atomic lattices the relationship between u and m^* can be expressed in the form $um^{*5/2} = \text{const}$. In particular, for $m^*/m_0 = 0.25$, $u/u_0 = 32$. As is seen from the plot of $\alpha^2\sigma$, the value of $(\alpha^2\sigma)_{max}$ for the lattice with $m^*/m_0 = 1/4$ is four times larger than for the lattice with $m^*/m_0 = 1$.

The formula describing the dependence of α and $\alpha^2\sigma$ on σ contains the interrelated quantities u and m^*. According to the quantum theory, for atomic lattices $um^{*5/2} = u_0 m_0^{5/2}$, whilst for polar lattices $um^{*3/2} = u_0 m_0^{3/2}$. Therefore for polar lattices α can be written down as

$$\alpha = \frac{k}{e}\left[3 + \ln\frac{2e(2\pi m_0 kT)^{3/2}}{h^3} - \ln\frac{\sigma}{u_0}\right], \qquad (48)$$

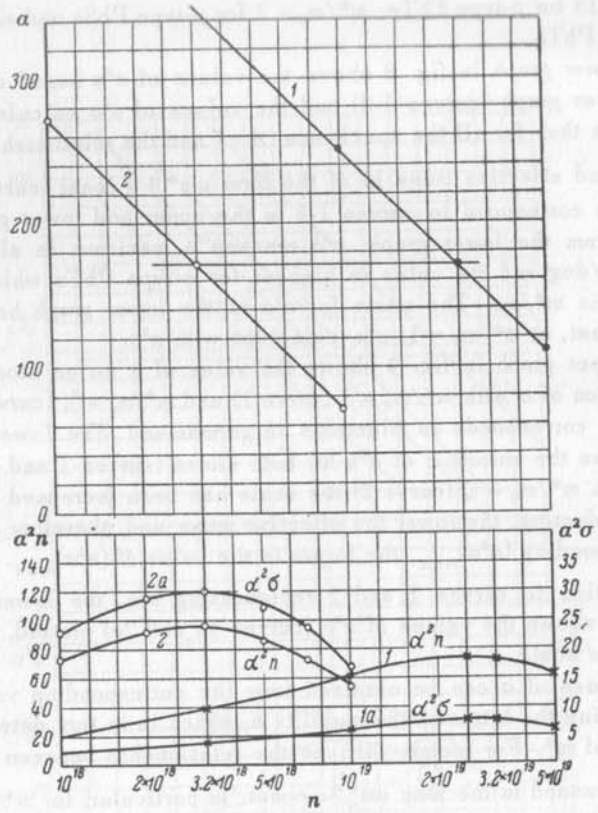

Fig. 9

and for atomic lattices as

$$\alpha = \frac{k}{e}\left[2 + \ln\frac{2e(2\pi m_0 kT)^{3/2}}{h^3} - \ln\frac{\sigma}{u_0}\times\frac{m}{m_0}\right] =$$

$$= \frac{k}{e}\left[\left(2 + \ln\frac{m_0}{m^*}\right) + \ln\frac{2e(2\pi m_0 kT)^{3/2}}{h^3} - \ln\frac{\sigma}{u_0}\right]. \qquad (49)$$

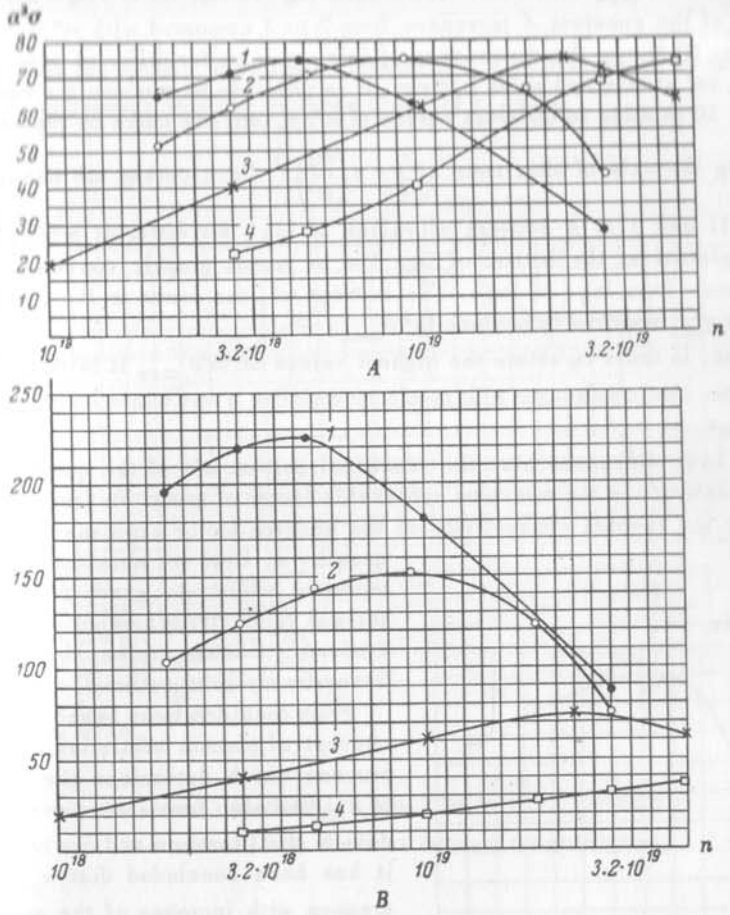

Fig. 10. *A* - ionic lattice $n/n_0 = (m_0/m^*)^{3/2}$; *B* - atomic lattice $n/n_0 = (m_0/m^*)^{5/2}$; *1* - $m^*/m_0 = 1/3$; *2* - $m^*/m_0 = 1/2$; *3* - $m^*/m_0 = 1$; *4* - $m^*/m_0 = 2$.

We can infer from this that for polar lattices neither a at a given σ, nor $(a^2\sigma)$ depends on m^*/m_0. On the other hand, for atomic lattices the value of $(a^2\sigma)_{max}$ increases with decreasing m^*/m_0; for $m^*/m_0 = 2.7$ the value of the constant A increases from 2 to 3 compared with $m^*/m_0 = 1$.

Fig. 10 shows the dependence of $(a^2\sigma)$ on $\log n$ for different values of m^*/m_0 for atomic and polar lattices. It is possible to combine the curves in fig. 10 relating to different values of m^*/m_0 into one curve by replacing n along the axis of abscissae by $\epsilon = n\left(\frac{m_0}{m^*}\right)^{3/2}$. Such curves are shown in figs. 11 and 11a. A network of values of $\log n$ for different m^*/m_0 has been plotted at the bottom of fig. 11a to permit graphic conversion of abscissae from $\log\epsilon$ to $\log n$. The smaller m^*, the lower is the concentration n_{opt} required to produce $(a^2\sigma)_{max}$.

Thus, in order to obtain the highest values of $(a^2\sigma)_{max}$ it is desirable to select semiconductors with maximum mobility u and minimum effective mass m^*.

We have discussed here the electrical portion $a^2\sigma$ of the quantity z, which determines the maximum achievable factor of merit. No less important is the thermal conductivity of the semiconductor expressed by the quantity κ. Here we should aim at a minimum value. An exact theory of thermal conductivity has not yet been evolved. Certain rules, however, have already been outlined.

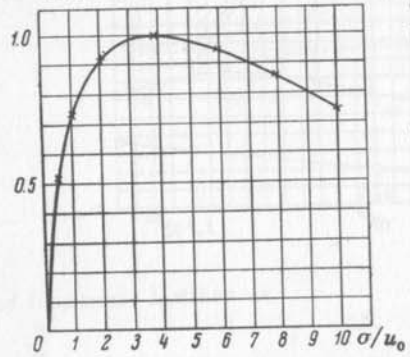

Fig. 11. Atomic lattice

From considerations based on the concept of phonon scattering as the process which determines the value of κ_{ph} and also from a comparison of data in the literature and our results it has been concluded that κ_{ph} decreases with increase of the atomic weight and with the reduction of the hardness of the material. κ_{ph} for ionic compounds has a lower value than for atomic compounds.

The above calculations were based on the assumption that $(a^2\sigma)_{max}$ would coincide with the condition $z_{max} = \left(\frac{a^2\sigma}{\kappa}\right)_{max}$ which holds only

$$\frac{u}{u_0} = \left(\frac{m_0}{m^*}\right)^{5/2}$$

in cases when κ is independent of σ. Of the two terms of which the thermal conductivity is composed,

$$\kappa = \kappa_{ph} + \kappa_{el},$$

only the phonon component of thermal conductivity is independent of σ, whereas the second, electronic component κ_{el}, is determined by the value of σ, increasing with the increase of σ, viz $\kappa_{el} = L\sigma$.

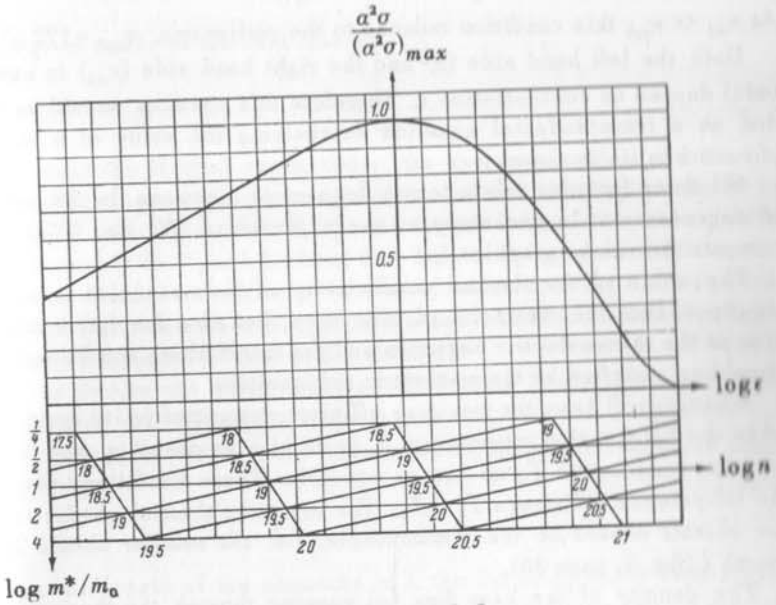

Fig. 11a. Ionic lattice: $u/u_0 = (m_0/m^*)^{3/2}$, $\epsilon = n(m_0/m^*)$.
The numbers down the sides indicate the ratio m^*/m_0.

This second component can be neglected only when $\kappa_{el} \ll \kappa_{ph}$, which is far from being always the case. In the general case, when κ_{ph} and κ_{el} are quantities of the same order, the condition $\alpha_{opt} = 172\ \mu V/deg$ is no longer valid.

Instead of investigating the condition z_{max} we shall consider the equivalent condition $(1/z)_{min}$:

$$\frac{1}{z} = \frac{\kappa_{ph}}{a^2\sigma} + \frac{\kappa_{el}}{a^2\sigma} = \frac{\kappa_{ph}}{a^2\sigma} + \frac{L}{a^2}.$$

α is related to σ by the equation $\alpha = C - \frac{k}{e}\ln\sigma$, whence $\frac{d\sigma}{d\alpha} = -\frac{\sigma}{\frac{k}{e}}$.

By equating $\frac{d\left(\frac{1}{z}\right)}{d\alpha} = 0$, we obtain

$$\alpha_{opt} = 2\frac{k}{e}\left(1 + \frac{\kappa_{el}}{\kappa_{ph}}\right) = 172\left(1 + \frac{\kappa_{el}}{\kappa_{ph}}\right)\ \mu\text{V/deg}. \qquad (40a)$$

At $\kappa_{el} \ll \kappa_{ph}$ this condition reduces to the earlier one, $\alpha_{opt} = 172\ \mu$V/deg.

Both the left hand side (α) and the right hand side (κ_{el}) in equation (40a) depend on concentration n. Therefore this equation should be regarded as a transcendental equation determining the value of n at which $\alpha^2\sigma$ reaches its maximum.

All these formulae relate to non-degenerate electrons. In the presence of degeneracy it is necessary to use expressions (26) and (26a) and to compute the values graphically.

The value of the thermal conductivity of thermocouples is not only important from the viewpoint of efficiency, but also for determining the size of the thermoelectric batteries and for establishing conditions which should be satisfied by thermoelectric refrigerators.

A battery will have the maximum efficiency permitted by its composition when the hot junction temperature T_1 is as high as possible, and the cold junction temperature T_0 as low as possible. These conditions determine the temperature difference $T_1 - T_0$. The lower the thermal conductivity κ, the shorter should be the thermocouple, i.e. the smaller should be the length l (fig. 1, page 36).

The density of the heat flux (q) passing through the thermoelement (thermal energy in watts passing through a section with an area of 1 cm^2) can be expressed in the form:

$$q = \kappa\frac{T_1 - T_0}{l}. \qquad (50)$$

When l is specified it is necessary to ensure a certain value of q and, conversely, when the heat flux density is specified the length of the battery elements l is governed by thermal conductivity κ.

In practical thermoelements, the efficiency of which does not exceed 10%, the bulk of the power delivered by the heat source passes to the cold junctions by thermal conduction. Therefore the power loss from the heat source is primarily governed by the heat flow through the branches of the thermoelement. The electric power delivered by the battery can be represented as ηQ_h, where $Q_h = qS$ (S is the total cross section area of the battery):

$$W = \eta qS = \eta\kappa\frac{T_1 - T_0}{l}S.$$

The power produced by every cm^3 of the battery, i.e. the specific power, is equal to

$$w = \frac{W}{Sl} = \eta\kappa(T_1 - T_0)\frac{1}{l^2}, \qquad (51)$$

or, at a given value of the heat flux q,

$$w = \eta q\frac{1}{l}. \qquad (51a)$$

The lower the thermal conductivity, the shorter should be the thermoelements for a given temperature difference, and the higher should be heat flux density at a given W. As the length l decreases, the specific power increases as l^2, and the heat flux density increases l times.

Finally, thermal conductivity is also of importance for the determination of thermal stresses created in the battery and deformations suffered by it under conditions of non-uniform heating.

Let us denote the temperature coefficient of linear expansion by p. As a result of the temperature difference $T_1 - T_0$ between the hot and cold ends of the battery, their linear dimensions P, which were initially equal, will differ by

$$\Delta P = p(T_1 - T_0)P.$$

When the length of the elements is l, the bending, which each branch of the thermoelement undergoes under the effect of the temperature gradient $\frac{T_1 - T_0}{l}$ is described by the radius of curvature

$$R = \frac{P}{\Delta P}l = \frac{1}{p(T_1 - T_0)}l. \qquad (52)$$

For example, when $p = 2\times10^{-5}$ deg^{-1}, $T_1 - T_0 = 300$°K and $l = 0.6$ cm, then $R = 100$ cm.

As a result of bending, the initially flat surface of the hot junction, fixed at one end, will move at the other end by a distance

$$\Delta l = \frac{P^2}{2R} = P^2\frac{p(T_1 - T_0)}{2l}. \qquad (52a)$$

With the above assumptions, when the width of the battery is $P = 10$ cm, the other end will move away from the plane by a distance $\Delta l = 0.5$ cm,

or when the centre of the battery is fixed its edges will move by 2.5 mm.

When the free bending of the battery is impeded, the stresses generated in the battery may bring about its failure due to cracking. At a given temperature difference $(T_1 - T_0)$ these stresses are the more harmful, the smaller is l and the larger is P.

* * *

So far we have assumed that one branch of the thermoelement consists of a semiconductor with purely hole conductivity and the other with purely electronic conductivity. When free electrons with a concentration of n_- and mobility u_-, and holes with a concentration n_+ and mobility u_+, are simultaneously present in one and the same branch, Pisarenko's formula takes on the following form

$$\alpha = \frac{k}{\sigma}\left\{n_-u_-\left[A + \ln\frac{2(2\pi m_-^* kT)^{3/2}}{h^3} - \ln n_-\right] - n_+u_+\left[A + \ln\frac{2(2\pi m_+^* kT)^{3/2}}{h^3} - \ln n_+\right]\right\}. \quad (53)$$

In the special case of a chemically pure semiconductor without admixtures, when $n_-m_+^{3/2} = n_+m_-^{3/2} = nm^{3/2}$, α becomes

$$\alpha = \frac{k}{\sigma}\left\{(n_-u_- - n_+u_+)\left[A + \ln\frac{2(2\pi m^* kT)^{3/2}}{h^3 n}\right]\right\}.$$

When $n_-u_- = n_+u_+$, then $\alpha = 0$. In general, however, the values of α for semiconductors with a mixed conductivity mechanism are appreciably lower than for impurity semiconductors with current carriers of one sign. Semiconductors in which the ratio u_-/u_+ is very high form an exception. InSb, for example, is known to have $u_-/u_+ > 80$. For such impurity-free semiconductors to possess an adequate concentration n, it is essential that the width of the forbidden zone should not exceed certain limits.

* * *

We have not taken into account in our calculations the Thomson heat generated (or absorbed) by the current in the branches of the thermoelement in which there is a temperature gradient $(T_1 - T_0)/l$.

It should be noted that when the condition for the maximum of $(\alpha^2\sigma)$ is satisfied and α has a constant value of ±172 μV/deg throughout the entire circuit, then the Thomson coefficient $\tau = 0$, and, therefore, the Thomson heat is also equal to zero. When, however, this condition is not satisfied

and $\frac{\partial\alpha}{\partial T} \neq 0$, then, owing to the Thomson heat, α_1 at the hot junction has to be replaced by the mean value

$$\bar{\alpha} = \frac{\alpha_1 + \alpha_0}{2}. \quad (54)$$

It is also necessary to specify with greater precision what is understood by the properties of the materials, κ and ρ, in expression (30), when the temperature T varies. Both κ and ρ are functions of temperature and it is necessary to substitute in equation (30)

$$\kappa\rho = \frac{1}{T_1 - T_0}\int_{T_0}^{T_1}\kappa\rho\,dT.$$

Between the limits $T_0 = 300°K$ and $T_1 = 600°K$, κ changes approximately by a factor of 2 and ρ by a factor of 4 to 5.

$\bar{\kappa}$ should not be regarded as the mean value of κ, but the inverse value of the mean thermal resistance $1/\kappa$, which increases linearly with temperature:

$$\bar{\kappa} = \frac{2}{\frac{1}{\kappa_0} + \frac{1}{\kappa_1}}. \quad (55)$$

It would be erroneous to think that $\bar{\kappa} = \kappa_1$ at the hot junction on the assumption that we are only interested in the loss of heat by thermal conduction from the hot junction of the thermoelements. In reality the temperature gradient at this end $\left(\frac{\partial T}{\partial x}\right)_{T=T_1}$ is not equal to $\frac{T_1 - T_0}{l}$ when κ is a function of T. In the stationary case the temperature gradient is distributed in the branches of the element in such a way that

$$\kappa_1\left(\frac{\partial T}{\partial x}\right)_{T=T_1} = \bar{\kappa}\,\frac{T_1 - T_0}{l}, \quad (56)$$

where $\bar{\kappa}$ is given by expression (55).

In order to determine the mean resistivity ρ entering into expressions for z and η it is necessary to know the law governing the changes of ρ with temperature and temperature distribution along the rod. The latter is governed by the dependence of κ or $1/\kappa$ on T. Since $1/\kappa \propto T$, the temperature distribution along a cylindrical rod may be described by the equations

$$\frac{dT}{T} = C dx, \quad T = T_1 e^{cx}, \quad C = \frac{1}{l} \ln \frac{T_0}{T_1},$$

where x is the distance from the hot junction.

For the majority of semiconductors, temperature dependence of ρ can be expressed in the form $\rho T^{-n} = \text{const}$; then

$$\bar{\rho} = \frac{\int_0^l \rho dx}{l} = \frac{\int_{T_0}^{T_1} \rho(T) \frac{dx}{dT} dT}{l} = \frac{\text{const}}{Cl} \int_{T_0}^{T_1} \frac{T^n}{T} dT = \frac{\text{const}}{Cl} \int_{T_0}^{T_1} T^{n-1} dT,$$

$$\bar{\rho} = \frac{1}{n} \times \frac{\text{const}}{Cl} (T_1^n - T_0^n) =$$

$$= \frac{1}{n} \times \frac{1}{C} \times \frac{\rho_1 - \rho_0}{l} = \frac{1}{n} \ln \frac{T_1}{T_0} (\rho_1 - \rho_0), \qquad (57)$$

and in the general case of an arbitrary function $\rho(T)$

$$\bar{\rho} = \frac{1}{Cl} \int_{T_0}^{T_1} \rho(T) \frac{1}{T} dT = \ln \frac{T_1}{T_0} \int_{T_0}^{T_1} \rho(T) \frac{1}{T} dT. \qquad (57a)$$

Pisarenko's formula describes α as a function of three quantities: m^*, T and n. Experiments show that by introducing impurities into the semiconductor or creating an excess of one of the constituents of the main substance in the lattice, n can be varied within wide limits without significantly affecting the value of m^*.

Impurities may not only alter the carrier concentration but may also affect the sign of the current carriers. When excess or impurity atoms become ionised in the lattice giving up their electrons into the free band they produce electronic conductivity; on the other hand when impurity atoms pick up electrons from the band filled with valence electrons, hole conductivity is produced. Thus, an excess of lead in PbS produces electronic conductivity, and an excess of sulphur, hole conductivity; in both cases the number of current carriers increases. Excess of Mg in the semiconducting alloy Mg_3Sb_2 produces an electronic current flow mechanism,

and an excess of Sb, a hole current flow mechanism; electrical conductivity increases in this process from 10^{-9} to 0.1 and to 1000 $ohm^{-1} \times cm^{-1}$. Excess of oxygen or lack of copper (which amounts to the same thing) in cuprous oxide Cu_2O brings about a sharp increase of hole conductivity from 10^{-9} to 10^{-2} $ohm^{-1} \times cm^{-1}$. In all the examples listed above, atoms with a low ionisation potential, which give up electrons easily in vacuo (such as Mg, Pb), also give up electrons in the crystal, thus raising the concentration of free electrons; atoms of electrically negative elements, which produce negative gaseous ions (such as O, S), become sources of hole conductivity. It may be inferred that we are dealing in these cases with lattices in which ionic bonds predominate.

There exist, however, semiconductors in which an excess of any of its components raises the electrical conductivity, whilst producing carriers of one kind only which are characteristic of the substance. A semiconducting alloy of this type is ZnSb, in which both an excess of Zn and an excess of Sb increase hole conductivity without changing carrier sign. There are several semiconductors, in which - as in ZnSb - the sign of current carriers is always the same, whatever impurities are introduced.

In semiconductors with pure valence bonds, the sign of current carriers introduced by impurities depends on the number of valence electrons in the atom. This, for example, is true for Ge and Si. Here each of the pair of atoms should provide one electron for the chemical bond. When the place of an atom in the main lattice is occupied by an atom of a different chemical nature, the latter should provide as many electrons for bonds with the adjacent atoms as there are in the main atoms in the lattice. When there are more valence electrons in an impurity atom than is required for this purpose, the surplus of electrons passes over into the free zone. When there are not enough valence electrons, they are supplemented by electrons from the filled zone, leaving behind a corresponding number of holes.

In the previously cited example of Ge and Si each atom has four valence electrons, which saturate four valence bonds with adjacent atoms. Elements of groups I, II and III of Mendeleev's periodic system, which have a deficiency of valence electrons, produce hole conductivity, whilst elements of Group V produce electronic conductivity.

It is important to note that this rule is valid only for substitutional impurities which occupy the place of one of the lattice atoms. In the case of interstitial impurities, when the extraneous atoms take up positions within lattice cells and create local lattice defects, the sign of the conductivity depends primarily on whether the impurity atom is electrically positive or negative. In such cases one would expect that the elements

in the first columns would produce electronic conductivity and elements belonging to groups VI and VII hole conductivity (as in the case of ionic compounds).

Finally, an impurity may occupy defect sites and vacancies, which usually occur as a result of different diffusion velocities of the constituents. In such cases the electron mobility usually increases and the sign of conductivity depends on the conditions of binding of the impurity atom.

Admixture of impurity atoms or a departure from the exact stoichiometric composition of the compound also affects other properties of the semiconductor: as a rule the electron and hole mobilities decrease and the thermal conductivity also falls. An impurity providing positive ions reduces the electron mobility, whilst negative ions reduce hole mobility. In all cases the cause is the higher concentration of scattering centres.

If the conditions for electron and phonon scattering were the same, the ratio of the mobility u to the phonon thermal conductivity κ_{ph} would not be affected by the introduction of impurities. In this case $\kappa_{ph}/u = \text{const}$.

In reality, however, as has already been pointed out, the conditions of electron and phonon scattering differ. Under no conditions can κ_{ph} be regarded as directly proportional to u.

Whilst most phonons have a wavelength ranging from one to a few atomic distances and are therefore scattered on all lattice distortions of the order of atomic distances, the wavelength of electronic waves extends over a few tens atomic distances; therefore electrons are scattered on defects of this size only to a small degree.

Fig. 12 shows the thermal conductivity κ_{ph} for PbSe in which various amounts of PbTe have been dissolved. Whereas κ_{ph} in approx. 50% solutions decreases 2.5 times and the free path length of phonons in such solutions does not exceed two lattice constants, the electron mobility does not decrease, or it becomes even higher than in pure PbTe and PbSe.

The ratio κ_{ph}/u in solid solutions is, therefore, particularly favourable for thermoelements.

However, negligible amounts of certain impurities (concentrations of less than 0.1%) reduce the mobility of Ge many times, whilst the lattice component of its thermal conductivity only decreases to a half on the addition of as much as 3% of other impurities, e.g. silicon atoms.

The introduction of various impurities into the semiconductor is the principal method available enabling us to alter semiconductor parameters (α, σ, κ) in the desired direction. It must be remembered, however, that impurities not only increase free charge concentration n, but may also decrease free charge mobility u, so that σ cannot be regarded as proportional to n; in fact σ grows more slowly than n. Introduction of impurities

does not lead only to an increase of the electronic part of thermal conductivity together with σ, but also to a simultaneous decrease of the phonon thermal conductivity. When these circumstances are taken into account, $\alpha^2\sigma$ is found to reach a maximum at thermal emf values slightly different from 172 μV/deg.

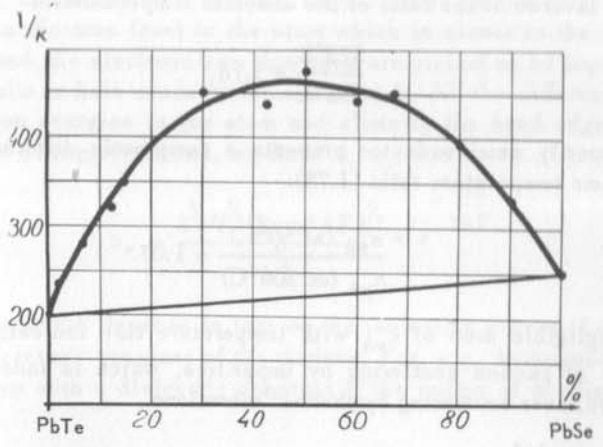

Fig. 12

The presence of impurities in the semiconductor, which affects the electron concentration, mobility, and thermal conductivity at a given temperature, also affects the temperature dependence of these quantities.

Scattering centres introduced by the impurities reduce the thermal conductivity of the semiconductor and slow down the rise of thermal resistance $1/\kappa$ with temperature.

These effects of impurities are well illustrated in fig. 13, which shows the results of measurements of the thermal conductivity κ of both pure lead telluride (curve 1) and lead telluride containing large amounts of impurities (curve 2). Having determined the thermal conductivity and electrical conductivity of both specimens in the temperature range from –40° to 300°C, we could separate the phonon part of thermal conductivity κ_{ph} on the basis of the Wiedemann-Franz law (curves 1a and 2a).

Fig. 13 demonstrates the reduction of the phonon part of thermal conductivity caused by the introduction of impurities. At 50°C κ_{ph} decreases to a half, viz from 25×10^{-3} to 12.2×10^{-3}. It is also found that in the

pure substance κ_{ph} is approximately inversely proportional to absolute temperature.

$$\frac{\kappa_{ph}\ (\text{at } 50^\circ\text{C})}{\kappa_{ph}\ (\text{at } 300^\circ\text{C})} = 1.85,$$

whilst the inverse of the ratio of the absolute temperature is

$$\frac{573^\circ\text{K}}{323^\circ\text{K}} = 1.78.$$

The impurity semiconductor presents a completely different picture. For the same temperature ratio (1.78):

$$\frac{\kappa_{ph}\ (\text{at } 50^\circ\text{C})}{\kappa_{ph}\ (\text{at } 300^\circ\text{C})} = 1.07.$$

Such a negligible drop of κ_{ph} with temperature rise indicates the predominance of phonon scattering by impurities, which is independent of temperature, over scattering by thermal vibrations.

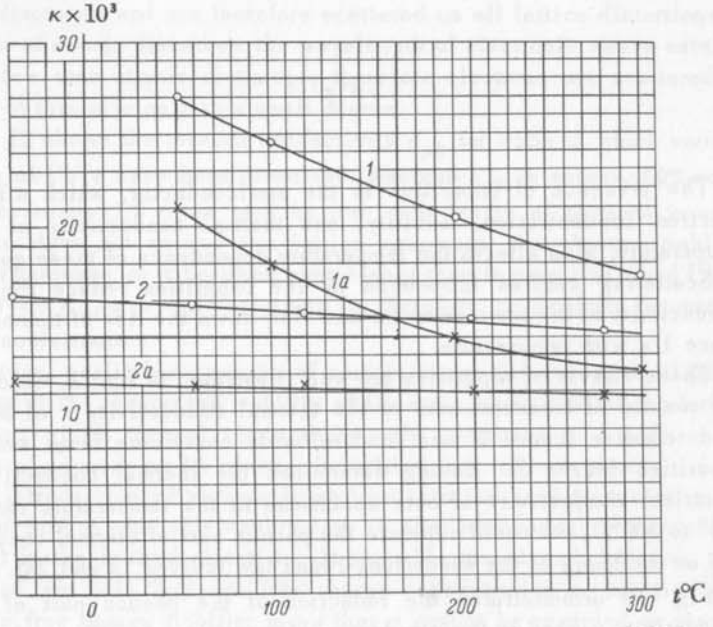

Fig. 13. The effect of impurities on the thermal conductivity of PbTe.

The effect of impurity atoms on the electron concentration n depends on the ionisation energy ΔE in the given substance, in other words on the energy level of the electrons in the atom with respect to the boundary of the forbidden band.

When the energy level of an electron in an atom is close to the conduction band, this leads to electronic conductivity; on the other hand when there is an electron level in the atom which is closer to the edge of the valence band, the electrons from this band are picked up by impurity atoms which results in hole conductivity. Denoting by ΔE the difference between the electron energies in the atom and close to the band edge, and by N the number of impurity atoms, we find

$$n_+ = \frac{2^{1/2} N^{1/2} (2\pi m^* kT)^{3/4}}{h^3} \times e^{-\frac{\Delta E}{2kT}}$$

The energy ΔE depends in turn on the ionisation potential of the atom and the dielectric constant of the medium. For, e.g., hydrogen-like atoms in a medium with a dielectric constant ϵ, the radius of the first quantum orbit is

$$r = 0.535 \times \epsilon \times 10^{-8}\ \text{cm}.$$

When ϵ is of the order of 10 or more, r is appreciably larger than the lattice constant and the medium can be regarded as continuous without introducing a large error. We have then

$$\Delta E = E_0 \times \frac{1}{\epsilon^2} = \frac{13.5}{\epsilon^2}\ \text{eV}.$$

As a rule, interstitial impurities distort the lattice more than substitutional impurities, particularly in the region encompassing the bulk of the electric field of the ion. Therefore, when the above formula is applied to interstitial impurities without modifying the value of ϵ, the resulting value of ΔE is not always accurate.

The temperature dependence of the electronic part of thermal conductivity κ_{el} is given by the Wiedemann-Franz law

$$\kappa_{el} = 1.72 \times 10^{-8} \sigma T.$$

When σ rises with temperature, as happens in semiconductors with a low electrical conductivity, κ_{el} increases with temperature at a steeper rate than T.

In semiconductors with a low resistivity, which are mainly used in the construction of highly efficient thermoelements, n often remains

approximately constant over a wide temperature range, whilst the mobility u decreases with temperature; consequently σ decreases with temperature, this decrease usually being steeper than the increase of T.

In impurity-free substances the mobility decreases with temperature rise according to the law $uT^{3/2} = \text{const}$ or $uT^{5/2} = \text{const}$. When n is constant, κ_{el} decreases with temperature either as $T^{-1/2}$ or as $T^{-3/2}$.

Finally, let us consider the conditions most frequently encountered in semiconductor thermobatteries, when the electrons are produced by impurity atoms. It is possible for the impurities here to be the principal factor governing the scattering of electronic and thermal waves. In comparison with scattering by impurities, which does not vary with temperature, scattering by thermal vibrations, which is proportional to the absolute temperature, then plays a secondary role. Therefore, in such impurity semiconductors, the phonon part of thermal conductivity varies little with temperature (fig. 13). On the other hand, as has already been noted, the temperature dependence of the electronic part of thermal conductivity is governed by the temperature dependence of the product σT.

Electron scattering by ionised impurity atoms increases with decreasing electron velocity, and the mean electron velocity in non-degenerate semiconductors is proportional to T. Therefore the mobility in such semiconductors, when it depends on scattering by ionised impurities (as often happens at low temperatures), increases, and not decreases, with rise of temperature.

The predominance of scattering by ionised impurities has also another important effect on the thermoelectric properties of the semiconductor: the dependence of the free path length l on the kinetic energy ϵ has in this case the form

$$l \propto \epsilon^2 .$$

Therefore the constant term in Pisarenko's formula becomes equal to 4, and the expression for the impurity conductivity for a single type of carrier becomes

$$\alpha = \pm \frac{k}{e}\left[4 + \ln \frac{2(2\pi m^* kT)^{3/2}}{h^3 n}\right].$$

The optimum value of $\alpha = 172\left(1 + \frac{\kappa_{el}}{\kappa_{ph}}\right)\mu\text{V/deg}$ is reached at higher values of n than in the case when the first term in the square bracket is equal to 2.

Introduction of impurities reduces the mobility to a lesser degree than it increases n, so that the electrical conductivity σ at a given value of α is higher and consequently $\alpha^2\sigma$ has also a higher value. Since impurities reduce the phonon thermal conductivity κ_{ph}, the value of $z = \frac{\alpha^2\sigma}{\kappa}$ increases on the introduction of ionised impurities when the number of ions is sufficiently large to govern the mechanism of electron scattering.

Introduction of a large quantity of impurities producing free charges of the same sign frequently raises the carrier concentration to a level at which a degenerate system is formed. As the concentration increases, α decreases; however, in the degeneracy range α decreases with σ less steeply than in the non-degenerate state.

Calculations of the optimum value of α in the case of degeneracy have to be carried out by graphical methods, using tables for the function $F_r\left(\frac{\mu}{kT}\right)$. In the case of advanced degeneracy, when $\frac{\mu}{kT} \gg 2$, the semiconductor can be regarded as a metal with a low concentration of free charges and with r equal to 2. The condition of the minimum of

$$\frac{1}{z} = \frac{\kappa_{ph}}{\alpha^2\sigma} + \frac{L}{\alpha^2}$$

leads in the general case to the differential equation

$$\frac{d\left(\frac{1}{\sigma}\right)}{d\alpha} = \frac{2}{\alpha}\left(\frac{1}{\sigma} + \frac{L}{\kappa_{ph}}\right),$$

where L may range from $2\frac{k^2}{e^2}T$ to $3.3\frac{k^2}{e^2}T$, depending on the extent of degeneracy.

By plotting α as a function of $1/\sigma$, it is possible to find the value of α_{opt} for a given value of L/κ_{ph}.

After having discussed a number of topics related to the selection of materials for thermoelectric power generators, we shall consider now a few specific examples with some numerical results.

As we have seen, the figure of merit of a thermoelement under the selected optimum conditions is governed by the electron mobility and the phonon thermal conductivity in the range $T_1 - T_0$. The total thermal conductivity here always exceeds its electronic part.

Let us assume that for an atomic lattice we have attained the conditions $\alpha = 172\ \mu\text{V/deg}$, $\sigma \approx 4u$, and take the values of 10^{-2} and 2×10^{-2} for κ_{ph}. Further, we shall take $T_0 = 300°\text{K}$. Tables 3 and 4 show the values of z and η for these conditions.

The optimum values of the efficiency η are listed in table 5 for both heat sources with a temperature $T_1 = 373°K$, as well as for very high temperature heat sources ($T_1 = 1800°K$), assuming in all cases that $T_0 = 300°K$, $\kappa_{ph} = 10 \times 10^{-3}$ and $u = 400$ cm²/sec × V.

TABLE 3
THE VALUE OF $z \times 10^3$ AS A FUNCTION OF u AND κ_{ph}

u cm²/sec × V	$\kappa_{ph} \times 10^3$ W/deg × cm	
	10	20
100	1.01	0.54
200	1.78	1.0
400	2.85	1.78
800	4.1	2.8
1000	4.4	4.3
2000	5.5	5.4
10000	6.5	6.2

We shall make numerical calculations for thermoelectric generators on the following assumptions:

1) $T_1 = 370°K$, $T_0 = 300°K$, $\sigma = 1600$ ohm^{-1} × cm^{-1}, $\kappa_{ph} = 20 \times 10^{-3}$, $\kappa_{el} = 7.2 \times 10^{-3}$, $\alpha = 230$ μV/deg, $z = 3.1 \times 10^{-3}$, $\eta = 3.6\%$.

2) $T_1 = 600°K$, $T_0 = 300°K$, $\sigma = 1600$ ohm^{-1} × cm^{-1}, $\kappa_{ph} = 15 \times 10^{-3}$, $\kappa_{el} = 10.8 \times 10^{-3}$, $\alpha = 295$ μV/deg, $z = 5.4 \times 10^{-3}$, $\eta = 18\%$.

In both cases, the attainment of $\alpha = 230$ or 295 μV/deg at an electrical conductivity $\sigma = 1600$ ohm^{-1} × cm^{-1} requires a very high mobility. Unfortunately, there are few known materials with such a mobility, the phonon thermal conductivity of which at room temperature does not exceed 20×10^{-3} W/cm × deg.

TABLE 4
THE VALUE OF η_{opt} (%) AT $T_0 = 300°K$ AS A FUNCTION OF MOBILITY u.

u cm²/sec × V	$\kappa_{ph} \times 10^3$ W/deg × cm			
	10	20	10	20
	$T_1 = 600°K$		$T_1 = 1000°K$	
100	6.1	3.7	12.8	7.7
200	9.2	6.1	18.5	12.8
400	12.6	9.2	24.3	18.5
800	15.8	12.5	26.8	24.3
1000	16.1	13.6	29.5	25.5
2000	18.2	16.3	32.5	29.5
10000	20.0	19.4	34.5	34.2

The following conditions conform more closely to the properties of real materials:

3) $T_1 = 600°K$, $T_0 = 300°K$, $\sigma = 1000$ ohm^{-1} × cm^{-1}, $\kappa_{ph} = 20 \times 10^{-3}$, $\kappa_{el} = 6.5 \times 10^{-3}$, $\alpha = 200$ μV/deg, $z = 1.5 \times 10^{-3}$, $\eta = 8.2\%$.

TABLE 5
η_{opt} (%) AT $T_0 = 300°K$, $z = 2 \times 10^{-3}$ AND $u = 400$ cm²/sec × V AS A FUNCTION OF T_1

T_1°K	373	600	1000	1800
η_{opt}	3.55	12.6	24.3	37.5
$\eta_{thermodynamic} = \frac{T_1 - T_0}{T_1}$	19.5	50.0	70.0	83.0
$\frac{\eta_{opt}}{\eta_{thermodynamic}}$	18.0	25.0	35.0	45.0

In the last case the optimum value of α would have been 225 μV/deg at the same electron mobility, $\sigma = 875$ ohm^{-1} × cm^{-1}, $\kappa_{el} = 6.3 \times 10^{-3}$, $z = 1.7 \times 10^{-3}$, $\eta = 9\%$.

* * *

Let us formulate the conditions for achieving high efficiency. It has been shown that the material should be characterised by as high a value of $z = \alpha^2\sigma/\kappa$ as possible, and be capable of operation up to very high temperatures T_1 of the heat source.

For this purpose:

1. The phonon component of the thermal conductivity of the semiconductors should be as low as possible. This condition should be satisfied by substances with a low Debye temperature, consisting of heavy molecules weakly bound to each other. The value of κ_{ph} can be further reduced by the introduction of impurities and the formation of solid solutions, provided these impurities do not simultaneously reduce the electron mobility by a similar amount.

2. The mobility of current carriers (electrons or holes) should be as high as is compatible with condition 1. The mobility should preferably not be reduced much by the introduction of impurities which raise the electrical conductivity σ. This condition will be best satisfied by atomic or molecular lattices with the predominance of acoustic vibrations in the

thermal spectrum. The mobility can be slightly increased by thorough annealing and in some cases by the introduction of impurity atoms tending to occupy empty lattice sites and reduce any lattice distortion.

3. One of the arms should consist of a purely hole type and the other of a purely electronic type semiconductor. For this purpose semiconductors should be selected which have low ionisation energy ΔE, and a forbidden band of such a width that the concentration should be determined solely by impurity atoms up to the hot junction temperature. Only at high ratios of electron-to-hole mobilities is it possible to employ semiconductors with a narrow forbidden band.

4. The electron concentration throughout the entire element, from the hot junction temperature T_1 to the cold junction temperature T_0, should be so adjusted that the thermal emf $\alpha = 172\left(1 + \frac{\kappa_{el}}{\kappa_{ph}}\right)\mu$V/deg at the temperatures prevailing in the various portions of the element. To satisfy this requirement it is necessary to make the thermoelement arms with a variable impurity content or construct them from several parts. In the low temperature zone the impurity concentration should be lower than in the high temperature zone since the value of α at a given m^* (effective mass of current carriers) is governed by the ratio $T^{3/2}/n$.

5. An important requirement for practical applications of the material is its stability to chemical influences, in particular to oxidation, and good mechanical strength and elasticity are necessary to prevent the thermoelement from cracking under the effect of thermal stresses.

6. In addition to materials suitable for the arms of the thermoelement it is also necessary to find a material for the metallic bridge connecting the arms which should create neither additional electrical resistances at the boundary with the semiconductors, nor additional thermal stresses.

The last two conditions become particularly important when, instead of a single thermoelement, one is considering a pile consisting of a large number of thermoelements. With a thermal emf of 172 μV/deg in each arm and a temperature difference of 300°, each element generates about 0.1 V. Consequently it is necessary to connect, e.g., 1000 elements in series to produce a 100 V pile. Therefore, a flexible bond is required between the couples of the pile and the hot and cold sources in order to avoid damage by thermal stresses.

2.3 Vacuum thermoelements. The low efficiency of semiconductor thermoelements is primarily due to the conduction of heat from the hot junction to the cold junction. Electron scattering in the thermoelement and the transfer of energy, accumulated over a free path length, to the lattice, together with the transfer of thermal energy by heat waves, create an unfavourable relationship between mobility and thermal conductivity.

From this point of view it is of interest to consider a thermoelement based on thermionic emission in vacuo. Such a generator of electrical energy may, e.g., consist of a number of plates kept at a high temperature T_1 and separated by vacuum from another set of plates maintained at a lower temperature T_2. Emission increases so steeply with temperature that even at $T_1 - T_2 > 200°$ the emission of plates at temperature T_2 can be practically neglected in comparison with the emission of the hotter plates. The difference between the kinetic energies in such a system creates an emf of a corresponding magnitude. The current is, however, limited by the space charge; reduction of the space charge is the main problem which has to be overcome in vacuum thermoelectric generators.

Instead of being transferred through lattice heat conduction, the heat will here pass through the vacuum by radiation. Nevertheless, since the emissivity is fully determined by one to two atomic layers, i.e. an outer layer 10^{-7} cm thick, whereas a layer of an order of 0.25×10^{-4} participates in the radiation and reflection of infra-red rays, it is possible to produce surfaces characterised by high electronic emission and low radiation.

The reflection coefficient can be increased to 95-97% and the radiation coefficient can be correspondingly decreased. In this way heat conduction, which is the main source of losses, could be substantially reduced in vacuum electric power generators.

Vacuum generators can obviously operate only at high temperatures, viz $T_1 > 900$°K, whilst there would be no sense in decreasing the temperature T_2 below the limit at which electronic emission substantially decreases.

Taking $T_1 = 1000$°K and $T_2 = 700$°K, the thermodynamic efficiency becomes 30% and the efficiency of the thermopile 10%. The temperature difference from 700° to 300°K could be utilised in a semiconductor thermoelement with an efficiency of, e.g., 10%, thus bringing the total efficiency to 20%.

The power balance of such a device will be found to be favourable as a result of an increase of the efficiency of the thermoelement. Possibilities of practical utilisation of high temperature heat sources in a combination of a vacuum thermoelement with a solid state generator will depend on the specific power output of such a generator, its dimensions and cost, all of which depends to a large extent on the attainable emission current density.

CHAPTER 3

OTHER APPLICATIONS OF THERMOELEMENTS

3.1 Cooling. The problem of the thermoelectric refrigerator is discussed in detail in the section on thermoelectric cooling. We are therefore presenting here only the principal results relating to this application.

Thermoelectric refrigerators utilise the Peltier effect consisting of the generation or absorption of heat at the junction between two conductors when a current is passed through a thermoelectric circuit (fig. 1, p. 36). We shall choose the direction of the current I so that the heat is absorbed from the cooled volume at a temperature T and generated at a room temperature T_0. The power absorbed at the cold junction is then

$$Q = \alpha I T$$

and that generated at the hot junction

$$Q_0 = \alpha_0 I T_0.$$

The Joule heat generated in the thermoelement is

$$W = I^2 r$$

where r is the resistance of both branches of the thermoelement. Half of W proceeds to the hot junction and the other half to the cold junction.

The heat transferred from the hot junction to the cold junction by conduction is

$$Q_h = k(T_0 - T).$$

In addition it is necessary to take into account the power consumed by the current flowing against the potential difference between the hot and cold junctions,

$$Q_p = \alpha I (T_0 - T).$$

The coefficient of performance K is equal to the ratio of the power absorbed by the cold junction to the electrical power consumed by the thermoelement

$$K = \frac{\alpha I T - \frac{1}{2} I^2 r - k(T_0 - T)}{I^2 r + \alpha (T_0 - T) I} \tag{58}$$

As in the case of the thermoelectric generator we shall describe the thermal conductance* of the thermoelement k and its resistance r by the specific parameters for the two branches κ_1 and κ_2, ρ_1 and ρ_2 and the dimensions of the branches S_1 and S_2, $l_1 = l_2 = l$. As in the case of the thermoelectric generator K is maximum when

$$\frac{S_1}{S_2} = \sqrt{\frac{\rho_1}{\rho_2} \times \frac{\kappa_2}{\kappa_1}} \; ;$$

under these conditions

$$kr = (\sqrt{\kappa_1 \rho_1} + \sqrt{\kappa_2 \rho_2})^2.$$

In the expression for K we shall multiply the numerator and denominator by r and replace Ir by V. Dividing the numerator and denominator by V we obtain

$$K = \frac{\alpha T - \frac{1}{2} V - kr(T_0 - T)\frac{1}{V}}{V + \alpha (T_0 - T)}.$$

We shall select the potential difference between the ends of the thermoelement so as to make K maximum. For this purpose we shall equate $\frac{\partial K}{\partial V}$ to zero which gives

$$V_{opt}^2 - \frac{4kr}{\alpha} \times \frac{T_0 - T}{T_0 + T} V_{opt} - 2kr \frac{(T_0 - T)^2}{T_0 + T} = 0,$$

whence

$$V_{opt} = \frac{2kr}{\alpha} \times \frac{T_0 - T}{T_0 + T} \left[1 + \sqrt{1 + \frac{1}{2} z (T_0 + T)} \right].$$

Putting again

$$\sqrt{1 + \frac{1}{2} z (T_0 + T)} = M,$$

we obtain

$$V_{opt} = \alpha (T_0 - T) \frac{1}{M - 1} \tag{59}$$

* In this chapter K is used to denote the coefficient of performance and k the thermal conductance of the thermoelements.

and the value of the coefficient of performance corresponding to this value of V

$$K = \frac{T}{T_0 - T} \times \frac{M - \frac{T_0}{T}}{M + 1} . \tag{60}$$

The maximum temperature drop $(T_0 - T)_{max}$ attainable at a given value of M will be obtained by equating K to zero. In this case we have from (59) $M = \frac{T_0}{T}$ and

$$(T_0 - T)_{max} = \frac{1}{2} z T^2 ; \tag{61}$$

in this case $V_{opt} = aT$ and the power consumption $W = \frac{a^2}{r} T^2 = kzT^2$.

The first multiple in the expression for K represents the thermodynamic efficiency of a reversible Carnot cycle, and the second multiple the reduction of efficiency due to the irreversible processes of thermal conduction and Joule heat generation.

It is easily seen from the expression

$$\frac{1}{K} = \left(\frac{T_0}{T} - 1\right) \frac{M + 1}{M - \frac{T_0}{T}}$$

that the coefficient of performance K decreases (and $\frac{1}{K}$ increases) with increasing $\frac{T_0}{T}$ and, for a given $\frac{T_0}{T}$, with decreasing M, i.e. decreasing value of $\frac{1}{2} z (T_0 + T)$.

Taking for example $z = 2 \times 10^{-3}$, $T_0 = 300°K$, and $\Delta T = 30°K$, we have $M = 1.225$, and $K = 10 \times \frac{0.144}{2.255} = 0.64$.

Since the conditions which have to be satisfied by the material of the thermoelement in order to achieve maximum K can, as previously, be reduced to the maximum value of $z(T_0 + T)$, the selection of materials will be governed by the same considerations as before, except, of course, the effect of temperature on the materials.

Table 6 and fig. 14 give the dependence of the value of K_{opt} on z and the temperature difference $(T_0 - T)$. In addition to the value of $(T_0 - T)_{max}$, following from expressions (59) and (61), table 6 also shows the corresponding values for thermoelectric batteries consisting of two stages arranged

in series $\left(T_0 - \frac{T_0 + T}{2}\right)$ and $\left(\frac{T_0 + T}{2} - T\right)$. It may be shown that, when the coefficients of performance of the individual stages are K_1 and K_2, the overall coefficient of performance for the two stages in series will be

$$K = \frac{1}{\frac{1}{K_1} + \frac{1}{K_2} + \frac{1}{K_1 K_2}} \tag{62}$$

and when $K_1 = K_2$

$$K = \frac{K_1}{2 + \frac{1}{K_1}} .$$

Straightforward calculation shows that the use of two stages increases appreciably the value of K only when $K < 1$. It is in practice useless to increase the number of stages above two.

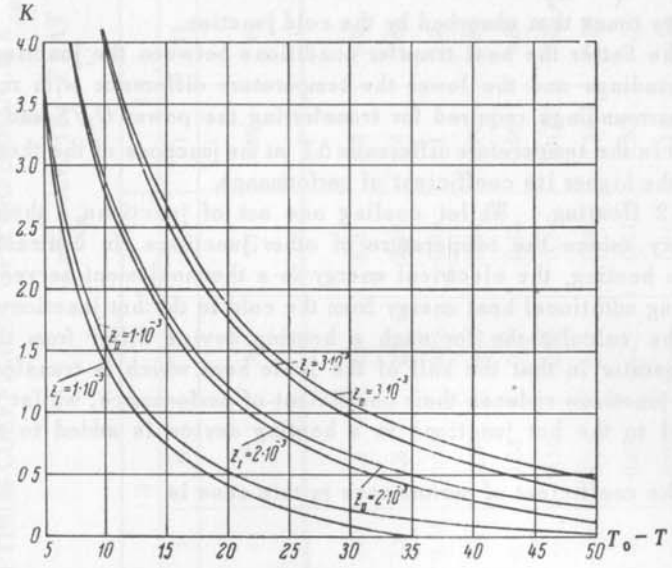

Fig. 14.

When, however, it is intended to achieve the maximum temperature drop without paying attention to energy consumption, each new stage will decrease the temperature by a value somewhat smaller than $T\frac{Tz}{2}$. When z is independent of temperature, the reduction of temperature is proportional to T^2, where T is the final temperature achieved by cooling. Therefore

successive stages will give smaller and smaller temperature drops. When for example $z = 2 \times 10^{-3}$ and $T_0 = 300°K$, the first stage will produce a temperature drop of 59°, the second somewhat less than 40°, the third less than 29°, the fourth less than 22°, etc. The power consumption steeply increases with the increasing number of stages. The maximum temperature drop which may be achieved with a single stage at $z = 2 \times 10^{-3}$ and $T = 100°K$ is only 8.5°.

The main condition governing the efficiency of a cooling device as well as of a generator is the heat flux across the thermopile. In a generator this depends mainly on heat conduction. The amount of heat transferred to the hot junctions is only slightly greater than that removed from the cold junctions. These conditions are somewhat different for a refrigerator: to the power Q_c removed from the cold end of the thermoelectric battery is added electric energy which often considerably exceeds Q_c (it is equal to Q/K), and the energy which has to be removed from the hot junction is $Q_h = Q_c\left(1 + \frac{1}{K}\right)$. When $K = 0.25$ the power removed from the hot junction is five times that absorbed by the cold junction.

The better the heat transfer conditions between the junctions and the surroundings and the lower the temperature difference with reference to the surroundings required for transferring the power Q_h/S and Q_c/S, the lower is the temperature difference ΔT at the junctions of the thermoelement and the higher its coefficient of performance.

3.2 Heating. Whilst cooling one set of junctions, a thermoelectric battery raises the temperature of other junctions. In contrast to direct Joule heating, the electrical energy in a thermoelement serves for transporting additional heat energy from the cold to the hot junctions.

The calculations for such a heating device differ from those for a refrigerator in that the half of the Joule heat which is transferred to the cold junctions reduces their coefficient of performance, whilst that transferred to the hot junctions in a heating device is added to the Peltier heat.

The coefficient of performance in this case is

$$K = \frac{\alpha I T + \frac{1}{2} I^2 r - k(T - T_0)}{I^2 r + \alpha I (T - T_0)} = \frac{\alpha T + \frac{1}{2} V - kr(T - T_0)\frac{1}{V}}{V + \alpha(T - T_0)}.$$

Its maximum is obtained from the condition $\frac{\partial K}{\partial V} = 0$ which gives

TABLE 6

THE OPTIMUM COEFFICIENT OF PERFORMANCE K_{opt} AND $(T_0 - T)_{max}$ AS FUNCTIONS OF $z = \frac{\alpha^2}{\kappa\rho}$ AND $(T_0 - T)$ AT $T_0 = 300°K$

$z \times 10^3$	1.0		1.5		2.0		2.5		3.0		5	
stages	1	II	I	II	I	II	I	II	I	II	I	$\frac{T}{T_0 - T}$
$(T_0-T)_{max}$ / T_0-T	33	60	45	80	56	93	65	106	72	117	100	
5	3.6	3.7	4.9	5.0	6.3	6.3	7.6	7.6	8.9	8.9	12.4	59
10	1.4	1.6	2.2	2.25	2.8	2.85	3.3	3.4	4.1	4.15	6.1	29
20	0.44	0.52	0.83	0.89	1.1	1.2	1.45	1.5	1.8	1.85	2.7	14
25	0.2	0.30	0.55	0.64	0.78	0.86	1.0	1.05	1.3	1.35	2.0	11
30	0.1	0.23	0.33	0.45	0.56	0.65	0.78	0.85	0.96	1.06	1.6	9.0
35	—	0.16	0.21	0.34	0.41	0.50	0.56	0.66	0.74	0.85	1.3	7.6
40	—	0.11	0.12	0.26	0.29	0.38	0.44	0.56	0.58	0.70	1.02	6.5
45	—	0.07	—	0.21	0.20	0.31	0.33	0.44	0.45	0.58	0.84	5.7
50	—	0.03	—	0.15	0.11	0.24	0.22	0.33	0.33	0.47	0.68	5.0

$$V_{opt} = \frac{a(T - T_0)}{M - 1},$$

where $M = \sqrt{1 + \frac{1}{2} z(T_0 + T)}$.

At V_{opt}

$$K = \frac{T}{T - T_0}\left(1 - 2\frac{M - 1}{Tz}\right).$$

At $z = 2 \times 10^{-3}$, $T_0 = 270°$ and $T - T_0 = 30°$, $M = 1.255$, $Tz = 0.6$ we have $\frac{T}{T - T_0} = 10$ and $K = 1.5$.

The values of K_{opt} are tabulated below for various z and $(T - T_0)$. The values of K can be raised by using two stages. With three successive stages, each raising the temperature by $\Delta T/3$, the coefficient of performance is still higher than with two stages, each raising the temperature by $\Delta T/2$. Thus, in raising the temperature by 30° from 300° to 330°K the coefficient of performance is

z	K_I	K_{II}	K_{III}
1×10^{-3}	1.30	1.38	1.46
1.5×10^{-3}	1.40	1.47	1.55
2×10^{-3}	1.65	1.68	1.71

It follows from table 7 that the advantages of thermoelectric heating for general heating purposes become appreciable at $z > 2 \times 10^{-3}$, particularly when the temperature difference between the junctions does not exceed 40°. At $z = 5 \times 10^{-3}$ and $\Delta T = 40°$ only half of the heat is supplied by the electric power fed into the battery; the other half is pumped by the thermoelements from the cold junctions utilising low temperature heat sources, such as water in rivers or pipelines. When $\Delta T = 30°$ the same result is obtained at $z = 3 \times 10^{-3}$.

The smaller ΔT, the greater are the advantages of thermoelectric heating. Thus, e.g., when $z = 3 \times 10^{-3}$ the electric power required to raise the temperature of water by 10° and 5° is, respectively, five and eight times less than that required by conventional electric heaters.

In the case of cooling by a small ΔT, the electric power required to cool by 10° and 5° is, respectively, four and eight times less than that consumed by conventional electrical cooling devices (assuming $z = 3 \times 10^{-3}$).

TABLE 7

THE OPTIMUM COEFFICIENT OF PERFORMANCE K_{opt} AS A FUNCTION OF z AND $T - T_0$ AT $T_0 = 300°K$

$z \times 10^3$	stages / $T - T_0$	1.0		1.5		2.0		2.5		3.0		4		5		10		$\frac{K_{opt}}{K_I}$
		1	II	I	II	I	II	I	II	I	II	I	II	I	II	I		
5		4.9		5.8		7.0		8.3		9.7		11.6		13.6		21		61
10		3.1		3.5		4.0		4.6		5.2		6.2		7.3		10.6		31
15		2.1		2.3		2.7		3.1		3.7		4.4		5.0		7.3		21
20		1.8	1.8	2.1	2.1	2.3	2.3	2.6		3.0		3.6		4.0		5.6		16
25		1.6	1.65	1.75	1.8	2.0	2.05	2.3		2.5		3.1		3.5		4.7		13
30		1.3	1.38	1.4	1.47	1.65	1.68	1.8	1.8	2.15	2.15	2.5	2.5	2.8	2.8	4.0		11
40		1.0	1.25	1.2	1.32	1.45	1.5	1.6	1.7	1.8	1.8	2.1	2.1	2.3	2.3	3.2		8.5
50		1.0	1.18	1.05	1.22	1.25	1.34	1.45	1.5	1.6	1.6	1.8	1.85	2.0	2.05	2.7		7.0

3.3 Measuring techniques. Thermocouples have been used for temperature and radiant energy measurements for many years. Until the last few decades these were the only applications of thermocouples.

Thermal emf's of semiconductors are at least one order of magnitude higher than in metals. Semiconductors may have α reaching 1000 μV/deg, whilst metals give no more than 20 μV/deg, and metal alloys up to 50 μV/deg. Measurement of the temperature difference between the junctions is usually carried out with the aid of a potentiometric scheme in which the current is equal to zero. It would appear that semiconductors would give sensitivities ten times higher. In spite of this, semiconductors have not found a wide practical application in temperature measurement.

Semiconductor resistors - thermistors - are finding increasing application.

Thermopiles acting as radiant energy receivers are made of metal alloys. It has been recently found that some of these alloys are typical semiconductors, although not the best ones by far, either with regard to the thermal emf or efficiency. The sensitivity of a thermopile is governed by the electrical energy generated by the absorbed radiant energy, and to permit the amplification of extremely small radiations it is necessary to use emf's as large as possible.

The conditions for the optimum efficiency are the same as those derived for generators, whilst the requirements for thermopiles feeding an amplifier can be reduced to the attainment of the maximum emf's and are far from having been achieved in available instruments. The rational selection of semiconductor materials would make it possible to increase the sensitivity of thermopiles.

Photoconductors and bolometers are finding an increasing application in practice. In addition, the sensitivity of the available radiant energy detectors is already close to the maximum attainable, which is governed by the noise level. Therefore an increase of their efficiency is of no interest for practical purposes.

The existence of semiconductors with melting points up to 4000°C on the one hand, and technical processes involving very high temperatures, which exceed those which can be withstood by metals, on the other hand, leads us to expect that semiconductor thermocouples will find an increasing application in this temperature range.

The form of semiconductor thermocouples will probably differ from the thin wire construction used in the current metallic thermocouples.

3.4 Sound generators. In chapter 2 mention was made of thermal deformations taking place in a semiconducting plate when a current is passed through it; the plate bends into a spherical shape with a radius

$$R = \frac{l}{p(T_1 - T_2)}$$

where l is plate thickness, p coefficient of linear thermal expansion, and $(T_1 - T_2)$ temperature difference between the two opposite faces of the plate.

In order to calculate this temperature difference we shall consider that an alternating current is passed through the plate, the frequency of the current being such that there will be enough time for the heating of one face and the cooling of the other face to spread to the central plane of the plate, the temperature of which remains constant (since here we are neglecting the Joule heat amounting, in this case, to approximately 1% of the Peltier heat developed at the faces).

Let the current density in the plate be I. The Peltier heat generated and absorbed per 1 sec in a plate with a 1 cm² area is then $Q = \alpha IT$. At a frequency of N c/s the heat generated in a half period is equal to $\frac{1}{2N}\alpha IT$ joules. This energy will heat one half of the plate and cool the other half by

$$\Delta T = \frac{1}{2N}\alpha IT\frac{2}{cl},$$

where c is the specific heat (per cm³);

$$T_1 - T_2 = 2\Delta T = \frac{2}{N}\alpha IT\frac{1}{cl}$$

and

$$R = \frac{N}{2} \times \frac{l^2 c}{p\alpha IT}.$$

We shall put, as an example, $N = 50$ c/s, $l = 10^{-2}$ cm, $c = 2$ joule/cm³, $p = 2 \times 10^{-5}$ deg^{-1}, $\alpha = 2 \times 10^{-4}$ V/deg, $I = 40$ A/cm², and $T = 300$°K; this gives

$$T_1 - T_2 = 4.8°\text{C} \quad \text{and} \quad R \approx 100 \text{ cm}.$$

When the plate is a circular membrane 5 cm in diameter, the amplitude of forced oscillations will in this case be equal to 0.6 mm. Such a membrane may serve as a powerful source of sound waves of the order of 2 W. A membrane 10^{-3} cm thick would generate sound waves with a frequency of 10,000 c/s.

3.5 Crystallisation. Peltier heat $Q = \alpha IT$ is generated or absorbed at the interface between the solid and liquid phases of one and the same conductor, as well as at the boundary between two different substances.

The heat evolved in crystallisation can be removed not only in the usual manner by thermal conduction, but also, through the Peltier effect, by the flow of electrons.

Let us consider the conditions of crystallisation at a boundary with an area of 1 cm² when the melting point is T_0. We shall assume that a current with a density of I A/cm² is supplied to metallic blocks which are good conductors and the temperature of which is maintained at T_0.

We shall denote the specific heat of fusion by q cal/gm $= 4.19q$ joule/gm $= Q$ joule/gm; the density of the solid phase by d gm/cm³; the thermal emf between the solid and liquid phases by α V/deg; the resistivity of the liquid by ρ_1 ohm × cm; the resistivity of the solid phase by ρ_2 ohm × cm; the thickness of the liquid layer by L_1 cm; the thickness of the solid phase by L_2 cm; and the rate of growth of the solid phase by $\frac{\Delta L}{\Delta t}$ cm/sec.

The power developed or absorbed at the boundary is

$$W = \alpha I T_0 - \frac{1}{2} I^2 (\rho_1 L_1 + \rho_2 L_2).$$

Since the temperatures at the boundary between two phases and at the electrodes are equal, there is no doubt that the Joule heat will be equally divided between the electrodes and the boundary. The second term represents, here, the power supplied to the boundary from solid and liquid phases; the first term is the Peltier heat removed by current I, expressed as power.

The power W determines the rate of crystallisation:

$$\frac{\Delta L}{\Delta t} = \frac{W}{Qd} = \frac{\alpha I T_0 - \frac{1}{2} I^2 (\rho_1 L_1 + \rho_2 L_2)}{Qd}.$$

The rate of crystallisation will be a maximum at a current density I_{opt} satisfying the equation

$$\frac{d \frac{\Delta L}{\Delta t}}{dI} = 0$$

or

$$I_{opt} = \frac{\alpha T_0}{\rho_1 L_1 + \rho_2 L_2}.$$

At this value of $I = I_{opt}$

$$\frac{\Delta L}{\Delta t} = \frac{1}{2} \frac{(\alpha T_0)^2}{Qd(\rho_1 L_1 + \rho_2 L_2)}.$$

TABLE 8

	q	d	$\alpha \times 10^6$	T_0	$\rho_2 \times 10^6$	I_{opt} A/cm²	$\left(\frac{\Delta L}{\Delta t}\right)_{I=I_{opt}}$ cm/sec	$\left(\frac{\Delta L}{\Delta t}\right)_{I=100\ \text{A/cm}^2}$
Zn	26	7.1	8	693	20	280	1.0×10^{-3}	0.63×10^{-3} cm/sec = 2.3 cm/hr
Bi	14	9.8	29-62	544	240	110	2.6×10^{-3}	2.5×10^{-3} cm/sec = 9 cm/hr
Cs	4	1.9	10	300	19	150	7×10^{-3}	0.63×10^{-2} cm/sec = 23 cm/hr
Ge*	120	5.5	~100	1250	1300	~100	2.2×10^{-2}	4.5×10^{-3} cm/sec = 16.4 cm/hr at I = 10 A/cm²

* The May 1957 issue of the Journal of Electronics, pp. 597-608, contains a paper by W. G. Pfann, K. E. Benson and J. H. Wernick concerning the use of the Peltier effect for the crystallisation of well-conducting liquids and in particular semiconductors.

However, as the authors of the article themselves point out, their treatment differs substantially from our approach.

I consider the most important advantage of the Peltier effect to consist of the possibility of carrying out crystallisation under isothermal conditions at the melting point. This prevents the appearance of thermal stresses and plastic deformations. It is probably also the only method of preparing perfect crystals by zone melting. The possibility of creating p-n junctions by varying the magnitude or direction of the current was self-evident.

On the other hand, Pfann et al. are mainly interested in this last process. Consequently, there was no need for us to consider the temperature gradient; all that was necessary was to assess the magnitude of the current which would not appreciably affect the constancy of the temperature, whereas in the aforementioned paper it is equally natural to take into account primarily the transport of the Peltier heat along the temperature gradient.

In the Russian edition of this book the value of the thermal emf at the boundary between solid and liquid germanium was listed as $\alpha = 15 \times 10^{-6}$ V/deg. At the time of writing of the book our measurements had not been completed and this value appeared to be the smallest of all the possible ones. It was important to show that even at such low values of α it was possible to attain adequate crystallisation velocities.

The pronounced effect of the plastic deformation of Ge and Si on the value of α impedes its measurement at the melting point. However, when α is determined by extrapolation in the solid and liquid states, the resulting value of $\alpha_{sol} - \alpha_{liq}$ is close to 100 μV/deg. It is this value that is used in the calculations of parameters listed in the last line of table 8.

A. F. Ioffe

July 1957

When $I \ll I_{opt}$ the second term in the expression for W becomes small in comparison with the first term and it is sufficiently accurate to assume that $\frac{\Delta L}{\Delta t} \simeq \frac{aIT_0}{Qd}$. The rate of crystallisation is then proportional to the current density.

Table 8 shows the data for some metals and semiconductors. It is assumed that L_1 and L_2 have such values that $\rho_1 L_1 + \rho_2 L_2 = \rho_2$.

Peltier heat is absorbed or generated with no inertia at the very surface where the crystallisation or melting process takes place, and the Peltier heat input exceeds the Joule heat input up to current densities of several hundreds A/cm². Therefore the current flow under these conditions governs the progress of crystallisation over the entire surface across which the current passes.

For the removal of impurities and the production of very pure substances use is made of so-called zone melting, in which a furnace moved along a cylindrical specimen creates a narrow molten zone slowly progressing along the rod together with the furnace.

The moving furnace can be replaced by passing current through the specimen; the current will continuously fuse the solid rod at one end and crystallise the melt at the same rate at the other end.

The molten zone, without changing its width, will move under the effect of a current, of density I, at a velocity of

$$v = \frac{I}{100}\left(\frac{\Delta L}{\Delta t}\right)_{I=\ 100\ \text{A/cm}^2}$$

as has been calculated previously.

Without listing other possible applications of the Peltier heat for the crystallisation process it may be noted that the Peltier heat presents us with a new method for controlling the crystallisation process under constant temperature conditions.

3.6 Examples of thermoelectric devices. There are still many remote inhabited places in the world where electrical energy is not available. As a rule, in such places, kerosene is used for providing light. A kerosene lamp provides a large amount of heat which may be utilised for producing enough electrical energy for operating a radio receiver or even a transmitter set.

Fig. 15 shows a photograph of a kerosene lamp manufactured in the U.S.S.R. over the glass of which is mounted a tube consisting of thermoelements. The inside of the tube is heated by the hot combustion gases and the outside is cooled with the aid of a set of radiators. The temperature difference created in this way amounts to 250-300°C; this gives a few watts of electrical energy for feeding a radio receiver set.

Fig. 15

Fig. 16 shows a more powerful battery rated at 15-20 W which is mounted on a kerosene burner and used to feed radio transmitters used in agricultural work. Thermoelectric batteries are used in tractors in place of dynamos.

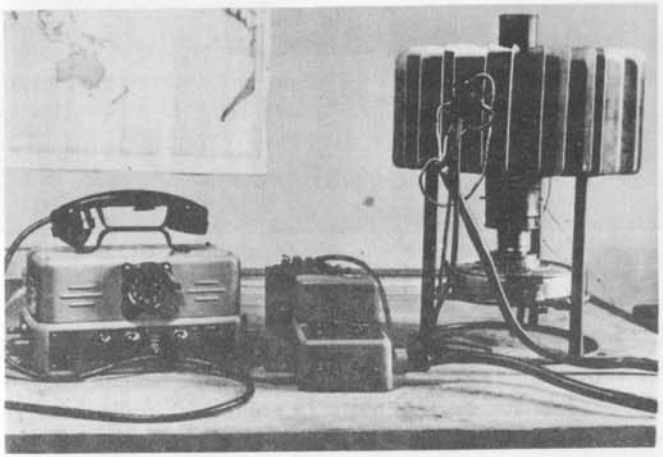

Fig. 16

More powerful generators with capacities of 200 and 500 W are also being manufactured. These generators use all types of fuels (firewood or petrol) and are intended for the far North. A furnace generating 200 W consumes approximately 2 kg of firewood per hour.

There is also an experimental thermoelectric battery in operation generating 100 W, utilising solar energy.

Fig. 17

Cooling devices utilising thermoelements include a water-cooled domestic refrigerator shown in fig. 17. The total weight of semiconductor materials used in its cooling units is around 50 gm and its energy consumption is approximately 50 W.

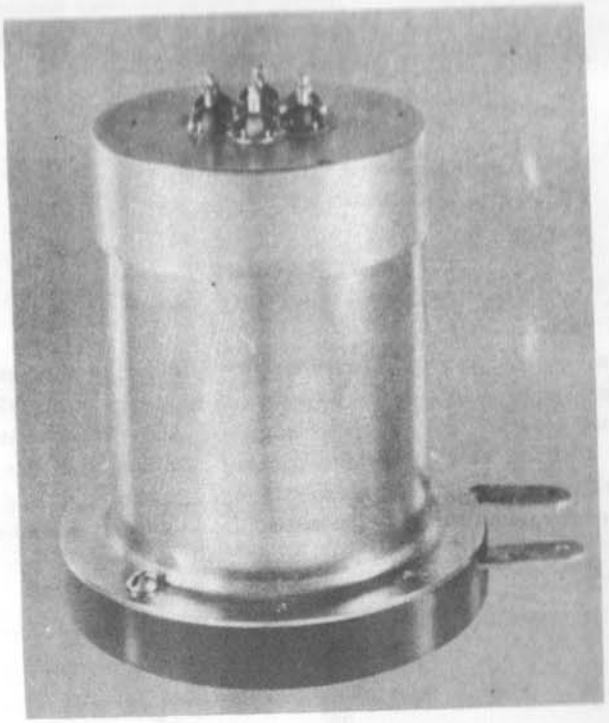

Fig. 18

Fig. 18 shows a thermostatic device for electronic equipment featuring automatic cooling and heating.

APPENDICES

1. Summary of principal formulae for calculating the thermoelectric properties of semiconductors in the presence of a degenerate electron gas. In the most general case, applicable to both a non-degenerate and a degenerate electron gas in semiconductors, the formulae for calculating thermoelectric properties can be written down in the following form.

a. The case of scattering by constant frequency oscillations ($r=-1$):

$$\alpha = \pm\frac{k}{e}\left[(1+e^{-\mu^*})\,F_0(\mu^*) - \mu^*\right],$$

$$\sigma = \frac{16\pi m^* e^2}{3h^3} \times \frac{l_0}{1+e^{-\mu^*}},$$

$$\kappa_{el} = \frac{16\pi m^* l_0}{3h^3}\,k^2T\left[2F_1(\mu^*) - (1+e^{-\mu^*})\,F_0^2(\mu^*)\right],$$

$$A = \left[2F_1(\mu^*) - (1+e^{-\mu^*})\,F_0^2(\mu^*)\right](1+e^{-\mu^*}),$$

$$\frac{\kappa_{el}}{\sigma} = A\left(\frac{k}{e}\right)^2 T,$$

where $\mu^* = \dfrac{\mu}{kT}$ is the reduced chemical potential, $l = \dfrac{l_0}{\epsilon}$ is the free path length, and $F_0(\mu^*)$ and $F_1(\mu^*)$ are Fermi integrals.

The formula for the coefficient in the Wiedemann-Franz law yields the following limiting values: in the classical case $A = 1$; in the case of complete degeneracy $A = \dfrac{\pi^2}{3}$.

In the intermediate case of partial degeneracy A should be calculated from the general expression.

b. The general case contains all forms of scattering in addition to the preceding one:

$$\alpha = \pm\frac{k}{e}\left[\frac{r+2}{r+1} \times \frac{F_{r+1}(\mu^*)}{F_r(\mu^*)} - \mu^*\right],$$

$$\sigma = \frac{16\pi m^* e^2}{3h^3}\,l_0(T)\,(kT)^{r+1}(r+1)\,F_r(\mu^*),$$

$$\kappa_{el} = \frac{16\pi m^* l_0(T)k}{3h^3}(kT)^{r+2}\left[(r+3)\,F_{r+2}(\mu^*) - \frac{(r+2)^2}{(r+1)} \times \frac{F_{r+1}^2(\mu^*)}{F_r(\mu^*)}\right],$$

$$n = 4\pi\left(\frac{2m^*kT}{h^2}\right)^{3/2} F_{1/2}(\mu^*),$$

where $F_r(\mu^*)$ are Fermi integrals of the type $F_r(\mu^*) = \displaystyle\int_0^\infty \frac{x^r\,dx}{e^{x-\mu^*}+1}$, n is the current carrier concentration in the conduction band, and $l = l_0(T)\epsilon^r$ is the free path length.

The Wiedemann-Franz coefficient for the general case is given by the expression

$$A = \left[\frac{(r+3)}{(r+1)} \times \frac{F_{r+2}(\mu^*)}{F_r(\mu^*)} - \frac{(r+2)^2}{(r+1)^2} = \frac{F_{r+1}^2(\mu^*)}{F_r^2(\mu^*)}\right].$$

It can be shown that A has the following limiting values: in the classical case $A = r + 2$; in the case of complete degeneracy $A = \pi^2/3$.

In the case of partial degeneracy use should be made of the general formulae.

Thus, using combinations of these expressions and the tables of Fermi functions listed in Appendix 2, it is possible to calculate theoretically, taking account of degeneracy, the values of the thermoelectric quantities or their combinations in relation to μ^* or the concentration n.

2. Reference tables of Fermi functions. Fermi functions for all the cases of interest are given in the range $\mu^* = -4$ to $\mu^* = 4$. Outside this range at $\mu^* < -4$, formulae for the non-degenerate case will give results not more than 1% in error, and at $\mu^* > 4$ when the electron gas is highly degenerate use can be made of formulae of the quantum theory of metals when the errors will not exceed 1-2%.

In this case, Fermi functions can be approximated by the following expression:

$$\int_0^\infty \frac{f(\epsilon)\,d\epsilon}{e^{\frac{\epsilon-\mu}{kT}}+1} = \int_0^\mu f(\epsilon)\,d\epsilon + \frac{\pi^2}{6}(kT)^2\left(\frac{df(\epsilon)}{d\epsilon}\right)_{\epsilon=\mu} +$$

$$+ \frac{7\pi^4}{360}(kT)^4\left(\frac{d^3 f}{d\epsilon^3}\right)_{\epsilon=\mu} + \ldots$$

μ^*	$F_0(\mu^*)$	$F_{1\frac{1}{2}}(\mu^*)$	$F_1(\mu^*)$	$\frac{2}{3}F_{3\frac{1}{2}}(\mu^*)$	$F_2(\mu^*)$	$F_{5\frac{1}{2}}(\mu^*)$	$F_3(\mu^*)$	$F_4(\mu^*)$
—4	0.018	0.016	0.018	0.016	0.037	—	0.101	0.439
—3	0.049	0.043	0.049	0.044	0.099	0.20	0.298	1.194
—2	0.127	0.115	0.131	0.117	0.266	0.56	0.805	3.231
—1	0.313	0.290	0.339	0.307	0.705	1.43	2.160	8.721
0	0.693	0.678	0.823	0.769	1.803	3.68	5.682	23.340
1	1.313	1.396	1.806	1.774	4.312	8.55	14.390	60.981
2	2.127	2.502	3.513	3.691	9.445	17.60	34.300	159.290
3	3.049	3.977	6.096	6.902	18.870	31.90	75.730	363.690
4	4.018	5.771	9.627	11.752	34.490	—	154.300	814.640

Data for the function $F_{5/2}(\mu^*)$ have been obtained by graphic extrapolation.

Part 2

THERMOELECTRIC COOLING

INTRODUCTION

In 1911 Altenkirch* developed the theory of thermoelectric cooling and derived thermodynamic expressions for the principal parameters of a thermoelectric refrigerator. Altenkirch, basing his considerations on the assumption that metals, which followed the Wiedemann-Franz law, were the best materials for thermoelements - an assumption which was quite natural at the beginning of this century - reached the incorrect conclusion that thermoelectric refrigerators were uneconomical and therefore could not find practical application.

A. F. Ioffe** developed the theory of semiconductor thermoelements in 1949, and showed that, from an economical point of view, semiconductor refrigerators could compete with modern refrigerating machines. A year later work was started at the Laboratory (now Institute) for Semiconductors of the Academy of Sciences of the U.S.S.R. with the aim of checking this theory experimentally. The prototype domestic refrigerator constructed in 1953 had a coefficient of performance of 20% when the temperature inside the refrigerator was 24°C below room temperature.

Thermoelements have now been developed which can produce a temperature drop of more than 60°C, which opens the way for a number of practical applications of thermoelectric cooling. The Institute for Semiconductors of the Academy of Sciences of the U.S.S.R. is working, in conjunction with Institutes representing various branches of industry, on the use of semiconductor thermoelements for cooling and thermostatic control of individual blocks of electronic equipment and special instruments.

Our aim here is to outline the current state of the problem of thermoelectric cooling.

* E. Altenkirch, *Phys. Zs.*, **12**, 920, 1911.

** A. F. Ioffe: "Energeticheskie osnovy termoelektricheskikh batarei iz poluprovodnikov" (Energetic principles of semiconductor thermoelectric batteries), published by the Academy of Sciences of the U.S.S.R., 1949.

CHAPTER 1

THEORY OF THERMOELECTRIC COOLING

1.1 Thermodynamic theory. Thermoelectric generators are based on the use of the Seebeck effect. If the junctions in a circuit consisting of two different conductors are maintained at different temperatures T_1 and T_0, an emf appears in the circuit

$$E = (a_1 - a_2)(T_1 - T_0), \tag{1}$$

where a_1 and a_2 are the thermal emf coefficients of the arms of the thermoelement with reference to some standard material.

Thermoelectric cooling makes use of the reverse phenomenon, namely the Peltier effect. When an external source of emf is connected to such a circuit, heat is generated at one junction and absorbed at the other junction. The amount of heat generated or absorbed in one second is

$$Q_\Pi = \Pi I, \tag{2}$$

where I is the current and Π is the Peltier coefficient, which is related to the thermal emf coefficient by the expression

$$\Pi = (a_1 - a_2)T, \tag{3}$$

where T is the temperature of the corresponding junction.

There also exists a third thermoelectric phenomenon, the Thomson effect, the nature of which is as follows: when there is a temperature drop $T_1 - T_0$ along a conductor through which an electrical current is flowing, then, in addition to the Joule heat, Thomson heat is generated or absorbed within the conductor

$$Q_r = r(T_1 - T_0)I, \tag{4}$$

where r is Thomson coefficient which is related to the thermal emf coefficient by the expression

$$r = T\frac{da}{dT}. \tag{5}$$

We shall first of all assume that in the temperature range T_0 to T_1 the thermal emf coefficient is constant and therefore $r = 0$. We shall also assume that the thermal conductivity and electrical conductivity of the arms of the thermoelement are constant.

When the junction at which heat is generated is maintained at a constant temperature T_0, then the other junction will cool down until the sum of the heat transferred from the surroundings (Q_0) and the heat flowing along the arms of the thermoelement (Q_T) becomes equal to the absorbed Peltier heat. The steady state condition is therefore

$$Q_\Pi = Q_0 + Q_T. \tag{6}$$

The heat flux Q_T reaching the cold junction along the arms of the thermoelement consists of two parts:

1) the heat transferred by thermal conduction

$$Q_t = K(T_0 - T_1), \tag{7}$$

where K is the thermal conductance of the thermoelement arms; and

2) half of the Joule heat generated within the arms of the thermoelement

$$Q_J = \frac{1}{2}I^2R. \tag{8}$$

(It can be readily shown that, irrespective of the value of the temperature gradient, the Joule heat is equally divided between the hot and cold junctions.) Therefore equation (6) can be written down in the form

$$Q_0 = \Pi I - \frac{1}{2}I^2R - K(T_0 - T_1), \tag{9}$$

or

$$T_0 - T_1 = \frac{\Pi I - \frac{1}{2}I^2R - Q_0}{K}. \tag{10}$$

It follows from expression (10) that, under otherwise equal conditions, the temperature difference $T_0 - T_1$ across the thermoelement is a maximum when the cold junction is perfectly insulated thermally ($Q_0 = 0$); when, on the other hand, the cold junction is in thermal contact with an object which is to be cooled (e.g. the internal chamber of a refrigerator cabinet

or some other apparatus), the temperature drop will be smaller. In both cases the thermoelement operates as a refrigerating machine with the electron gas playing the part of the cooling agent.

The principal parameter characterising a refrigerating machine is the coefficient of performance

$$\epsilon = \frac{Q_0}{W}, \tag{11}$$

where Q_0 is the heat removed in unit time from the cooled object and W is the power consumption.

In the case of thermoelectric cooling, the power consumption consists of two parts W_J and W_{th}:

$$W = W_J + W_{th}. \tag{12}$$

W_J denotes the power generated in the arms of the thermoelement, i.e.

$$W_J = I^2 R, \tag{12a}$$

and W_{th} the power required for overcoming the thermal emf, i.e.

$$W_{th} = EI = (a_1 - a_2)(T_0 - T_1)I. \tag{12b}$$

Therefore,

$$W = I[(a_1 - a_2)(T_0 - T_1) + IR] \tag{13}$$

and according to (9), (11), and (13)

$$\epsilon = \frac{(a_1 - a_2)IT_1 - \frac{1}{2}I^2R - K(T_0 - T_1)}{I[(a_1 - a_2)(T_0 - T_1) + IR]}. \tag{14}$$*

It will be seen from expressions (10) and (14) that both the temperature difference across the thermocouple and the coefficient of performance depend on the current I. By equating the derivatives $\frac{\partial(T_0 - T_1)}{\partial I}$ and $\frac{\partial \epsilon}{\partial I}$ to zero we can find the optimum values of the current and the corresponding maximum values of the temperature difference and the coefficient of performance. Straightforward calculations yield the following results:

1) the temperature difference $\Delta T = T_0 - T_1$ reaches its maximum value ΔT_{max} at a current

* See equation (14a) on p. 115.

$$I_m = \frac{(a_1 - a_2)T_1}{R}. \tag{15}$$

When, in addition, $Q_0 = 0$

$$\Delta T_{max} = \frac{(a_1 - a_2)^2}{RK} \times \frac{T_1^2}{2} = \frac{1}{2} zT_1^2, \tag{16}$$

where

$$z = \frac{(a_1 - a_2)^2}{RK}; \tag{16a}$$

2) the coefficient of performance ϵ reaches its maximum value for a current of

$$I_0 = \frac{(a_1 - a_2)(T_0 - T_1)}{\left(\sqrt{1 + \frac{1}{2}z(T_0 + T_1)} - 1\right)R}$$

and for a potential difference over the thermoelement of

$$\left.\begin{aligned} v_0 &= I_0 R + (a_1 - a_2)(T_0 - T_1), \\ \text{or} \quad v_0 &= \frac{(a_1 - a_2)(T_0 - T_1)\sqrt{1 + \frac{1}{2}z(T_0 + T_1)}}{\sqrt{1 + \frac{1}{2}z(T_0 + T_1)} - 1}, \end{aligned}\right\} \tag{18}$$

whence

$$\epsilon_0 = \frac{T_1}{(T_0 - T_1)} \times \frac{\sqrt{1 + \frac{1}{2}z(T_0 + T_1)} - \frac{T_0}{T_1}}{\sqrt{1 + \frac{1}{2}z(T_0 + T_1)} + 1}. \tag{19}$$*

For the sake of simplicity we shall assume initially that both arms of the thermoelement possess equal thermal conductivities ($\kappa_1 = \kappa_2 = \kappa$), equal electrical conductivities ($\sigma_1 = \sigma_2 = \sigma$), and equal, but opposite, thermal emf coefficients ($|a_1| = |a_2| = a$). We shall also assume that the cross-

* See equation (19a) on p. 115.

section areas of the elements S_1 and S_2 and their lengths l_1 and l_2 are equal: $S_1 = S_2 = S$; $l_1 = l_2 = l$.

Under these conditions, assuming for the moment that α, σ, and κ are independent of temperature, we have

$$z = \frac{\alpha^2\sigma}{\kappa}. \tag{20}$$

Expressions (16) and (19) show that, under prescribed operating conditions (T_0 and T_1), the coefficient of performance and the maximum temperature drop depend only on the value of z, which describes the quality of the thermoelement; with increasing z the coefficient of performance tends towards its upper limit:

$$\epsilon_{max} = \frac{T_1}{T_0 - T_1}, \tag{21}$$

i.e. to the coefficient of performance of an ideal thermodynamic machine.

We should, therefore, investigate the conditions under which z reaches its maximum value.

1.2 **Conditions for maximum efficiency of the thermoelements.** The properties of the substance which enter into the expression for z (the thermal emf coefficient α, the electrical conductivity σ, and the thermal conductivity κ) are not independent of each other; they are all functions of the concentration of free electrons (or holes) n. This relationship is shown qualitatively in fig. 1. The electrical conductivity σ is roughly

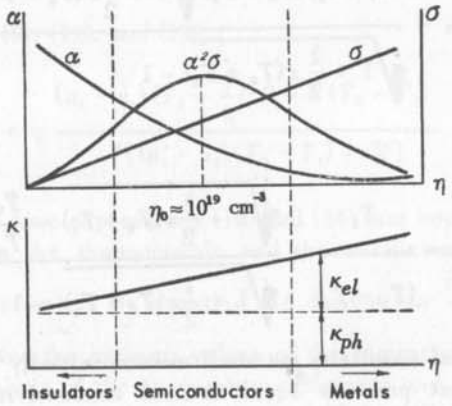

Fig. 1

proportional to the carrier concentration n. The thermal emf α, on the other hand, tends to zero with an increase of the number of carriers, and increases indefinitely as the carrier concentration decreases.

The thermal conductivity κ is the sum of a lattice thermal conductivity κ_{ph} and an electronic thermal conductivity κ_{el}:

$$\kappa = \kappa_{ph} + \kappa_{el}; \tag{22}$$

to a first approximation κ_{ph} is independent of n, whilst κ_{el} is proportional to n.

It is seen from fig. 1 that the numerator of the expression for z has a maximum at carrier concentrations of the order of 10^{19} cm^{-3}, i.e. approximately 1000 times smaller than the free electron concentration in metals. The part played by the electronic thermal conductivity is then relatively small in comparison with the lattice thermal conductivity and, therefore, the maximum of the expression for z is only very slightly shifted from the maximum of $\alpha^2\sigma$ towards lower electron concentrations. The value of z for insulators is small owing to their negligible electrical conductivity, and for metals and alloys owing to their very low thermal emf coefficient.

These qualitative considerations explain the reason why the efficiency of metallic thermocouples is very low and why, consequently, thermoelectric generators and refrigerators have not yet found wide technical applications. By using semiconducting substances as materials for the branches of the thermoelements and by a suitable selection of their carrier concentration it is possible to increase the efficiency of thermoelements by tens of times.

In order to formulate these qualitative considerations quantitatively we ought to use expressions for the thermal emf coefficient, electrical conductivity, and thermal conductivity derived from the quantum theory.

We are giving below the most general expressions for the thermal emf coefficient α, the electrical conductivity σ, the thermal conductivity κ, and the free carrier concentration n which are valid both for semiconductors and metals*. All these quantities are expressed as functions of the reduced chemical potential μ^*:

$$\mu^* = \frac{\mu}{kT}, \tag{23}$$

where μ is chemical potential, and k the Boltzmann constant. There is no need for deriving the relevant expressions here; the reader will find them

* A. G. Samoilovich and L. L. Korenblit, *Usp. Fiz. Nauk*, 57, No. 4, 578, 1955.

in several textbooks, monographs, and articles. We reproduce these formulae in their exact form:

$$\alpha = \pm\frac{k}{e}\left[\frac{r+2}{r+1}\times\frac{F_{r+1}(\mu^*)}{F_r(\mu^*)}-\mu^*\right], \tag{24}$$

$$n = \frac{4\pi(2mkT)^{3/2}}{h^3}F_{1/2}(\mu^*), \tag{25}$$

$$\sigma = \frac{16\pi m l_0(T)e^2}{3h^3}(kT)^{r+1}F_r(\mu^*), \tag{26}$$

$$\kappa_{el} = \frac{16\pi m l_0(T)(kT)^{r+2}}{3h^3}\left[(r+3)F_{r+2}(\mu^*)-\frac{(r+2)^2F_{r+1}^2(\mu^*)}{(r+1)F_2(\mu^*)}\right]. \tag{27}$$

We use here the following notation:

1) l is the electron free path length, which depends on the energy ϵ of the electron and the temperature; in the general case this dependence has the form

$$l = l_0(T)\epsilon^r, \tag{28}$$

where r is an exponent which depends on the electron scattering mechanism (for atomic lattices $r = 0$; for ionic lattices below the Debye temperature $r = \frac{1}{2}$ and above the Debye temperature $r = 1$; for scattering by impurity ions $r = 2$);

2) $F_{1/2}(\mu^*)$, $F_2(\mu^*)$, etc. are Fermi integrals:

$$F_r(\mu^*) = \int_0^\infty x^r f dx, \tag{29}$$

where $x = \frac{\epsilon}{kT}$ is the reduced kinetic energy, and f is the Fermi distribution function

$$f = \frac{1}{e^{x-\mu^*}+1}. \tag{30}$$

Fermi integrals are available in tabulated form* and the problem of finding μ^* corresponding to the maximum value of z can be solved numerically. There exists, however, another much more convenient method of solving this problem.

If it is assumed that the optimum μ^* lies within the range of carrier concentrations for which classical statistics are still valid (i.e. $\mu^* < -2$), then the expressions for the electrical conductivity, thermal conductivity, and thermal emf coefficient are considerably simplified. In this case μ^*, α, σ, and κ_{el} can be explicitly expressed as functions of carrier concentration n:

$$\mu^* = -\ln\frac{2(2\pi mkT)^{3/2}}{h^3 n}, \tag{31}$$

$$\alpha = \pm\frac{k}{e}(r+2-\mu^*) = \pm\frac{k}{e}\left[r+2+\ln\frac{2(2\pi mkT)^{3/2}}{h^3 n}\right], \tag{32}$$

$$\sigma = enu, \tag{33}$$

$$\kappa_{el} = (r+2)\left(\frac{k}{e}\right)^2 T\sigma. \tag{34}$$

If the condition $\frac{\partial z}{\partial n} = 0$ in fact gives $\mu^* < -2$, then this assumption will be substantiated.

When the above approximate formulae are substituted in the expression for z, then the condition $\frac{\partial z}{\partial n} = 0$ gives a transcendental equation for determining the optimum carrier concentration; this equation can be solved graphically or by the method of successive approximations.

Before solving it we shall make one further simplification by assuming that, at the optimum carrier concentration, the electronic thermal conductivity is small as compared with the lattice thermal conductivity (which, in general, follows from the graphical solution). If this assumption is correct then it is permissible as a first approximation to regard the thermal conductivity as independent of the carrier concentration and seek the maximum of the numerator in the expression for z and, then, to introduce corrections by the method of successive approximations.

* O. Madelung, *Zs. f. Naturforsch.*, 9a, Nos. 7-8, 667, 1954.

In this form the solution of the problem is extremely simple. From (32) and (33)

$$\alpha^2\sigma = \left(\frac{k}{e}\right)^2 \left[r + 2 + \ln \frac{2(2\pi mkT)^{3/2}}{h^3 n}\right]^2 enu.$$

The condition

$$\frac{\partial \alpha^2\sigma}{\partial n} = 0 \tag{35}$$

yields two solutions. One,

$$r + 2 + \ln \frac{2(2\pi mkT)^{3/2}}{h^3} = 0, \tag{35a}$$

corresponds to the minimum value of $\alpha^2\sigma$, and the other is

$$r + 2 + \ln \frac{2(2\pi mkT)^{3/2}}{h^3 n} = 2, \tag{35b}$$

or

$$\ln \frac{2(2\pi mkT)}{h^3 n} = r, \tag{35c}$$

or

$$\mu^* = r. \tag{35d}$$

Hence the optimum thermal emf is

$$\alpha_0 = 2\frac{k}{e} = 172\ \mu\text{V/deg}, \tag{36}$$

the optimum concentration,

$$n_0 = \frac{2(2\pi mkT)^{3/2} e^r}{h^3}, \tag{37}$$

and the maximum value of z,

$$z = 1.2 \times 10^{-7} \frac{\mu}{\kappa_{ph}} \left(\frac{m}{m_0} \times \frac{T}{T_0}\right)^{3/2} e^r, \tag{37a}$$

where m_0 is the free electron mass and T_0 is room temperature, equal to 293°K. (The subscript zero refers, here and further on, to values of α, σ, and n corresponding to the maximum value of $\alpha^2\sigma$.) We shall now introduce corrections taking account of the dependence of the total thermal conductivity (expression (22)) on the carrier concentration.

According to expressions (32), (33), (34), and (22)

$$z = \frac{\alpha^2\sigma}{\kappa_{ph} + \kappa_{el}} = \frac{k^2 u}{e\kappa_{ph}} \times \frac{(A - \ln n)^2 n}{1 + Bn}, \tag{38}$$

where

$$A = r + 2 + \ln \frac{2(2\pi mkT)^{3/2}}{h^3} \tag{39}$$

and

$$B = \frac{(r+2)\left(\frac{k}{e}\right)^2 Tue}{\kappa_{ph}}. \tag{40}$$

As has been mentioned earlier, the condition $\frac{\partial z}{\partial n} = 0$ yields a transcendental equation for determining the optimum value of n, which will be denoted by n_1:

$$\ln n_1 = \ln n_0 - 2Bn_1, \tag{41}$$

or

$$\ln\left(1 + \frac{n_1 - n_0}{n_0}\right) = -2Bn_1. \tag{41a}$$

Since, even for $n = n_0$, $Bn_0 = \frac{\kappa_{el}}{\kappa_{ph}}$ is usually less than unity, we are entitled to expand the left hand side of expression (41a) into a series

and confine ourselves to the first term in the expansion (the error in doing this will not exceed a few percent); hence

$$\frac{n_1 - n_0}{n_0} \approx -2Bn_1$$

and

$$n_1 \approx \frac{n_0}{1 + 2Bn_0}. \tag{42}$$

Equation (41) can be solved exactly by a graphical method. For this purpose it is most convenient to rewrite it, using equation (32), in the following form

$$\alpha_1 = \alpha_0 + 2\frac{k}{e} \times \frac{\kappa_{el}}{\kappa_{ph}} = 172(1 + Bn_1). \tag{43}$$

By plotting α from equation (32) and the right hand side of expression (43) as functions of n, we can find n_1 as the abscissa of the point of intersection of these curves.

Obviously, the correction will be the greater, the higher the ratio of mobility to lattice thermal conductivity.

All the foregoing calculations are based on the approximate expressions (32) and (33) which are valid only for a non-degenerate electron gas. We shall not consider in detail the corrections on taking degeneracy into account, since, as we have already mentioned, a solution cannot be obtained in this case in a simplified general form.

All the calculations were also carried out by Bok* using the exact expressions (24), (26), and (27). It was found that the optimum value of the thermal emf varied within the range from 150 to 400 μV/deg, depending on the mechanism of carrier scattering, i.e. the exponent r in the expression for the free path length (28), and the ratio of electron mobility to lattice thermal conductivity.

Such great deviations from expression (36) should not cause any surprise. In fact, according to (35d) the approximate theory yields for the optimum conditions $\mu^* = r$, i.e. $\mu = 0$ for an atomic lattice, $\mu^* = +\frac{1}{2}$ for an ionic lattice at temperatures below the Debye temperature and $\mu^* = +1$ at temperatures above the Debye temperature. For scattering by impurity ions $\mu^* = +2$.

Therefore the optimum value of μ^* is found to be, in all cases, outside the limits of applicability of classical statistics ($\mu^* > -2$) on which the foregoing approximate theory is based. This unfortunate situation is alleviated by the following two circumstances:

1) expression (32) for the thermal emf derived by Pisarenko for a non-degenerate electron gas ($\mu^* < -2$) gives reasonably accurate values of the thermal emf even in the case of relatively high degeneracy, as has been demonstrated by Kontorova*; this is because the deviations of numerical values of the first term in the expression (24) for the thermal emf,

$$\frac{r+2}{r+1} \times \frac{F_{r+1}(\mu^*)}{F_r(\mu^*)},$$

and the second term, μ^*, from the approximate values,

$$\frac{r+2}{r+1} \times \frac{F_{r+1}(\mu^*)}{F_r(\mu^*)} \approx r + 2$$

and

$$\mu^* \approx \frac{2(2\pi mkT)^{3/2}}{h^3 n}$$

tend to compensate each other;

2) in the vicinity of the maximum, the figure of merit of the thermoelement z is a quadratic function of $n - n_0$; therefore, as has been shown by calculations, deviations of 50% from the optimum concentration n_0 reduce the value of z by only 6%.

Consequently, conditions (36) and (37) for α_0 and n_0 are not critical and the foregoing expressions are sufficiently accurate for qualitative analysis, and in the majority of cases also for quantitative calculations; our subsequent considerations will therefore be based on these equations.

According to expression (37a) the figure of merit of the thermoelement is proportional to the ratio of carrier mobility to lattice thermal conductivity. From expression (37) we find that z has a maximum at a certain carrier concentration.

The foregoing analysis implies, therefore, that the development of materials for the arms of the thermoelement can be reduced to the solution of two basic problems:

1) finding materials with maximum ratios of current carrier mobility to lattice thermal conductivity and methods of obtaining a further increase of this ratio;

2) creating in these materials carrier concentrations satisfying condition (37).

* B. I. Bok, Unpublished Report. Institute for Semiconductors of the U.S.S.R. Academy of Sciences.

* T. A. Kontorova, *Zhur. Tekh. Fiz.*, 24, No. 7, 1291, 1954.

From expression (37a) one might also conclude that the figure of merit of the thermoelement increases with increasing effective mass, exponent r in the expression for the electron free path length, and temperature. Such a conclusion would, however, be premature. The reason is that the carrier mobility u entering into expression (37a) also depends to a large extent on these three factors.

The theoretical dependence of mobility on temperature and effective mass has the following form:

a) for atomic lattices

$$u = a_1 m^{-5/2} T^{-3/2}; \tag{44}$$

b) for ionic lattices at temperatures below the Debye temperature

$$u = a_2 m^{-3/2} e^{\theta/T}, \tag{45}$$

and at temperatures above Debye temperature

$$u = a_3 m^{-3/2} T^{-1/2}; \tag{46}$$

c) for scattering by impurity ions

$$u = a_4 m T^{3/2}. \tag{47}$$

Comparison of expression (37a) with (44), (45), (46), and (47) demonstrates that for atomic lattices z is inversely proportional to effective mass, for ionic lattices it is independent of effective mass, and for scattering by impurity ions z increases with increasing effective mass;

d) finally, in recent times a wide class of substances has been investigated, the binding in which has an intermediate character between atomic, ionic, and metallic; the temperature dependence of the mobility for these substances is given by the formula

$$u = a_5 T^{-3}, (5/2) \tag{48}$$

(the dependence of mobility on effective mass for this class of substances has not yet been established). It has not yet been found to be theoretically possible to estimate the value of the constant a which enters the expression for the mobility; it can only be stated that mobility in atomic lattices is tens and even hundreds of times higher than in purely ionic lattices; therefore substances with an ionic lattice are not good materials for thermoelements and we shall not consider them any further.

Considerable experimental material, collated and systematised by Zhuze* shows that the mobility is highest in substances in which the bonds are of an intermediate character between atomic and metallic. These substances which include several intermetallic compounds and some materials grouped under (d) are the most suitable materials for thermoelements.

The introduction into the lattice of impurity ions, which become additional scattering centres for electrons, always reduces the mobility. However, at the same time the value of the exponent r increases (e.g. from 0 to 2 in an atomic lattice) and therefore according to equation (32) the thermal emf also increases. Therefore, an introduction of a measured amount of impurities may bring about an increase in $\alpha^2\sigma$ in spite of the attendant drop in mobility. Preliminary experiments in this direction have not so far yielded positive results.

In order to derive the temperature dependence of z from expression (37a), we must take into account the temperature dependence of the thermal conductivity. Leaving aside the case of temperatures below the Debye temperature, which have not yet found any practical applications, we find that the thermal conductivity κ_{ph} is inversely proportional to temperature in the case of scattering of phonons by phonons (ideal lattice) and is independent of temperature in the case of scattering of phonons by lattice defects. Both these laws have been confirmed by investigations carried out by E. D. Devyatkova and P. V. Gul'tyaev of the Institute for Semiconductors.

TABLE 1

	Ideal lattice ($\kappa_{ph} \propto T^{-1}$)	Imperfect lattice (κ_{ph} = const)
Scattering by impurity ions $u \propto T^{3/2}$	$z \propto T^4$	$z \propto T^3$
Atomic lattice $u \propto T^{-3/2}$	$z \propto T$	z = const
Substances belonging to group (d) (see p. 108) $u \propto T^{-3}$	$z \propto T^{-1/2}$	$z \propto T^{-3/2}$

* V. P. Zhuze, *Zhur. Tekh. Fiz.*, 25, No. 12, 2079, 1955.

Thus the temperature dependence of z may have the forms shown in table 1.

In substances belonging to group (d) z rises with decreasing temperature; this class of substances is therefore the most suitable for very low temperature cooling.

As follows from expression (37), the optimum concentration of electrons at which z reaches its maximum value is a function of temperature:

$$n_0 \propto T^{3/2}.$$

Therefore carrier concentration should be made to correspond to the working temperature range. From this point of view the most suitable material for thermoelements would be such a substance in which n would depend on temperature according to the law (37), as a result of which the thermal emf coefficient would retain its optimum value ($\alpha = 172\ \mu V/deg$) over a wide temperature range. Such substances, however, do not exist in nature.

In addition to conventional semiconducting materials, in which the carrier concentration is an exponential function of temperature, several other substances have recently been investigated in which the carrier concentration remains constant over a wide temperature range.* These substances may serve as materials for semiconductor thermoelements since they satisfy conditions (36) and (37) better than conventional semiconductors. Conditions (36) and (37) can be exactly satisfied over a wide temperature range by making the arm of the thermoelement from a range of materials or from a single material with a varying impurity concentration.

In order to attain the maximum of $z = \alpha^2\sigma/\kappa$ we ought to satisfy conditions at which the lattice thermal conductivity of the substance is a minimum. As yet there is no exact theory of thermal conductivity or sufficient experimental data to permit a straightforward answer to this problem. A. F. Ioffe's qualitative theory leads, however, to the following conclusions:

* In these substances the activation energy of impurity centres decreases steeply with increase of their concentration and becomes equal to zero at $N = 10^{18}$ to 10^{19} cm^{-3}. Consequently all impurity centres become ionised even in the vicinity of the absolute zero and the carrier concentration n remains constant ($n = N$) up to temperatures at which intrinsic conductivity appears. The theory of such substances, known as semi-metals, was developed by K. S. Shifrin (see A. G. Samoilovich and L. L. Korenblit, *Usp. Fiz. Nauk*, 57, No. 4, 578, 1955).

1) According to experimental data the thermal conductivity of an ideal crystalline lattice at temperatures above Debye temperature is proportional to T^{-1}, i.e. to the sensible heat of the crystal. It may therefore be inferred that the thermal conductivity of various substances at a given temperature is also governed by the sensible heat, and consequently decreases with decreasing Debye temperature.

$$\theta \propto \sqrt{\frac{f}{M}}, \tag{49}$$

where M is the mass of atoms or ions forming the lattice and f is the elastic binding coefficient. Therefore, the thermal conductivity would be expected to be minimum in crystals, consisting of heavy atoms or ions, with a low Young's modulus.

2) The finite free path length of phonons is a consequence of the anharmonicity of the atomic and ionic vibrations; the larger the amplitude of vibration the greater is the degree of anharmonicity. Furthermore, for a given sensible heat, the lattice thermal conductivity decreases with increasing anharmonicity factor in the expression for the elastic deformation of the lattice. From the macroscopic viewpoint, anharmonicity manifests itself in thermal expansion of the lattice. Therefore, the minimum thermal conductivity can be expected to occur in crystals with a large thermal expansion coefficient.

3) In non-degenerate semiconductors, the wavelength of electronic waves, at room temperature, λ_{el}, is tens of times larger than the interatomic distance ($\lambda_{el} \approx 10^{-6}$ cm), whereas most of the normal lattice vibrations occur at a wavelength λ_{ph}, which is of the order of the lattice constant ($\lambda_{ph} \approx 10^{-8}$ cm). This difference between λ_{el} and λ_{ph} makes it possible to create non-homogeneities in the crystal lattice which are effective in scattering phonons but which virtually do not scatter electron waves, i.e. do not reduce the carrier mobility. Such non-homogeneities can, in particular, be produced by the introduction into the lattice of neutral impurity atoms or by the formation of solid solutions based on chemical compounds crystallising in similar lattices.

1.3 **Taking account of the Thomson heat in the energy balance of the thermoelement.** It follows from equations (36) and (37) that the best materials for thermoelements are those in which the thermal emf coefficient is constant:

$$\alpha = 2\frac{k}{e} = 172\ \mu V/deg,$$

whilst the carrier density varies according to the law

$$n = AT^{3/2}.$$

In the theory presented in the preceding paragraph we have considered the ideal conditions at which

$$r = T\frac{d\alpha}{dT} = 0.$$

As has been mentioned earlier, the materials actually used for the arms of thermoelements are usually semi-metals, i.e. substances in which the carrier concentration is constant and the thermal emf, according to equation (32), rises with rising temperature. In this case the Thomson coefficient is different from zero, and according to equations (5) and (32) can be written in the form

$$r = \frac{3}{2} \times \frac{k}{e} = 129\ \mu\text{V/deg}. \tag{50}$$

We should now take into account the effect of the Thomson heat on the heat balance of the thermoelement. This effect will manifest itself primarily in a redistribution of temperature along the arms of the thermoelement. Until now we have assumed that the temperature gradient along the arms of the thermoelement is constant and, therefore, that the density of the heat flux towards the cold junction of the thermoelement can be expressed by the formula

$$Q_h = \kappa \frac{T_0 - T_1}{l}. \tag{51}$$

The effect of Joule heat on the temperature distribution has been taken into account approximately by assuming that half of it proceeds towards the hot junction of the thermoelement and half towards the cold junction.

In order to solve this problem more rigorously, it is necessary to find the temperature distribution along the arms of the thermoelement, taking into account both the Joule and Thomson heats, and then find the density of the heat flux from the exact expression

$$Q_h = -\kappa \nabla T. \tag{52}$$

Let the x axis be directed along the arms of the thermoelement and let the origin coincide with the cold junction of the thermoelement; equation

(52) will now take on the following form

$$Q_h = -\kappa\left(\frac{dT}{dx}\right)_{x=0}. \tag{52a}$$

In order to calculate Q_h from equation (52a), we must know the temperature distribution along the arms of the thermoelement

$$T = f(x).$$

As before, we shall neglect the temperature dependence of the thermal conductivity and the electrical conductivity, and replace the true values of these parameters as functions of temperature by average values in the working temperature range. In a thermoelectric generator, both electrons and holes move from the hot junction towards the cold junction; in addition to the Joule heat, Thomson heat is also generated in the entire volume of the thermoelement arms. In a thermoelectric refrigerator the electrons and holes move in the opposite direction and therefore the Thomson heat has to be deducted from the Joule heat. Consequently, the steady-state condition for a unit volume of a thermoelement arm will in this case have the form

$$\kappa\frac{d^2T}{dx^2} - rj\frac{dT}{dx} + j^2\rho = 0. \tag{53}$$

The solution of the differential equation (53), taking account of boundary conditions ($T = T_1$ at $x = 0$, and $T = T_0$ at $x = l$), has the form

$$T = T_1 + \frac{T_0 - T_1 - \dfrac{w_\rho}{w_r}l}{1 - e^{\frac{w_r}{\kappa}l}}\left(1 - e^{\frac{w_r}{\kappa}x}\right) + \frac{w_\rho}{w_j}x, \tag{54}$$

where the following notation is used: $j^2\rho = w_\rho$ and $jr = w_r$. Hence we find from (52a) and (54) that the heat flux towards the cold junction is

$$Q_h = \kappa\left(\frac{dT}{dx}\right)_{x=0} = \kappa\left(\frac{T_1 - T_0 + \dfrac{w_\rho}{w_r}l}{1 - e^{\frac{w_r}{\kappa}l}} \times \frac{w_r}{\kappa} + \frac{w_\rho}{w_r}\right). \tag{55}$$

Expanding the exponent in equation (55) into a series and retaining the first two terms, we obtain

$$Q_h = \kappa \frac{T_0 - T_1}{l} + \frac{1}{2} j^2 \rho l - \frac{1}{2} r j (T_0 - T_1). \tag{56}$$

We have thus shown that, to a first approximation, half of the Joule heat in fact proceeds to the cold junction; we can now use equation (56) to calculate the effect of Thomson heat on the coefficient of performance of the thermoelement ϵ. Expression (9) for the cooling capacity of the thermoelement, after taking account of expression (56), takes the form

$$Q_0 = \Pi I - K(T_0 - T_1) - \frac{1}{2} I^2 R + r(T_0 - T_1) I, \tag{57}$$

where $\Pi = 2\alpha_1 T_1$, and α_1 is the value of the thermal emf coefficient at the temperature T_1. We can therefore rewrite expression (57) as follows:

$$Q_0 = 2\bar{\alpha} T_1 I - K(T_0 - T_1) - \frac{1}{2} I^2 R, \tag{58}$$

where

$$\bar{\alpha} = \alpha_1 + \frac{1}{2} r \frac{T_0 - T_1}{T_1}. \tag{59}$$

We shall now prove that $\bar{\alpha}$ is in fact equal to the mean value of the thermal emf coefficient in the temperature range $T_0 - T_1$. According to (32), we have for semi-metals (i.e. when n = const)

$$\alpha_0 - \alpha_1 = \frac{3}{2} \frac{k}{e} \ln \frac{T_0}{T_1} = r \ln \frac{T_0}{T_1} \approx r \frac{T_0 - T_1}{T_1},$$

whence

$$r \approx \frac{\alpha_0 - \alpha_1}{T_0 - T_1} T_1. \tag{60}$$

Substituting (60) into (59) we obtain

$$\bar{\alpha} = \alpha_1 + \frac{1}{2}(\alpha_0 - \alpha_1) = \frac{\alpha_1 + \alpha_0}{2}.$$

With the same degree of accuracy we can write for the emf

$$E = \int_{T_1}^{T_0} \alpha dT \approx \bar{\alpha}(T_0 - T_1). \tag{61}$$

Taking account of expressions (50a) and (61), expression (14) for the coefficient of performance becomes

$$\epsilon = \frac{2\bar{\alpha} I T_1 - \frac{1}{2} I^2 R - K(T_0 - T_1)}{I[2\bar{\alpha}(T_0 - T_1) + IR]}. \tag{14a}$$

Expression (14a) has the same form as (14), the only difference being that the thermal emf coefficient α, which has been regarded previously as independent of temperature, is now replaced by its mean value in the working temperature range. Therefore, without repeating the steps described in the previous paragraph, we are justified in expressing the maximum coefficient of performance in the form

$$\epsilon_0 = \frac{T_1}{T_0 - T_1} \times \frac{\sqrt{1 + \frac{1}{2}(T_0 + T_1)\bar{z}} - \frac{T_0}{T_1}}{\sqrt{1 + \frac{1}{2}(T_0 + T_1)\bar{z}} + 1}, \tag{19a}$$

where $\bar{z} = \frac{\bar{\alpha}^2 \sigma}{\kappa} = \frac{\bar{\alpha}^2}{\kappa\rho}$. It can also be shown that the temperature dependence of the electrical conductivity and the thermal conductivity can be, to a first approximation, taken into account by replacing the product $\kappa\rho$ in the value for $\bar{z}$ by its mean value in the working temperature range. Thus,

$$z = \frac{\bar{\alpha}^2}{\overline{\kappa\rho}},$$

where $\overline{\kappa\rho} = \frac{1}{T_0 - T_1} \int_{T_1}^{T_0} \kappa\rho \, dT$.

1.4 Multistage batteries. The maximum temperature drop which a thermoelement can provide is

$$(T_0 - T_1)_{max} = \frac{z T_1^2}{2}, \quad \text{or} \quad T_1 = \frac{\sqrt{1 + 2T_0 z} - 1}{z}. \tag{62}$$

The temperature can be reduced still further by using multistage cooling. It is obvious, however, that it is not possible to attain the minimum temperature given by expression (62) which corresponds to $\epsilon = 0$, and at the same time reduce the temperature still further using another stage, since the second stage will generate heat, which the first one will have to absorb. For the best utilisation of all stages of a multistage battery intended for the attainment of the lowest temperatures, the batteries should consist of stages of steeply decreasing power. With the aid of a multistage battery, it is also possible to achieve another result, namely to increase the coefficient of performance when the required temperature drop is close to the maximum attainable for the given z.

The coefficient of performance of a multistage battery is calculated as follows.

Let Q_1 be the refrigerating capacity of the battery stage which is in direct contact with the cooled object, ϵ_1 its coefficient of performance, and W_1 its power consumption. The respective values for the preceding stage will be denoted by Q_2, ϵ_2 and W_2, etc. From equation (11), $W_1 = Q_1/\epsilon_1$; therefore

$$\left.\begin{aligned} Q_2 &= W_1 + Q_1 = Q_1\left(1 + \frac{1}{\epsilon_1}\right), \\ Q_3 &= Q_2\left(1 + \frac{1}{\epsilon_2}\right) = Q_1\left(1 + \frac{1}{\epsilon_1}\right)\left(1 + \frac{1}{\epsilon_2}\right), \\ &\cdots\cdots\cdots\cdots\cdots\cdots \\ Q_{n+1} &= Q_1\left(1 + \frac{1}{\epsilon_1}\right)\left(1 + \frac{1}{\epsilon_2}\right)\cdots\left(1 + \frac{1}{\epsilon_n}\right). \end{aligned}\right\} \quad (63)$$

But Q_{n+1} is composed of two parts, namely the power consumed by the entire battery W and Q_1:

$$Q_{n+1} = W + Q_1 = Q_1\left(1 + \frac{1}{\epsilon}\right), \quad (64)$$

where ϵ is the coefficient of performance of the whole battery. Comparison of expressions (63) and (64) yields an expression for the coefficient of performance of a multistage battery:

$$1 + \frac{1}{\epsilon} = \prod_{i=1}^{i=n}\left(1 + \frac{1}{\epsilon_i}\right), \quad (65)$$

or

$$\epsilon = \frac{1}{\prod_{i=1}^{i=n}\left(1 + \frac{1}{\epsilon_i}\right) - 1}. \quad (66)$$

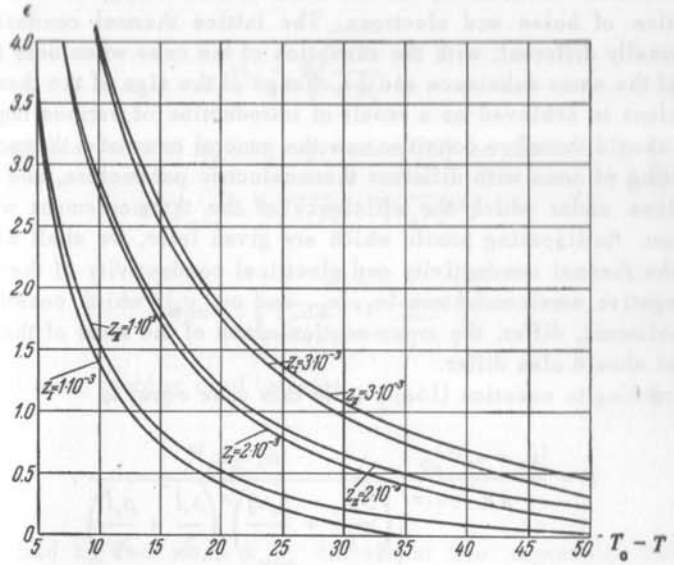

Fig. 2

Let us consider an example. When $z = 2 \times 10^{-3}$ and $\Delta T = 50°$, then for a single stage $\epsilon = 0.1$ (10%). With two stages $\Delta T_1 = \Delta T_2 = 25°$, $\epsilon_1 = \epsilon_2 = 0.8$, and the coefficient of performance of the whole battery is $\epsilon = 0.25$. Similarly, with three stages we obtain $\epsilon = 0.275$. This shows that the use of a three stage battery in this case is useless. Let us assume that for $z = 2 \times 10^{-3}$ we wish to reduce the temperature by 25° in two stages of 12.5°. The coefficient of performance for each stage would be $\epsilon_1 = 2$ and for both stages together $\epsilon = 0.8$, i.e. the same as for a single stage.

Fig. 2 shows the dependence of the coefficient of performance ϵ on temperature difference and z for a single stage and a two-stage thermobattery for $T_0 = 293°K$

1.5 Principles of calculations for thermoelectric batteries.

Selection of the ratio of the cross-section areas of the thermoelement arms. Until now we have assumed that the arms of the thermoelement consist of substances with equal electrical and thermal conductivity and equal, but opposite, thermal emf coefficients. In practice these conditions are not as a rule realised; even when it is possible to attain the same thermal emf coefficient for both arms of the thermoelement $|\alpha| = 172\,\mu$V/deg, the electrical conductivity of the arms differs owing to the different mobilities of holes and electrons. The lattice thermal conductivity is also usually different, with the exception of the case when both arms are made of the same substance and the change of the sign of the thermal emf coefficient is achieved as a result of introduction of various impurities.

We should therefore consider now the general case of a thermoelement consisting of arms with different thermoelectric parameters, and find the conditions under which the efficiency of the thermoelement will be a maximum. Anticipating proofs which are given later, we shall state that when the thermal conductivity and electrical conductivity of the positive and negative semiconductors (κ_1, κ_2, and σ_1, σ_2), which constitute the thermoelement, differ, the cross-section areas of the arms of the thermoelement should also differ.

According to equation (16a) z is in this case equal to

$$z = \frac{(a_1 - a_2)^2}{RK} = \frac{(a_1 - a_2)^2}{\left(\frac{S_1\kappa_1}{l} + \frac{S_2\kappa_2}{l}\right)\left(\frac{\rho_1 l}{S_1} + \frac{\rho_2 l}{S_2}\right)}, \tag{67}$$

where S_1 and S_2 are the cross-section areas of the branches of the thermoelement, l is their length, which will be assumed to be equal for both arms; and ρ_1 and ρ_2 the electrical resistivities of the materials. When the terms in the first bracket in the denominator of expression (67) are divided by S_2 and in the second bracket multiplied by S_2, this expression becomes more symmetrical in form, viz,

$$z = \frac{(a_1 - a_2)^2}{(\kappa_1 m + \kappa_2)\left(\frac{\rho_1}{m} + \rho_2\right)} = \frac{\bar{a}^2}{\overline{\kappa\rho}}, \tag{68}$$

where the following notation has been adopted: $m = \frac{S_1}{S_2}$, $\bar{a} = \frac{a_1 - a_2}{2}$ and $\overline{\kappa\rho} = \frac{\kappa_1 m + \kappa_2}{2} \times \frac{\rho_2 + \frac{\rho_1}{m}}{2}$. The denominator $\overline{\kappa\rho}$ in the expression for z is a

function of m and we can find $\overline{\kappa\rho}_{min}$, and therefore also z_{max}, from the condition $\frac{\partial\overline{\kappa\rho}}{\partial m} = 0$:

$$4\frac{\partial\overline{\kappa\rho}}{\partial m} = \kappa_1\rho_2 - \frac{\kappa_2\rho_1}{m^2} = 0$$

and

$$m_0 = \sqrt{\frac{\kappa_2\rho_1}{\kappa_1\rho_2}}; \tag{69}$$

substituting this value of m_0 into expression (68) we obtain

$$4\,\overline{\kappa\rho}_{min} = (\sqrt{\kappa_1\rho_2} + \sqrt{\kappa_2\rho_1})^2,$$

$$z_{max} = \left(\frac{a_1 - a_2}{\sqrt{\kappa_1\rho_2} + \sqrt{\kappa_2\rho_1}}\right)^2. \tag{68a}$$

The following problem is of interest.

Let

$$z_1 = \frac{a_1^2}{\kappa_1\rho_1}, \qquad z_2 = \frac{a_2^2}{\kappa_2\rho_2}.$$

We shall find by how much z_{max} calculated from expression (68a) is smaller than z_1, (i.e. by how much the properties of the thermoelement as a whole are inferior to the properties of the better of the two branches).

Let $\sqrt{z_1} = l_1$; $\sqrt{z_2} = l_2$; $\sqrt{z_{max}} = l_m$; $\sqrt{\kappa_1\rho_1} = k_1$; and $\sqrt{\kappa_2\rho_2} = k_2$.

Then

$$l_1 - l_m = \frac{a_1}{k_1} - \frac{a_1 - a_2}{k_1 + k_2} = (l_1 - l_2)\,\frac{1}{1 + \frac{k_1}{k_2}}.$$

The lower the resistivity of the given material the lower is the value of $k = \sqrt{\kappa\rho}$ characteristic of this material; at the limit this value tends to the Wiedemann-Franz constant. In order to prevent a large reduction of z_{max}, the carrier concentration should therefore be so selected that $\rho_1 \gg \rho_2$.

Design calculations of a single-stage battery. The starting quantities for the calculation are:

1) the parameters of the thermoelement arms: α_1, α_2; σ_1, σ_2; κ_1, κ_2;

$$z_{max} = \left(\frac{\alpha_1 - \alpha_2}{\sqrt{\kappa_1\rho_2} + \sqrt{\kappa_2\rho_1}}\right)^2 \quad \text{and} \quad m_0 = \sqrt{\frac{\kappa_2\rho_2}{\kappa_1\rho_1}};$$

2) the prescribed operating conditions: cold and hot junction temperatures T_1 and T_0, and the refrigerating capacity Q_0;

3) voltage of the power supply source V;

4) from design considerations it is also necessary to select the length of the thermoelement arms l (or, what amounts to the same thing, the thickness of the battery).

It can be readily shown that the surface area of the thermobattery for a given refrigerating capacity is proportional to l, whilst its volume is proportional to l^2; therefore in order to reduce the consumption of materials and weight of the thermobattery it is necessary to make l small. This, however, complicates the removal of heat from the hot junctions. In each specific case it is therefore necessary to select a certain optimum arm length.

Calculation steps:

1) expressions (18) and (19) are used to calculate the values of ϵ_0 and v_0, the power required for the battery $\mathbb{W} = Q_0/\epsilon_0$, and the operating current $I = \mathbb{W}/V$;

2) the number of thermoelements is now calculated

$$N = \frac{V}{v_0}, \tag{70a}$$

and then from expressions (17) and (18) the resistance of each thermoelement;

3) moreover, we have

$$R = l\left(\frac{\rho_1}{S_1} + \frac{\rho_2}{S_2}\right) = \frac{l}{S_1}(\rho_1 + m_0\rho_2). \tag{70b}$$

Knowing R, l, ρ_1, ρ_2, and m_0, we find from equation (70b) S_1 and $S_2 = \frac{S_1}{m_0}$.

It can be readily shown that the power consumption of the battery and its refrigerating capacity do not depend on the voltage of the power supply source V, the number of couples N, the surface area of the thermobattery

F, and its thickness l, but they depend only on the ratio of the last two quantities F/l, each of which can, by itself, be arbitrary. The amount of "cold" removed from 1 cm² of the battery $q = Q_0/F$ depends on the thickness of the battery, i.e. the length of the thermoelements l. This permits us to decrease l and F simultaneously, each by a times, which leads to a reduction of the volume, and an economy of material by a^2 times for the same capacity. The length of the thermoelement cannot be reduced below a certain limit because of junction resistances in the thermoelement and temperature drops across the layers of insulation between the battery and the radiators (which serve for heat exchange with the surroundings), fitted to the hot and cold thermoelement junctions. The reduction of l is expedient as long as the aforementioned junction resistances do not become comparable with the resistances of the arms, and the temperature drops at the thermal contacts of the battery with the radiators, and in the radiators themselves, are not comparable with the working temperature difference.

We have not yet taken into account the junction resistances r of the two junctions of the thermoelement. In practice they may always exist, and when they are taken into account the resistance of the thermoelement is expressed by the following formula:

$$R = 2r + 2\rho\frac{l}{S} = 2\frac{l}{S}\left(\frac{rS}{l} + \rho\right) = \frac{2l}{S}\left(\frac{r_0}{l} + \rho\right). \tag{71}$$

The quantity $r_0 = rS$ characterises the quality of the junction since $r = S^{-1}$ and r_0 does not depend on the contact surface area. (Since the contact between the arms can be achieved by welding or pressing, the term "soldering" will be replaced by the more general term "commutation".)

It can be readily shown that when the junction resistances are taken into account the expression for z takes on the form

$$z = \frac{\alpha^2}{\kappa\left(\rho + \frac{r_0}{l}\right)}.$$

Thus, from the viewpoint of attaining maximum z, l can be decreased as long as the condition $l\rho \gg r_0$ or $l \gg r_0/\rho$ is fulfilled. In order to avoid an appreciable temperature drop at the thermal contact between the battery and the radiator the following analogous condition should obtain: $l/\kappa \gg k_0^{-1}$ or $l \gg \kappa/k_0$ where κ is the thermal conductivity of the substance and k_0 the heat transfer by conduction across a unit contact surface area.

To eliminate the temperature drop in the radiators proper, the latter should have a large well-finned contact surface area with the surrounding medium. Heat transfer from the thermobattery to the outer surfaces of the radiators is achieved with the aid of good thermal conductors such as copper or aluminium, or even more effectively by a stream of liquid or vapour distilled in vacuo from the hot to the cold surface.

Apart from its power conversion aspects, the thermobattery should also satisfy specific mechanical requirements.

The temperature difference, which is unavoidable in all thermoelectric devices, produces a bending moment. For a coefficient of thermal expansion equal to approximately 2×10^{-5} and a temperature difference of 50°C, the linear dimensions of the hot junction are larger than those of the cold junction by 10^{-3} times the width of the battery. A battery with a 10 cm long side expands by 0.1 mm, so that when the thickness of the battery is 1 cm, the resulting bending has a radius of curvature equal to 10 m. To prevent cracking it is necessary to make the batteries somewhat elastic.

The effect of departures from optimum conditions. We have determined the ratio of the cross-section areas of arms of the thermoelement (m_0) for which z has the maximum value; earlier we have also found the optimum carrier concentration n_0 (equation (37)), electrical conductivity σ_0 (equation (33)), and optimum voltage drop across the thermoelement (equation (18)).

In practice, owing to uncontrollable variations in the technological processes, the specimens from which the battery is constructed have varying thermoelectric parameters α, σ, and κ. In general, the scatter of these parameters is within the limits of 10%. It is therefore important to find out how departures from the optimum conditions affect the properties of the battery.

Departures from the optimum ratio of cross-section areas of the arms. Expanding $\overline{\kappa\rho}$ as a Taylor series in powers of m close to m_0, and remembering that $\left(\frac{\partial\overline{\kappa\rho}}{\partial m}\right)_{m=m_0} = 0$, we find

$$\overline{\kappa\rho} - \overline{\kappa\rho}_{min} \approx \frac{1}{2}\left(\frac{\partial^2\overline{\kappa\rho}}{\partial m^2}\right)_{m=m_0}(m-m_0)^2. \tag{72}$$

From equation (69)

$$\frac{\partial^2\overline{\kappa\rho}}{\partial m^2} = \frac{2\kappa_2\rho_1}{m^3}; \tag{73}$$

using equations (72) and (73) we obtain

$$\frac{\kappa\rho - (\overline{\kappa\rho})_{min}}{(\overline{\kappa\rho})_{min}} = p\left(\frac{m-m_0}{m_0}\right)^2, \tag{74}$$

where the coefficient

$$p = \frac{\sqrt{\kappa_1\rho_1\kappa_2\rho_2}}{[\sqrt{\kappa_1\rho_1} + \sqrt{\kappa_2\rho_2}]^2} \leqslant \frac{1}{4},$$

since the geometric mean of two numbers is always smaller than or equal to the arithmetic mean, and so

$$\frac{\overline{\kappa\rho} - (\overline{\kappa\rho})_{min}}{(\overline{\kappa\rho})_{min}} \leqslant \frac{1}{4}\left(\frac{m-m_0}{m_0}\right)^2. \tag{75}$$

It follows from (75) that the value of $\overline{\kappa\rho}$ and therefore also of z depends very little on m. Thus, e.g., when $(m-m_0)/m_0 = 0.2$, $\overline{\kappa\rho}$ increases by only 1%. According to expression (75)

$$\frac{z_{max} - z}{z_{max}} \leqslant \frac{1}{4}\left(\frac{m-m_0}{m_0}\right)^2. \tag{75a}$$

Departure from the optimum carrier concentration. According to expression (37), the numerator $\alpha^2\sigma$ in the expression for z has a maximum at a certain carrier concentration. An optimum electrical conductivity corresponds to this optimum carrier concentration

$$\sigma_0 = en_0u = \frac{2(2\pi mkT)^{3/2}}{h^3}e^r ue. \tag{33a}$$

Let us find out by how much the efficiency of the thermoelement decreases when the electrical conductivity of the branches differs slightly from the optimum value. From (32), (33a), and (35) we have

$$\left.\begin{aligned} \alpha^2\sigma &= \frac{k^2}{e^2}(A - \ln\sigma)^2\sigma, \\ \frac{\partial(\alpha^2\sigma)}{\partial\sigma} &= \frac{k^2}{e^2}[(A-\ln\sigma)^2 - 2(A-\ln\sigma)], \\ \frac{\partial^2(\alpha^2\sigma)}{\partial\sigma^2} &= \frac{k^2}{e^2}\left[\frac{2}{\sigma} - \frac{2(A-\ln\sigma)}{\sigma}\right]. \end{aligned}\right\} \tag{76}$$

For $A - \ln \sigma_0 = 2$, i.e. $\sigma_0 = e^{A-2}$, we have

$$(\alpha^2\sigma)_{max} = 4\frac{k^2}{e^2}\sigma_0 . \tag{77}$$

Expanding $\alpha^2\sigma$ into a series in terms of $(\sigma - \sigma_0)$ and confining ourselves to the first three terms of the expansion, we obtain

$$(\alpha^2\sigma)_{max} - \alpha^2\sigma \approx \frac{1}{2}\left[\frac{\partial^2(\alpha^2\sigma)}{\partial\sigma^2}\right]_{\sigma=\sigma_0}(\sigma - \sigma_0)^2 .$$

From (76) and (77) we have

$$\left[\frac{\partial^2(\alpha^2\sigma)}{\partial\sigma^2}\right]_{\sigma=\sigma_0} = \frac{2}{\sigma_0}\frac{k^2}{e^2} .$$

Therefore,

$$(\alpha^2\sigma)_{max} - \alpha^2\sigma = \frac{k^2}{e^2} \times \frac{1}{\sigma_0}(\sigma - \sigma_0)^2$$

or, from (77)

$$\frac{(\alpha^2\sigma)_{max} - \alpha^2\sigma}{(\alpha^2\sigma)_{max}} \approx \frac{1}{4}\left(\frac{\sigma - \sigma_0}{\sigma_0}\right)^2 . \tag{78}$$

Expression (78) shows that the dependence of $\alpha^2\sigma$, and therefore also of z, on σ, close to the point $\sigma = \sigma_0$, bears the same character as the dependence of z on m close to the point $m = m_0$, i.e. a change of σ by 20% leads to a decrease of z by only 1%.

As may be seen from (75a) and (78), $\frac{z_{max} - z}{z_{max}}$ depends in exactly the same way on departures of m from the value m_0, as on departures of σ from σ_0.

Fig. 3 shows the dependence of $\frac{z_{max} - z}{z_{max}}$ on $\frac{\sigma - \sigma_0}{\sigma_0}$. The same graph can be used for finding the dependence of $\frac{z_{max} - z}{z_{max}}$ on $\frac{m - m_0}{m_0}$.

Dependence of $\alpha^2\sigma$ on temperature. According to (32), (33), and (35)

$$\alpha^2\sigma = \left(B + \frac{3}{2}\ln T\right)^2 CT^{-\beta} , \tag{79}$$

where $\beta = \frac{1}{2}$ for an ionic lattice and $\beta = \frac{3}{2}$ for an atomic lattice (it is assumed here that the carrier concentration n is independent of temperature). It has been mentioned earlier that experimental investigation of the dependence of the mobility on temperature has shown that for a number of semiconducting substances used for thermoelements the mobility is inversely proportional to the cube of the temperature; thus the case $\beta = 3$ is also of interest to us.

From (79) we have

$$\frac{\partial(\alpha^2\sigma)}{\partial T} = 3\left(B + \frac{3}{2}\ln T\right)CT^{-\beta-1} - \beta\left(B + \frac{3}{2}\ln T\right)^2 CT^{-\beta-1} , \tag{80}$$

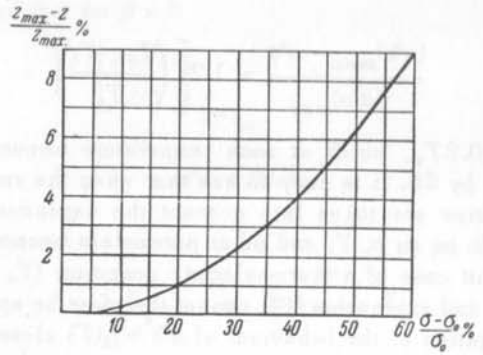

Fig. 3

$$\frac{\partial^2(\alpha^2\sigma)}{\partial T^2} = CT^{-\beta-2}\left[\frac{9}{2} - 3(2\beta+1)\left(B + \frac{3}{2}\ln T\right) + \beta(\beta+1)\left(B + \frac{3}{2}\ln T\right)^2\right] . \tag{81}$$

According to (80), $\frac{\partial(\alpha^2\sigma)}{\partial T} = 0$ at the temperature T_0 for which $B + \frac{3}{2}\ln T_0 = \frac{3}{\beta}$, whence $T_0 = e^{2/\beta - \frac{1}{2}B}$ and

$$(\alpha^2\sigma)_{max} = \frac{9}{\beta^2}CT_0^{-\beta} . \tag{82}$$

Comparing (77) and (82) we find that the respective maxima of $\alpha^2\sigma$ in elements with $T = \text{const}$, $\alpha^2\sigma = f_1(\sigma)$, and with $n = \text{const}$, $\alpha^2\sigma = f_2(T)$ do not

coincide. Only for an atomic lattice ($\beta = 5/2$) are both maxima at the same point

$$A - \ln\sigma = B + \frac{3}{2}\ln T = 2,$$

i.e. in this case we are not dealing with a relative maximum but with an absolute maximum. In this case according to (81)

$$\left[\frac{\partial^2(\alpha^2\sigma)}{\partial T^2}\right]_{T=T_0} = \frac{9}{2} C T_0^{-7/2}.$$

Expanding $\alpha^2\sigma$ into Taylor series close to the point T_0 we obtain

$$\frac{(\alpha^2\sigma)_{max} - \alpha^2\sigma}{(\alpha^2\sigma)_{max}} = 1.25\left(\frac{T_0 - T_1}{T_0}\right)^2. \tag{83}$$

For $T_0 - T_1 = 0.2\,T_0$, which at room temperature amounts to about 50°, $\alpha^2\sigma$ drops only by 5%. It is easy to see that when the remaining terms of the Taylor series are taken into account the dependence close to the maximum of $\alpha^2\sigma$ on m, σ, T, and other parameters becomes even weaker. However, in the case of a thermoelectric generator $(T_0 - T_1)/T_1$ usually exceeds unity and expression (83) cannot therefore be applied.

An investigation of the behaviour of $\alpha^2\sigma = f_2(T)$ close to the maximum for the cases $\beta = 1/2$ and $\beta = 3$ is of no great interest since this point lies beyond the working temperature range.

In fact, at the temperature T_w specified by the working conditions we select a carrier concentration at which $\alpha^2\sigma = f_1(\sigma)$ would reach a maximum; according to equation (35b) this corresponds to the condition

$$B_w + \frac{3}{2}\ln T_w = 2. \tag{84}$$

But at a given B_w the value of $\alpha^2\sigma = f_2(T)$ has a maximum when condition (82) is fulfilled

$$B_w + \frac{3}{2}\ln T_0 = \frac{3}{\beta}. \tag{82a}$$

From (84) and (82a) we obtain

$$\frac{T_0}{T_w} = e^{2/\beta - 4/3}, \tag{85}$$

whence, for $\beta = 5/2$, we find $T_0 = T_w$, for $\beta = 1/2$ we have $T_0 = 12T_w$, and for $\beta = 3$

$$T_0 = T_w e^{-5/3} \approx 0.53\,T_w. \tag{85a}$$

In order to establish the temperature dependence of $\alpha^2\sigma$, we shall expand $\alpha^2\sigma$ in a Taylor series in the vicinity of the point T_w, and, since at this point the first derivative is not equal to zero, we shall limit the expansion to the first two terms

$$\alpha^2\sigma = (\alpha^2\sigma)_{T=T_w} + \frac{\partial(\alpha^2\sigma)}{\partial T}(T - T_w).$$

From (80) we find that for $\beta = 3$

$$\left[\frac{\partial(\alpha^2\sigma)}{\partial T}\right]_{T=T_w} = -6\,C T_w^{-4},$$

$$\alpha^2\sigma = 4\,C T^{-3}$$

and, therefore,

$$\frac{(\alpha^2\sigma)_w - (\alpha^2\sigma)}{(\alpha^2\sigma)_w} = \frac{3}{2}\times\frac{T - T_w}{T_w}. \tag{86}$$

Effect of departures of the current I from the optimum value I_0 on ΔT_{max}. When the thermoelement operates with the cold junction perfectly thermally insulated, we find from (10)

$$\left.\begin{aligned} \Delta T &= \frac{\Pi I - \frac{1}{2}I^2R}{K} \\ \frac{\partial\Delta T}{\partial I} &= \frac{\Pi}{K} - \frac{IR}{K}, \\ \frac{\partial^2\Delta T}{\partial I^2} &= -\frac{R}{K}, \\ \frac{\partial^3\Delta T}{\partial I^3} &= 0. \end{aligned}\right\} \tag{87}$$

Expanding ΔT into a Taylor series close to the point $I = I_0$, we find, after straightforward transformations,

$$\frac{\Delta T_{max} - \Delta T}{\Delta T_{max}} = \left(\frac{I - I_0}{I_0}\right)^2. \tag{88}$$

According to (88), a departure of the current density from the optimum value by 20% results in a reduction of ΔT by 4%.

Effect of the change of supply voltage on the coefficient of performance. In a similar way we arrive at the following expression:

$$\frac{\epsilon_0 - \epsilon}{\epsilon_0} = 2\left(\frac{v - v_0}{v_0}\right)^2 \left(1 + \frac{1}{2\epsilon_0}\right). \tag{89}$$

CHAPTER 2

EXPERIMENTAL INVESTIGATION OF THE THERMOELECTRIC PROPERTIES OF SEMICONDUCTORS

The theory of thermoelectric cooling expounded in Chapter 1 is based on a number of deductions of theoretical physics: Thomson's thermodynamic relationships (3) and (5), Pisarenko's expressions for the thermal emf (32), the temperature dependence of the mobility (44) and (46), etc. All these deductions were to a greater or lesser extent in need of experimental verification.

Thomson's relationships do not follow directly from thermodynamics, but they can be deduced either by postulating the reversibility of thermoelectric processes, or on the basis of the principle of the symmetry of kinetic coefficients, the introduction of which involves additional hypotheses. Several investigations have been devoted to the measurement of α, Π, and τ and the verification of Thomson's relationships for metals. In the majority of these investigations the relationship (3) has been adequately substantiated, although very conflicting results have been obtained with regard to relationship (5).

Despite this we know only of two investigations in which the Peltier and Thomson effects have been studied for semiconductors. Königsberger and Weiss measured the Thomson coefficient for two semiconductors: Si and MoS_2. Gottstein* measured the thermal emf coefficient and the Peltier coefficient for these substances and used his and Königsberger's results for checking Thomson's relationships.

Relationship (3) was found to be in accordance with the experimental data; the quantities entering into expression (5), i.e. τ and $T\frac{d\alpha}{dT}$, were found to differ by a factor of 2 to 3.

It was therefore of interest to find out how semi-metals, which are at present used in thermoelectric generators and refrigerators, obey these relationships.

* G. Gottstein, *Ann. d. Phys.*, 43, 1079, 1914.

It was also of interest to determine the temperature dependence of the thermal emf and the mobility. Investigations of the temperature dependence of the mobility for semiconductors with an atomic lattice (Si, Ge, Zn, Sb, etc.) had yielded relatively good agreement with expression (44); however, there was no investigation confirming relationship (46).

For the majority of semiconductors Pisarenko's formula gives an unsatisfactory agreement with the experimental data. Since the substances used in thermoelements (PbS, PbSe, PbTe, Bi_2Te_3) occupy an intermediate position between purely ionic and atomic compounds, neither theoretical nor experimental investigations have yielded unequivocal answer to the problem of the temperature dependence of mobility in such substances. Some importance was therefore attached to a direct determination of the temperature dependence of the thermal emf and the mobility for such substances.

Finally, it was essential to verify the principal hypotheses of the theory of thermoelectric cooling experimentally.

2.1 Methods of investigating the thermoelectric properties of semiconductors.

Measurement of the Peltier and Thomson coefficients. For the simultaneous measurement of the Peltier and Thomson coefficients an instrument, which is shown schematically in fig. 4, was constructed.

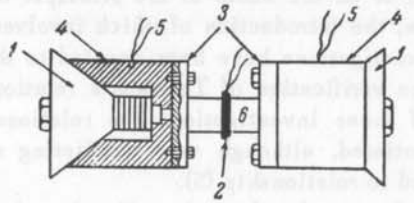

Fig. 4

The investigated specimen 6 was soldered to two plates 3 which were then screwed to cylindrical cups 4 with conical lids 1. All parts of the instrument (cups, lids, and plates) were made of red copper with ground contact surfaces. Inside each of the cups was housed a 0.1 mm diam. constantan wire heater with a resistance of 16 ohms, wound on a cylindrical extension of the lid. To each of the cups were soldered insulated copper and constantan wires 5, forming thermocouples for measuring the temperature difference across the specimen. The thermal emf of the specimen was measured with reference to copper using copper leads. Good contact at the interface between the specimens and the plates was achieved by careful tinning and soldering over the entire contact surface.

The Peltier heat was measured by the null method evolved by Gottstein. Current was allowed to flow through the specimen and at the same time

the electric heater mounted in the cup was switched on. The latter was cooled owing to the Peltier heat being absorbed at the cold junction. When the currents were such that the temperatures of both cups were equal, the Joule heat generated by the electric heater balanced the heat absorbed by the adjacent junction, heating the corresponding cup to the same temperature as that of the other cup, which was heated by the Peltier heat. Therefore, under these conditions the Joule heat was equal to twice the Peltier heat. The Peltier coefficient was determined from the formula

$$\Pi = \frac{I_h^2 R_h}{2I_0}, \tag{90}$$

where I_h and R_h are the current and resistance of the heater respectively and I_0 the current flowing through the specimen.

Measurement of the Thomson coefficient was carried out with the same instrument by comparing the Joule heat generated in the specimen with the Thomson heat. For this purpose one of the heaters was first switched on until a stationary temperature drop of 10-30° was established across the specimen. A current was then passed through the specimen for 1-2 minutes in a given direction, and after a pause of 10-15 minutes, required for allowing the apparatus to return to its initial stationary state, the current was passed in the opposite direction.

The temperature of the specimen when the current was flowing through it was measured with the aid of thermocouple 2, soldered to a copper foil strip 0.1 mm thick, which was in turn glued with Glyptal varnish to the centre of the specimen. Before taking the measurements, the emf of the thermocouple was balanced with the aid of a potentiometer. When the current started to flow the balance was upset by the heat generated in the specimen, the deflection of the galvanometer γ_1 with the current flowing in a given direction being proportional to the sum of the Joule heat

$$Q_J = I^2 R dt \tag{91}$$

(where R is the resistance of the specimen and τ the time), and the Thomson heat

$$Q_\tau = \tau I (T_1 - T_0) dt ; \tag{92}$$

when the current was flowing in the opposite direction, the galvanometer deflection γ_2 was proportional to the difference between these heats. The resistance of the specimen was measured before the tests. Galvanometer deflections were recorded at 15 second intervals from the instant of

switching on the current. Using expressions (91) and (92), the Thomson heat was calculated from the formula

$$Q_T = \frac{\gamma_2 - \gamma_1}{\gamma_1 + \gamma_2} I^2 R . \qquad (93)$$

Measurement of the thermal emf. Fig. 5a shows a diagram of an instrument usually employed for the measurement of the thermal emf of semiconductors.

The investigated specimen 1 is clamped with the aid of a load or a spring between two metal rods 2 and 3. On one of these rods (2) an electric heater 6 is wound so that it serves as a heat source, whilst the other

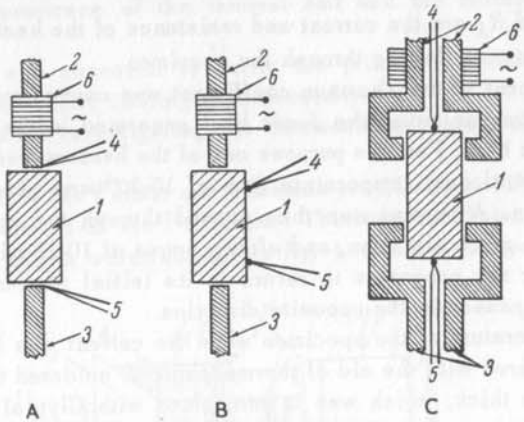

Fig. 5

rod (3) serves as a heat sink. To the tips of the hot and cold rods are soldered, or pressed in, metallic measuring thermocouples 4 and 5. The temperatures of the ends of the specimen T_1 and T_2 and its thermoelectric emf E_x, with reference to one of the branches of the measuring thermocouples, are measured by a null method. The thermal emf coefficient is then calculated from the formula

$$\alpha = \frac{E_x}{T_1 - T_2} . \qquad (94)$$

This very simple method suffers from a substantial defect, namely, a temperature drop always exists between the specimen and the rods; this drop is proportional to the heat flux and the thermal resistance of the

contacts. As a result of this, the measured temperature difference across the specimen is higher than the true one, and formula (94) gives too low a value for the thermal emf coefficient. This error can be appreciably reduced by arranging the thermocouples at one side of the 'main' heat flux, i.e. on one of the side faces of the specimen, as shown in fig. 5b.

The error is almost completely removed by eliminating the heat flux across the contact surface between the thermocouple and the specimen. For this purpose the portions of the thermocouple adjoining the contact surface should be maintained at a temperature equal to that of the ends of the specimen. Fig. 5c shows an instrument for measuring the thermal emf coefficient based on the above principle which was employed in this investigation. For studying the temperature dependence of the thermal emf, the entire instrument is mounted in an electrical furnace or in a special jacket in a Dewar vessel filled with liquid nitrogen.

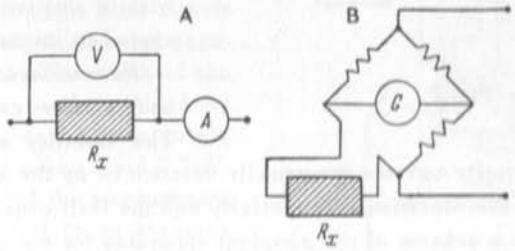

Fig. 6

The instrument shown in fig. 5b has an additional advantage in allowing the simultaneous measurement of the thermal emf coefficient and electrical conductivity; the heat source and sink act in this case as current conductors, and one of the branches of the thermocouples as probes for measuring the voltage drop.

Measurement of the electrical conductivity. The electrical conductivity of a semiconductor is calculated from the usual formula

$$\sigma = \frac{l}{R_x S} , \qquad (95)$$

where l is the length of the investigated specimen, S its cross-section area and R_x its resistance. The measurement of the electrical conductivity of semiconductors differs from that of metals in that in the former case R_x cannot be measured by the ammeter and voltmeter method (fig. 6a) or a bridge scheme (fig. 6b), since in both cases the results of measurement include a contribution from the contact resistances, which in the

case of semiconductor materials may exceed the resistance of the specimen itself many times. Therefore the electrical conductivity of semiconductors is usually measured by a probe method using the null arrangement shown in fig. 7.

Measurements may be carried out both with d.c. and a.c.; in the first case, in order to eliminate the thermal emf between the probes, E_x should be taken as a mean of two measurements taken with the current flowing in opposite directions. When making measurements with a.c., the null instrument may consist of a vibration galvanometer or a narrow band amplifier with a millivoltmeter connected to its output.

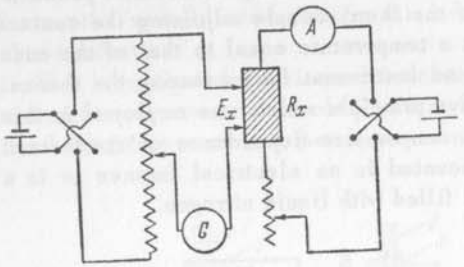

Fig. 7

Measurement of mobility and carrier concentration. The mobility and the concentration of majority carriers are usually determined by the simultaneous measurement of the electrical conductivity and the Hall constant.

Fig. 8 shows a scheme of the simplest apparatus for the measurement of these quantities with d.c. using a null method. Probes 1 and 2 serve for the measurement of the Hall emf, and probes 3 and 4 for the measurement of the electrical conductivity. In order to eliminate thermomagnetic effects and the potential difference between probes 1 and 2 due to their asymmetry, the Hall emf is determined as an average of four measurements, with opposite directions of the magnetic field, and opposite directions of current flow through the specimen.

Fig. 9 shows an apparatus for the measurement of the Hall effect with a.c., in which the thermomagnetic effects are eliminated, thus permitting a substantial simplification of the measurements; this scheme was used in the work described here. The a.c. source of 500 c/s consisted of a sound (frequency) generator. In order to match the load to the output impedance of the generator a step-down transformer was connected at the output of the generator which had a transformation ratio of 0.01. The current flowing through the specimen was measured by determining the voltage drop over a standard resistance of 10^{-3} ohm connected in series with the specimen. The voltage drop between the probes, the Hall emf, and the voltage drop across the standard resistance were measured using

an amplifier. The initial potential difference due to the asymmetry of Hall probes was balanced by feeding an alternating voltage tapped from a phase shifting bridge into the Hall emf circuit (both the amplitude and the phase had to be balanced). The measuring instrument consisted of a narrow band amplifier (see Vlasova and Stil'bans*) with a selenium rectifier and a d.c. millivoltmeter connected at its output.

In order to make the transmission band narrower, the second stage of the amplifier was based on a narrow transmission band RC phase filter circuit with combined positive and negative feedback. The width of the transmission band provided by this circuit was approximately 6 c/s and the noise level 0.3 μV, which permitted the measurement of the Hall emf to an accuracy of 1 μV. The amplifier output had provisions for connection to an oscillograph, making it possible to determine the carrier sign from the phase of the Hall emf. The carrier sign could also be determined by feeding a low alternating voltage, having a frequency of 500 c/s, to the input of the third stage.

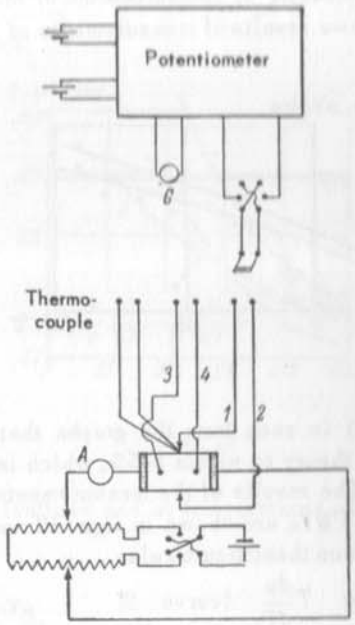

Fig. 8

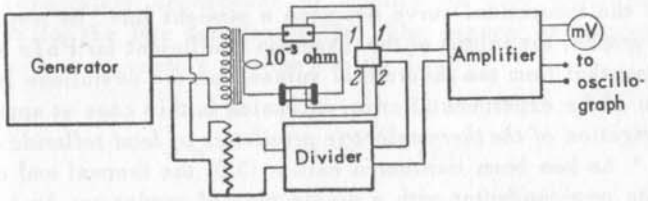

Fig. 9

* R. M. Vlasova and L. S. Stil'bans, *Zhur. Tekh. Fiz.*, 25, No. 4, 571, 1955.

The power supply consisted of an electronic voltage stabiliser.

2.2 Results of the experimental investigations of the thermoelectric properties of semiconductors.

Results of measurements of the Peltier and Thomson effects. Fig. 10 shows results of measurements of Π and α for a ZnSb specimen in the temperature range from –40 to +180°C. In order to carry out measurements at low temperatures the instrument described above was mounted in a Heppler-type thermostat; measurements at elevated temperatures were carried out in a specially designed furnace fed from a ferromagnetic voltage stabiliser. Fig. 11 shows the results of measurements of Π and α for a PbTe specimen in the temperature range from 21 to 110°C.

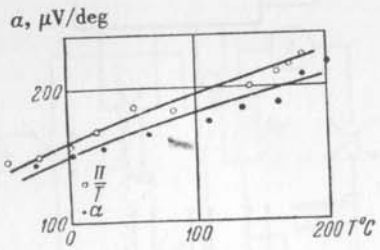

Fig. 10

It is seen from the graphs that in both cases the results agree with the theory to within 3–5%, which is within the experimental error.

The results of the measurements of the Thomson coefficient r for ZnSb and PbTe are shown in figs. 12 and 13 (curve 1); for the purpose of comparison these figures also show $T\frac{d\alpha}{dT}$ (curve 2) based on the data plotted in figs. 10 and 11, and theoretical curves (3) based on the measurements of the Hall effect. In the temperature range from –40°C to +180°C, the carrier concentration in ZnSb is constant and therefore the theoretical curve becomes a straight line. As may be seen from the graphs, the values of the Thomson coefficient for PbTe and ZnSb differ somewhat from the theoretical values, but the deviations lie within the limits of the experimental error, estimated in this case at approx. 10%.

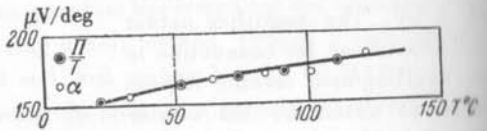

Fig. 11

*Investigation of the thermoelectric properties of lead telluride and lead selenide.** As has been mentioned earlier (32), the thermal emf of a non-degenerate semiconductor with a single type of carrier can be expressed by the formula

$$\alpha = \pm\frac{k}{e}\left[r + 2 + \ln\frac{2(2\pi mkT)^{3/2}}{h^3 n}\right].$$

* N. V. Kolomoets, T. S. Stavitskaya, and L. S. Stil'bans, *Izv. Akad. Nauk SSSR, Ser. Fiz.*, 27, No. 1, 73, 1957.

where the carrier free path length is, in the general case, given by

$$l = f(T)\epsilon^r . \tag{96}$$

Both the function $f(T)$ and r are governed by the mechanism of carrier scattering in the lattice of the substance.

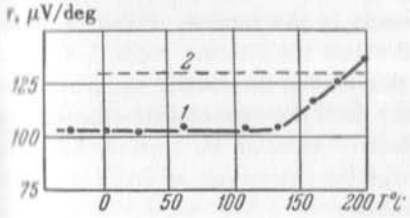

Fig. 12

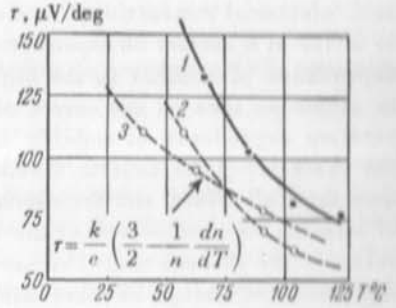

Fig. 13

For scattering by thermal lattice vibrations and at temperatures above the Debye temperature

$$l \propto \frac{\epsilon^r}{T}, \tag{97a}$$

where $r = 1$ for an ionic lattice and $r = 0$ for an atomic lattice; for scattering by lattice defects, $f(T)$ = const, and

$$l \propto \epsilon^r . \tag{97b}$$

In particular, for scattering by impurity ions $r = 2$, etc.

The temperature dependence of mobility is also governed by the expression for the free path length (96). The general expression for the mobility of non-degenerate carriers has the form

$$u \propto T^{-5/2}\int_0^\infty l(\epsilon)\, e^{-\epsilon/kT}\,\epsilon\, d\epsilon . \tag{98}$$

Therefore, according to (98) and (97a), we have for scattering by thermal lattice vibrations

$$u \propto T^{r-3/2}, \tag{99}$$

For scattering by defects, we have, according to (98) and (97b),

$$u \propto T^{r-1/2}. \qquad (100)$$

The above relationships show that the simultaneous measurement, in one and the same material, of the temperature dependence of the thermal emf, electrical conductivity, and carrier concentration makes it possible to arrive at a number of important physical conclusions. The temperature dependence of mobility in the high temperature range makes it possible to obtain an idea on the nature of bonds in the lattice, whilst the temperature dependence of mobility in the low temperature range indicates the character of the defects. Having determined the carrier concentration from the Hall effect, and the exponent r from the temperature dependence of mobility, we can determine the effective mass of the carriers from the value of the thermal emf. The investigation described in this paragraph represents an attempt to solve this problem.

As materials for the investigation we have selected lead telluride and lead selenide, as well as the solid solution PbTe-PbSe, since these substances were until very recently the best materials for the negative branch of the thermocouples. Apart from its theoretical interest, the investigation of the thermoelectric properties of these materials was also of major importance. The investigations were carried out on polycrystalline specimens prepared by sintering. Measurement of the thermal emf, electrical conductivity, and Hall effect, was carried out employing the usual methods described previously.

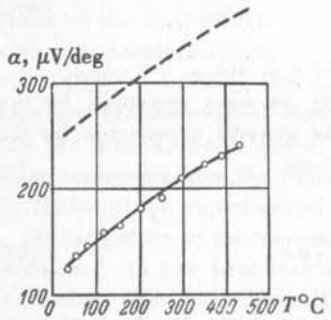

Fig. 14

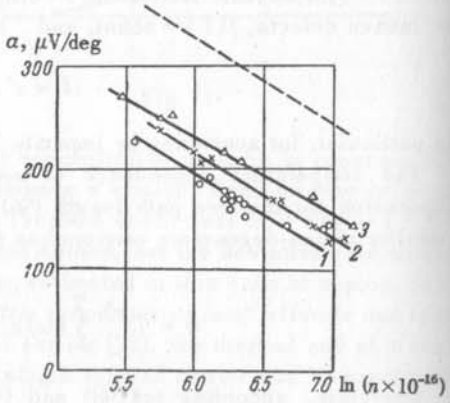

Fig. 15

The high temperature range. Fig. 14 shows the temperature dependence of the thermal emf for a specimen of n-type lead telluride with a carrier

concentration of $n = 9.9 \times 10^{18}$ cm^{-3} in the temperature range 0–450°C. The hatched line shows the theoretical dependence according to expression (32) on the assumption that $A = 2$ (both here and in subsequent considerations we shall denote by A the first term in Pisarenko's formula: $A = r + 2$) and $m = m_0$.

Fig. 15 shows the dependence of the thermal emf on carrier concentration at room temperature for n-type lead telluride (curve 1), and n-type (curve 2) and p-type (curve 3) lead selenide; the hatched line represents the theoretical curve constructed according to expression (32), assuming again that $A = 2$, $m = m_0$.

From figures 14 and 15 we can infer that:

1) the dependence of the thermal emf on temperature and carrier concentration agrees approximately with that given by theory;

2) the absolute experimental values of the thermal emf differ from the theoretical values by 120 μV/deg for lead telluride and somewhat less for lead selenide. This disagreement between the theoretical and experimental values of emf can be attributed to one of two causes: either, (a) the effective mass of the carriers is approximately 2.5 times lower than the free electron mass, or (b) the value of the first term in formula (1), taken in fact quite arbitrarily as $A = 2$, is incorrect.

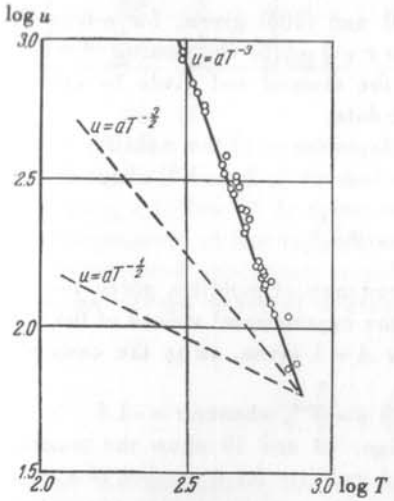

Fig. 16

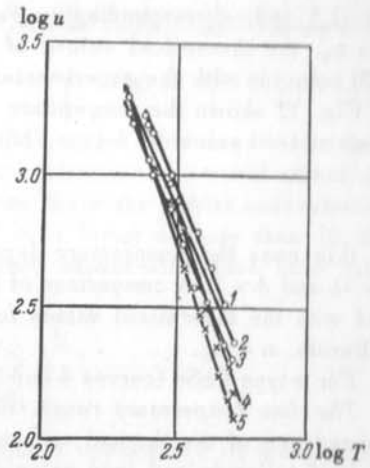

Fig. 17

We have already mentioned that a relationship between A and the temperature dependence of mobility exists. For an atomic lattice $r = 0$,

$A = 2$, and

$$u \propto T^{-3/2}, \tag{101}$$

whilst for an ionic lattice at temperatures above the Debye temperature $r = 1$, $A = 3$, and

$$u \propto T^{-1/2}. \tag{102}$$

With regard to their bond character, lead telluride and lead selenide occupy an intermediate position between these two limiting cases and it could have been predicted in advance that the value of r would lie between 0 and 1.

Fig. 16 shows, with logarithmic co-ordinates, the temperature dependence of the mobility for four specimens of lead telluride in the temperature range 300–700°K (curve 1). For the sake of comparison, the hatched curves represent the theoretical relationships (101) and (102). It follows from this graph that lead telluride obeys, with great accuracy, the law

$$u \propto T^{-3}. \tag{103}$$

Comparison of expressions (99) and (103) gives, for n-type PbTe, $r = -1.5$ and, correspondingly, $A = r + 2 = 0.5$. On putting $A = 0.5$ and $m \approx m_0$, the theoretical values of the thermal emf given by expression (32) coincide with the experimental data.

Fig. 17 shows the temperature dependence of the mobility for specimens of lead selenide; n-type PbSe (curves 1, 2, and 3) obeys the law

$$u \propto T^{-5/2}.$$

In this case the temperature dependence of mobility gives the values $r = -1$ and $A = 1$. A comparison of the experimental values of the thermal emf with the theoretical values for $A = 1$ gives, as in the case of lead telluride, $m \approx m_0$.

For p-type PbSe (curves 4 and 5) $u \propto T^{-3}$, whence $r = -1.5$.

The low temperature range. Figs. 18 and 19 show the temperature dependence of the thermal emf and mobility for a number of specimens of lead telluride and lead selenide with various carrier concentrations ($1 - 0.48 \times 10^{18}$, $2 - 3.8 \times 10^{18}$, $3 - 7.8 \times 10^{18}$) in the temperature range 100–700°K. It is seen from these figures that at temperatures below 200°K the temperature dependence of the thermal emf deviates from the theoretical curve constructed according to expression (32) (hatched curve) and the temperature dependence of the mobility deviates from the

law (103). The higher the carrier concentration, the higher the temperature at which the deviations from the laws established in the preceding paragraph are observed.

These deviations can be attributed to two causes: (a) the onset of degeneracy, and (b) a change in the scattering mechanism, i.e. transition from scattering by thermal lattice vibrations to scattering by ionised impurities.

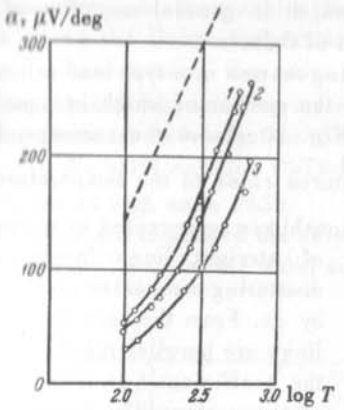

Fig. 18

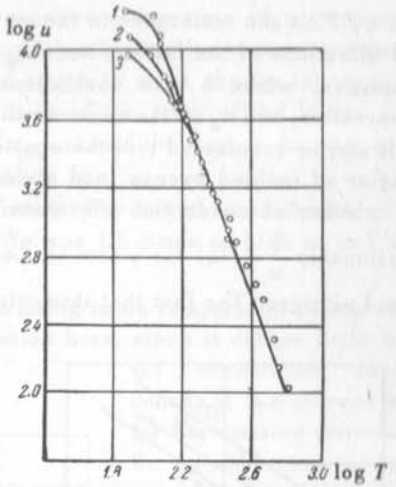

Fig. 19

The carrier concentration in the investigated specimens varied from $n_1 = 10^{18}$ to $n_2 = 10^{19}\,\text{cm}^{-3}$.* At these concentrations one would expect the onset of degeneracy at low temperatures. Since the carrier concentration in the investigated specimens varied by a factor of more than 10, the temperatures of the onset of degeneracy should also have been quite different:

$$\frac{T_1}{T_2} = \left(\frac{n_1}{n_2}\right)^{3/2}.$$

In reality, the changes in the temperature dependence of the mobility took place, for all specimens, within a narrow temperature range. Therefore, the cause of the departure of the experimental temperature dependence of the thermal emf from the theoretical dependence cannot be attributed to degeneracy.

* E. Z. Gershtein, T. S. Stavitskaya and L. S. Stil'bans (*Zhur. Tekh. Fiz.*, 27, No. 11, 2472–2483, 1957) later extended this range to 5×10^{17} to 2×10^{20} (Translator's note).

The carrier mobility, for scattering by thermal vibrations only, decreases with decrease of temperature so one would expect that scattering by lattice defects should become more noticeable at low temperature. The reciprocal of the mobility should then represent the sum of two terms:

$$\frac{1}{u} = aT^3 + bn_d , \qquad (104)$$

where aT^3 is the resistance to the movement of electrons due to the thermal vibrations of the lattice, and bn_d the resistance due to scattering by impurities, where b is a coefficient which in general may depend on temperature, and n_d is the concentration of defects.

It may be considered that the scattering centres in n-type lead telluride consist of ionised excess lead atoms, the number of which is equal to the number of conduction electrons. Fig. 20 shows the corresponding relationship $\frac{1}{u} = f(n)$ for a few temperatures close to the temperature of liquid nitrogen. The fact that this relationship is represented by a number of straight lines favours the scattering mechanism postulated by us. From the fact that these lines are parallel it follows that the coefficient b is independent of temperature. The departure of the temperature dependence of the thermal emf from the theoretical value observed in this temperature range may also be related to the change of the character of the scattering of electrons.

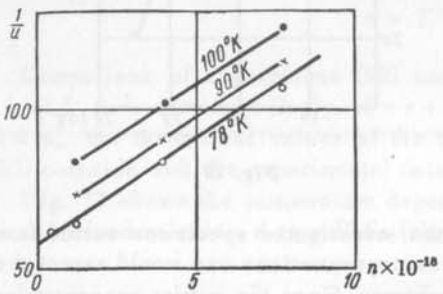

Fig. 20

As has been mentioned earlier, when the mobility follows the law $u = aT^{-3}$, the value of A in expression (32) should be close to unity. For scattering by impurity ions $l \propto \epsilon^2$, which should make the value of A in expression (32) equal to four. To each scattering mechanism there corresponds a certain value of A. The intermediate temperature range, in which the character of scattering changes, should be characterised by a gradual change in the value of A.

Thermoelectric properties of the PbTe-PbSe solid solution. According to equation (37a) the figure of merit of semiconductor thermoelements is proportional to the ratio of the carrier mobility u to the thermal conductivity of the crystalline lattice κ_{ph}. For lead telluride and lead selenide this ratio is relatively high, so these substances are good materials for

the branches of thermoelements. From this viewpoint, an even better substance is the solid solution PbTe-PbSe.

According to the ideas of A. V. Ioffe, at whose initiative a study of the aforementioned system was undertaken, replacement of a certain number of tellurium atoms by selenium atoms in lead telluride must lead to relatively small distortions of the crystalline lattice, owing to the isomorphism of PbTe and PbSe.

These distortions should be very ineffective for the scattering of electronic waves, the length of which reaches a few tens of angstroms at room temperature, but they should be quite effective for scattering thermal lattice vibrations, the wavelength of which is much shorter (at temperatures above the Debye temperature it is of the order of the lattice constant). Consequently, the ratio u/κ_{ph} should be higher for the solid solution than for the starting materials.

Experimental investigation confirmed this hypothesis: the value of u/κ_{ph} in the solid solution PbTe-PbSe was 1.5 times as high as in PbTe and twice as high as in PbSe.

We shall not reproduce the data relating to the temperature dependence of the thermal emf for the solid solution here, since it differs little from the temperature dependence of the thermal emf for the starting materials. We shall confine ourselves only to the discussion of the dependence of the carrier mobility on alloy composition and temperature.

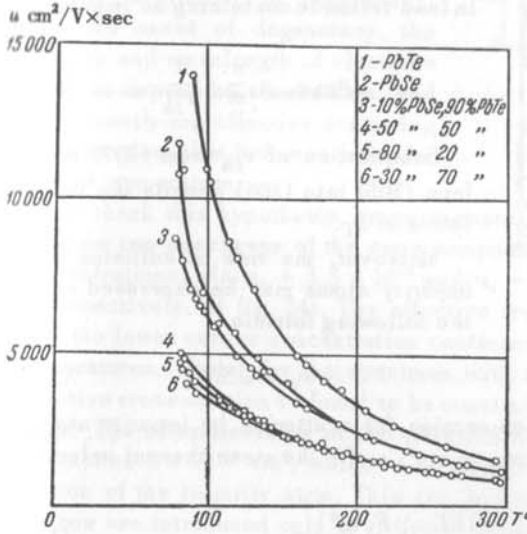

Fig. 21

Fig. 21 shows the dependence of mobility on temperature for specimens of various compositions. It is seen from this figure that the carrier mobility decreases with increasing departure of the composition of the specimens from that of the starting components. An exception here is the 50% PbSe–50% PbTe specimen (curve 4) in which the mobility at low temperatures is higher than in 30% PbSe–70% PbTe (curve 6) and 80% PbSe–20% PbTe (curve 5) specimens. This may

be attributed to the onset of ordering in specimens with 1:1 composition.

Fig. 22 shows the dependence of mobility on composition at various temperatures. These curves permit us to reach certain conclusions concerning the mechanism of electron scattering by neutral defects.

It is known that the carrier mobility for specimens of any composition may be expressed by the following general formula:

$$u = \frac{e}{m} r = \frac{e}{m} \times \frac{1}{\nu}, \tag{105}$$

where r is the relaxation time and $\nu = \frac{1}{r}$ is the number of collisions in a second. For a low percentage of lead selenide in lead telluride, it may be considered, to a first approximation, that the number of collisions per second ν represents the sum of collisions with thermal lattice vibrations ν_{th} and collisions with impurity atoms ν_i

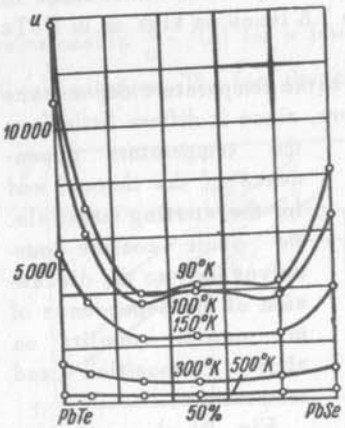

Fig. 22

$$\nu = \nu_{th} + \nu_i ; \tag{106}$$

ν_{th} may be calculated from the mobility in lead telluride containing no impurities

$$u_{\mathrm{PbTe}} = \frac{e}{m} \times \frac{1}{\nu_{th}} . \tag{107}$$

Substitution of ν_{th} from (107) and ν from (105) into (106) permits the calculation of ν_i.

Moreover, the rate of collision with impurity atoms may be expressed using the following formula:

$$\nu_i = \bar{v} S N_i , \tag{108}$$

where S is the effective cross-section for scattering by impurity atoms, N_i the number of impurity atoms in cm³; and $\bar{v}$ the mean thermal velocity:

$$\bar{v} = \sqrt{\frac{2kT}{m}} \times \frac{F_1(\mu^*)}{F_{1/2}(\mu^*)} , \tag{109}$$

where $F_1(\mu^*)$ and $F_{1/2}(\mu^*)$ are Fermi integrals, and μ^* is the reduced chemical potential.

Thus, having found ν_i as a function of temperature from the temperature dependence of the mobility, it becomes possible to obtain the effective scattering cross-section S as a function of temperature

$$S = \frac{\nu_i}{\bar{v} N_i} .$$

Fig. 23 shows the dependence of the effective scattering cross-section on temperature for specimens of different compositions with a carrier concentration $n = 6.5 \times 10^{18}$. It will be seen from the curves that the effective scattering cross-section decreases with decreasing temperature. This fact can be qualitatively explained as a result of the drop in the thermal velocity of electrons, and therefore an increase of the wavelength, with decreasing temperature. At temperatures below 200°K the decrease of the effective cross-section becomes less steep, which can be attributed to degeneracy. With the onset of degeneracy, the velocity and wavelength of electrons cease to depend on temperature, and consequently the effective scattering cross-section also becomes independent of temperature.

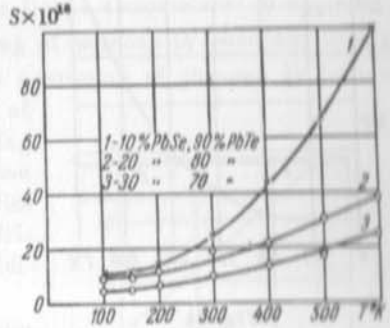

Fig. 23

To check this hypothesis, measurements were made of these relationships for two specimens of the same composition but with different carrier concentrations, viz $n_1 = 1.5 \times 10^{18}$ and $n_2 = 1.5 \times 10^{20}$, (see curves 1 and 2, respectively, of fig. 24). The effective cross-section for the specimen with the lower carrier concentration continues to drop down to the lowest temperatures, whilst for the specimen with the higher concentration the effective cross-section is found to be constant over the entire temperature range. The absolute value of the effective scattering cross-section does not exceed 2×10^{-16} cm², which is at least 10 times less than the cross-section of the impurity atom. This can be explained by the fact that distortions are introduced only by differences between the cross-sections of the impurity and normal atoms of the lattice.

Fig. 25 shows, using logarithmic co-ordinates, the dependence of the effective scattering cross-section on the electron velocity calculated according to expression (109). From the slope of the straight lines we find that

$$S \propto \bar{v}^4 \tag{110}$$

and since $\bar{v} \propto 1/\lambda$ (where λ is electron wavelength), we have

$$S \propto \frac{1}{\lambda^4}. \tag{110a}$$

Thus, in the case investigated here, we have found a formal analogy with Rayleigh's law for the scattering of light in the atmosphere.

Introduction of balanced impurities. We have established that for lead telluride the exponent r in the expression giving the dependence of free path length on energy is equal to 1.5 and, therefore, $A = 0.5$; for impurity ions $r = 2$ and $A = 4$. Therefore by introducing a sufficient amount of impurity ions into lead telluride it is possible to increase the first term in expression (32) by 3.5 units, which corresponds, at a given carrier concentration, to an increase in the thermal emf of

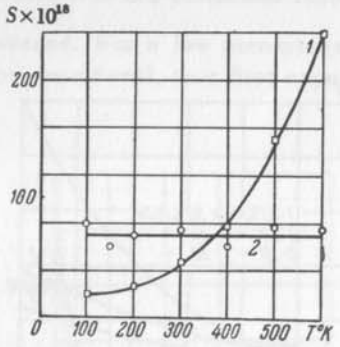

Fig. 24

$$\frac{K}{e} 3.5 = 86 \times 3.5 \approx 300\ \mu\text{V/deg}.$$

On the other hand, introduction of impurity ions brings about a decrease of mobility. Calculations show, however, that by introducing a measured amount of ions it is possible to attain a certain increase of the value of $\alpha^2\sigma$. In order to prevent the carrier concentration from changing it is necessary to introduce simultaneously equal quantities of donors and acceptors, to make both types of impurities balance each other as regards their effect on carrier concentration (hence the term 'balanced impurities').

Initial experiments, aimed at increasing $\alpha^2\sigma$ by the introduction of balanced impurities, carried out on lead telluride, did not yield positive results. Fig. 26 shows the experimentally obtained relationship between the first term in expression (32) and the logarithm of the electron concentration which could be explained by a change in the scattering mechanism. Later on, it was found, however, that

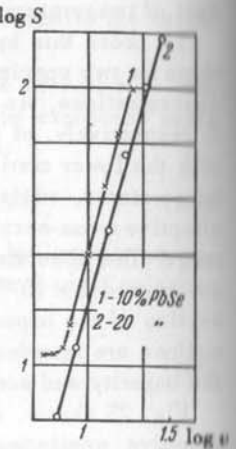

Fig. 25

the curve in fig. 26 served equally well for specimens with balanced and unbalanced impurities. Comparison of the experimental results with theory showed that the increase in the value of the first term in expression (32) was entirely due to degeneracy*.

2.3 Comparison of the theory of thermoelectric cooling with the experimental results.

Study of the temperature dependence of the figure of merit of thermoelements. The temperature dependence of the figure of merit of thermoelements z is governed by the temperature dependence of $\alpha^2\sigma$ and $\kappa = \kappa_{ph} + \kappa_{el}$.

The lattice thermal conductivity κ_{ph} depends on the phonon scattering mechanism. At temperatures above the Debye temperature: 1) $\kappa_{ph} \propto T^{-1}$ in ideal crystals, i.e. for the scattering of phonons by phonons; 2) κ_{ph} is independent of temperature for the scattering of phonons by lattice defects. Intermediate cases may, of course, also occur with both scattering mechanisms participating; in this case the numbers of collisions of phonons with phonons, and with defects, i.e. the reciprocals of the free path lengths, are additive.

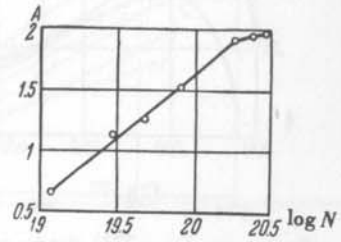

Fig. 26

The electronic thermal conductivity and its temperature dependence at low temperatures are related to the electrical conductivity by the Wiedemann-Franz law. At high temperatures an exciton mechanism of thermal conduction also begins to play an important part. These problems will not be considered here, since they have been discussed in detail in the paper by Ioffe and Ioffe**.

The temperature dependence of the numerator $\alpha^2\sigma$ in the expression for z is governed, according to expressions (32) and (33), by the temperature dependence of the carrier concentration and of the mobility. It has been mentioned earlier that in order that $\alpha^2\sigma$ should preserve its maximum value over a wide temperature range, the carrier concentration should, according to expression (37), rise gradually with temperature: $n_0 \propto T^{3/2}$. However, there are no substances in nature which follow such a law and, therefore, the materials for thermocouple arms consist as a rule of semimetals in which the carrier concentration is constant. Depending on the

* T. L. Koval'chik and Yu. P. Maslakovets, *Zhur. Tekh. Fiz.*, **26**, No. 11, 2417–2431, 1956; E. Z. Gershtein, T. S. Stavitskaya, and L. S. Stil'bans, *ibid*, 27, No. 11, 2472–2483, 1957, consider this in greater detail.

** A. V. Ioffe and A. F. Ioffe, *Izv. Akad. Nauk SSSR, Ser. Fiz.*, **20**, No. 1, 1956.

working temperature range, a suitable number of donors or acceptors is introduced into the semi-metal so as to fulfil condition (37) approximately within this particular temperature range.

Therefore the temperature dependence of $\alpha^2\sigma$ in semi-metals is entirely governed by the temperature dependence of mobility.

The negative arm of the thermoelement may be made of lead telluride in which the mobility is inversely proportional to the cube of the temperature, and the positive arm of antimony telluride with additions of some other materials; for this arm $u \propto T^{-3/2}$. Figs. 27 and 28 show the temperature dependence of $\alpha^2\sigma$ in these two cases for three carrier concentrations giving maxima of $\alpha^2\sigma$ in different temperature ranges, curve 1 at 220°K ($n = 3.5\times10^{18}$) curve 2 at 360°K ($n = 5.5\times10^{18}$), and curve 3 at 400°K ($n = 8.5\times10^{18}$).

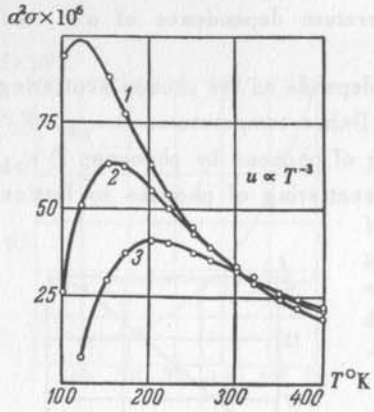

Fig. 27

It is seen from these graphs that the temperature at which $\alpha^2\sigma$ at a given carrier concentration has the highest value need not coincide with the temperature for which this concentration gives the maximum value of $\alpha^2\sigma$; in the first case ($u \propto T^{-3}$) these temperatures differ by a factor of 2, whilst in the second case ($u \propto T^{-3/2}$) they coincide.

Figs. 29, 30, and 31 show, respectively, the temperature dependences of α, σ, and $\alpha^2\sigma$ for six specimens of lead telluride with different carrier concentrations. Fig. 32 shows a comparison with the theoretical relationship of the experimentally determined temperature dependence of $\alpha^2\sigma$ for specimens No. 2 and No. 5.

Figs. 33, 34, and 35 show similar curves for three specimens of antimony telluride, and fig. 36 gives a comparison between experimental and theoretical relationships.

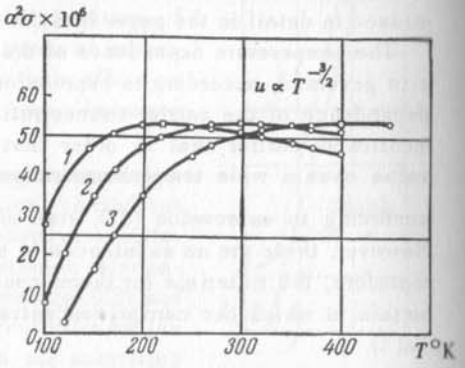

Fig. 28

These curves indicate qualitative agreement between the theoretical and experimental data, as well as substantial discrepancies, the explanation of which requires further study.

Measurement of the coefficient of performance and the maximum temperature drop. Tests on the thermoelements were carried out with the apparatus shown in fig. 37.

The thermoelement 7–7 was placed inside a brass bell jar 1 with a rubber vacuum seal at its base 14. The leads for the measuring thermocouples 2 and 3 (copper–constantan) were taken out through the vacuum seal at the base of the bell jar (not shown on the drawing). In the upper part of the bell jar there was a connection 4 to a forevacuum pump. On the outside of the bell jar, on an asbestos sheet, was wound a nichrome wire heater 5. The temperature of the wall of the bell jar was measured with the thermocouple 6.

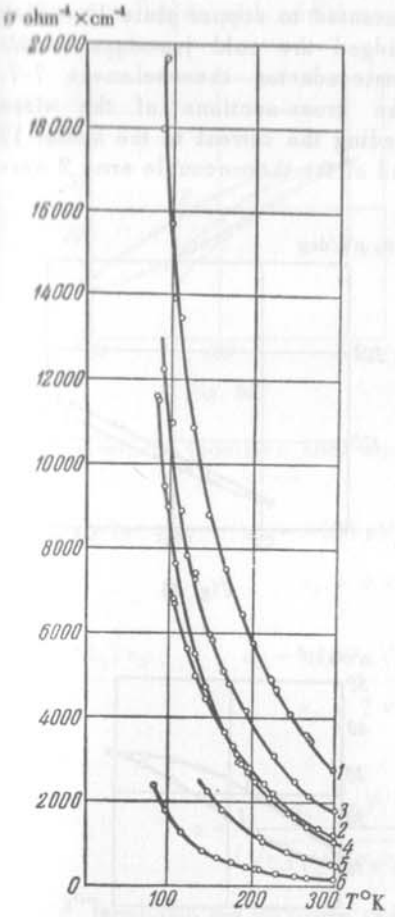

Fig. 29

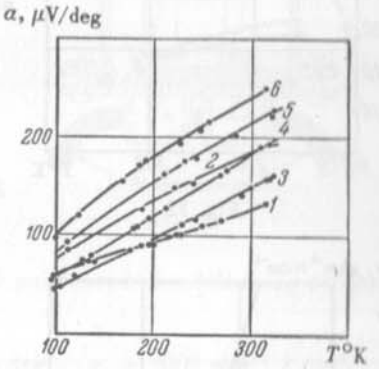

Fig. 30

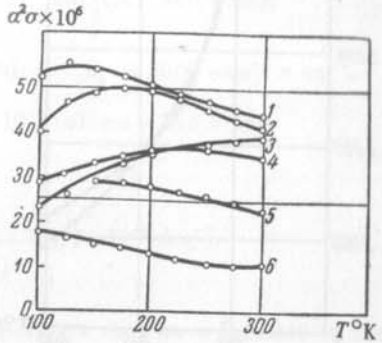

Fig. 31

The semiconductor thermoelement under investigation 7 was soldered to two brass bolts 8 insulated from the base. The heads of these bolts consisted of the chambers 9, through which was circulated a heat-absorbing liquid from a thermostat. The temperature of these chambers was measured with the thermocouple 10. A small constantan heater 12 providing the working load was cemented to copper plate 11, which bridged the cold junctions of the semiconductor thermoelement 7–7. The cross-sections of the wires feeding the current to the heater 12 and of the thermocouple arms 2 were

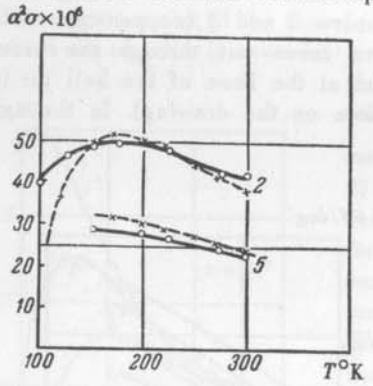

Fig. 32

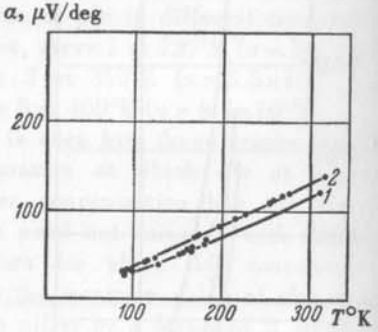

Fig. 33

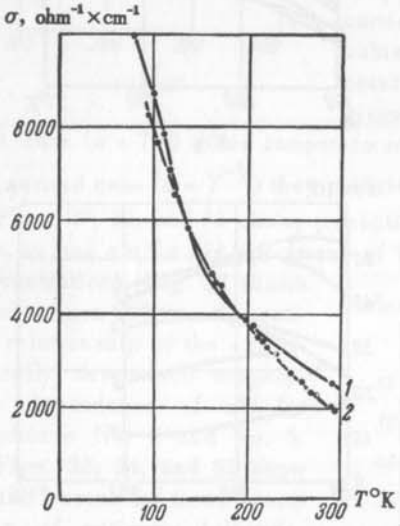

Fig. 34

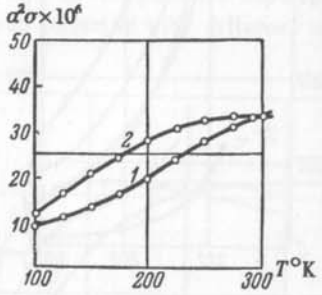

Fig. 35

selected so as to make the heat flux along their length negligible; the entire heat generated by the heater was therefore transferred to the cold junction of the thermoelement. Contacts 13 inserted through the vacuum seal served for introducing the current and measuring the voltage drop across the thermoelement under operating conditions.

During the experiments simultaneous readings could be taken of the hot junction temperature T_0, the cold junction temperature T_1, the heater power consumption W, the current through the thermoelement I, and the voltage drop across the thermoelement V. The thermoelement consisted of lead telluride (negative arm) and antimony telluride with additions of

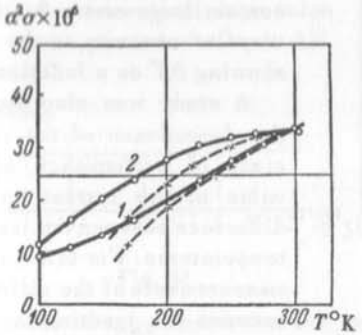

Fig. 36

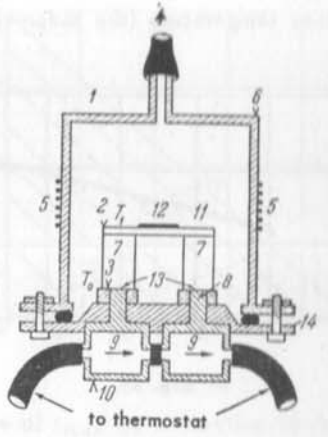

Fig. 37

other elements (positive arm) and possessed the following properties:

PbTe: $\alpha_1 = -130\ \mu V/deg$, $\sigma_1 = 2000\ ohm^{-1} \times cm^{-1}$, $\kappa_1 = 9 \times 10^{-3}$ cal/cm × sec × deg;

Sb_2Te_3: $\alpha_2 = +130\ \mu V/deg$, $\sigma_2 = 2000\ ohm^{-1} \times cm^{-1}$, $\kappa_2 = 7 \times 10^{-3}$ cal/cm × sec × deg.

Hence

$$z = \frac{(\alpha_1 - \alpha_2)^2}{(\sqrt{\kappa_1\rho_1} + \sqrt{\kappa_2\rho_2})^2} = 1.2\times10^{-3}\ deg^{-1}.$$

Fig. 38 shows the maximum temperature drop as a function of the hot junction temperature; the hatched line is the theoretical curve constructed on the basis of expression (16) taking into account the temperature dependence of z. It is seen from the graph that there is good agreement between the theoretical and experimental data.

The temperature drop across the thermoelement was also investigated as a function of the working current at different hot junction temperatures

(fig. 39). In fig. 40 a comparison is made between the experimental results (full lines) and theoretical relationships (hatched lines) for hot junction temperatures of +45°, +15°, and −30°C.

Fig. 41 shows the dependence of the optimum current on the cold junction temperature (the theoretical curve is shown by a hatched line).

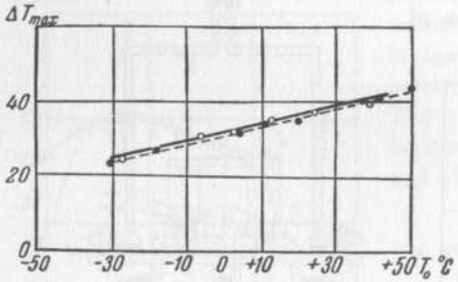

Fig. 38

It should be noted that the experimental values of I_{opt} contain large errors due to the very flat maximum on the curve showing ΔT as a function of I.

A study was also made of the dependence of the coefficient of performance on the value of the current and the difference between the junction temperatures. For this purpose measurements of the difference between the junction temperatures ($\Delta T = T_0 - T_1$) were made as a function of the load (the load was provided by the heater mounted at the cold junction). Variations of ΔT_0 (temperature difference in the absence of load) were achieved by adjusting the value of the current flowing through the thermoelement; measurements were also made of ΔT as a function of the load Q_0 at constant values of I.

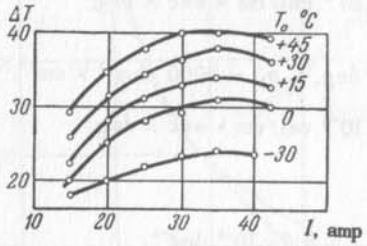

Fig. 39

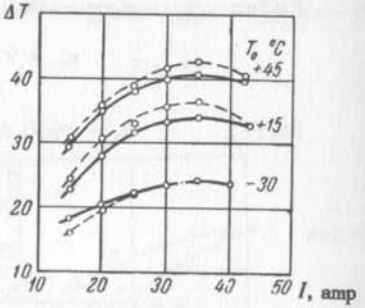

Fig. 40

According to equation (10) these relationships should be linear:

$$\Delta T = \Delta T_0 - \frac{Q_0}{K}.$$

The thermal conductivity of the thermoelement could be determined from the slope of these straight lines.

Fig. 42 shows a family of such lines for a thermoelement operating at a hot junction temperature $T_0 = +45°C$. The lines are parallel to each other. From the points of intersection of these lines with lines parallel to the axis of abscissae it is possible to determine the experimental dependence of ϵ on I at given T_0 and T_1 and to compare it with the theoretical expression (14). Having found, for each ΔT,

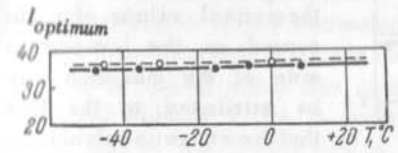

Fig. 41

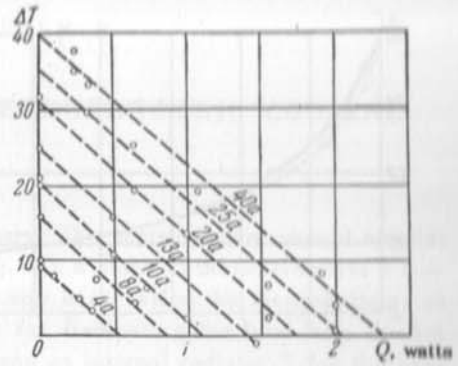

Fig. 42

the value of ϵ_{max} and drawn the curve of ϵ_{max} as a function of ΔT, the latter could be compared with expression (19).

Fig. 43 shows the experimental dependence of ϵ on I, with the values of ΔT°K marked by the side of each curve. The maximum of these curves shifts towards lower currents with decreasing ΔT.

In fig. 44 a comparison is made between the theoretical (hatched lines) and experimental (full lines) dependences of ϵ on I for $\Delta T_1 = 20°$ and $\Delta T_2 = 12°$. For $\Delta T_1 = 20°$ ϵ_1 was also measured directly as a function of I; this was done by

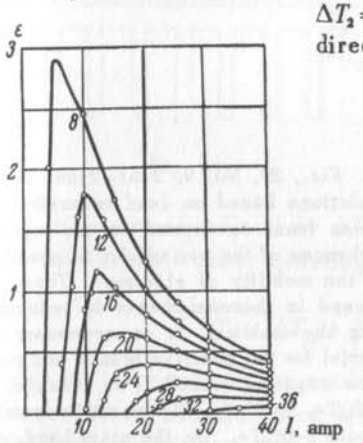

Fig. 43

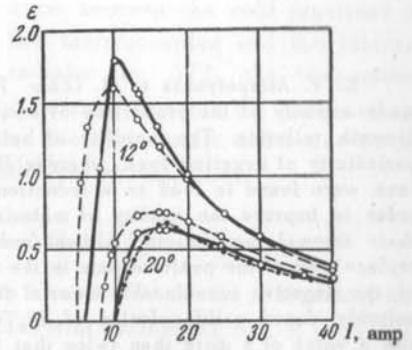

Fig. 44

varying I and Q_0 and maintaining ΔT constant and equal to 20°, and then calculating ϵ for each Q_0 from the measured values of Q_0, I, and V. This

curve is shown in fig. 44 by dashes and dots. It is seen that the two experimental curves corresponding to $\Delta T = 20°$ are in good agreement. The theoretical curve for $\Delta T = 20°$ has an identical shape, but lies everywhere above the experimental curve; the theoretical curve for $\Delta T = 12°$ is slightly below the theoretical curve.

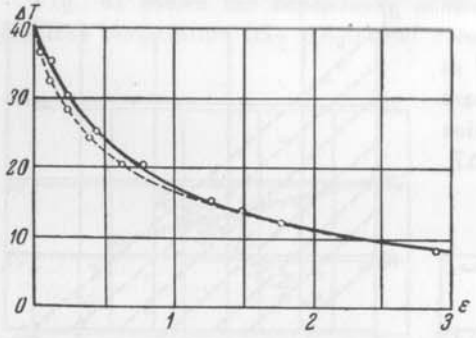

Fig. 45

The large discrepancies between experimental and theoretical values of ϵ observed on the low-current side of the maximum may be attributed to the fact that the errors in calculating ϵ are found to be much higher in this region.

Fig. 45 shows the experimental (full line) and theoretical (hatched line) dependences of ϵ_{max} on ΔT for the temperature range $T_0 = 45°C$ to $T_1 = +5°C$; the two curves are in good agreement.

On the basis of the evidence presented in this chapter it may be concluded that all the postulates listed in the preceding chapter, i.e. all the postulates of the theory of thermoelectric cooling, are in good agreement with experiment.

S. V. Airapetyants et al. (*Zhur. Tekh. Fiz.*, **27**, No. 9, 2167–2169, 1957) made a study of the properties of solid solutions based on lead telluride and bismuth telluride. The mobility of holes was found to depend on the regular periodicity of negative ions, whereas disturbances of the periodicity of positive ions were found to lead to a reduction of the mobility of electrons. Thus, in order to improve the quality of materials used in thermoelements by reducing their thermal conductivity without reducing the mobility, it is necessary to replace part of the positive ions in the material for the positive branch and part of the negative ions in the material for the negative branch. For example, a suitably doped solid solution of Bi_2Te_3–Sb_2Te_3 used for the positive branch has a value of z more than twice that for pure p-Bi_2Te_3. On the other hand, as shown by S. S. Sinani and G. N. Gordyakova (*Zhur. Tekh. Fiz.*, 26, No. 10, 2398–2399, 1956), 80% at. Bi_2Te_3–20% at. Bi_2Se_3 solid solution doped with 0.05% wt. CuBr has a value of z of around 2.5 and is eminently suitable for negative branches. (Translator's note)

CHAPTER 3

APPLICATIONS OF THERMOELECTRIC COOLING

3.1 Domestic refrigerators.

Construction of the thermobattery. The thermobattery should consist of the following main elements (fig. 46): a block of thermoelements 3 connected in series, which has until now been called the thermobattery, an external radiator 1, i.e. a device for dissipating the heat from the hot junctions of the thermocouples; and an internal radiator 2 for the heat exchange between the cold junctions and air inside the refrigerated chamber. We shall denote the temperature drop of the air inside the chamber with respect to the temperature of the surroundings by ΔT_A, the temperature difference between the internal radiator and air in the refrigerated chamber by $\Delta T'_B$, the temperature difference between the external radiator and the surrounding air by $\Delta T'_C$, the temperature difference between the cold junctions of the thermocouples and the internal radiator by $\Delta T''_B$, the temperature difference between the hot junctions and the external radiator by $\Delta T''_C$, and the temperature difference across the thermocouple under operating conditions by ΔT_0. Then

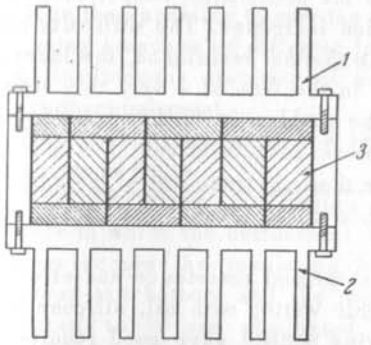

Fig. 46

$$\Delta T_0 = \Delta T_A + \Delta T'_C + \Delta T'_B + \Delta T''_C + \Delta T''_B .$$

Since ΔT_A depends on the conditions of operation of the refrigerator and the coefficient of performance decreases with increasing ΔT_0, it is obvious that the main problem in the construction of a battery is the reduction of the detrimental temperature drops $\Delta T'_C$, $\Delta T'_B$, $\Delta T''_C$ and $\Delta T''_B$.

Thermal contacts between radiators and thermoelements. The simplest way to eliminate $\Delta T''_C$ and $\Delta T''_B$ completely consists of soldering a copper or an aluminium plate to each internal and external thermoelement junction.

In this case the radiators would consist of a number of plates insulated from each other.

This design, which was used in the first thermobattery models, has a number of important shortcomings. Firstly, the free end of the plate forms a large lever with respect to the junction of the thermoelement, and therefore accidental contact with the plate may disturb commutation. Secondly, the current consumed by the thermoelement decreases with the decreasing cross-section area of the branches and such a construction makes it impossible to reduce this area, since when this is done the distance between the plates becomes too small for satisfactory heat exchange; the reduction of area is desirable from the point of view of selecting economical power supply sources. Finally, this design does not make it possible to extend the surface of the radiators sufficiently and thus keep the values of $\Delta T_C'$ and $\Delta T_B'$ within acceptable limits.

Good thermal contact between the stages of a multi-stage battery and between the batteries and the radiators is relatively difficult to achieve, particularly at high thermal loads, when the detrimental temperature drop across the layers of electrical insulation increases. The difficulty lies in the fact that, in order to decrease the thermal resistance, the layer of the electrical insulation must be made in the form of a very thin strong film with high thermal conductivity. The problem is further complicated because conventional electrical insulators have relatively low thermal conductivities. Moreover, in spite of the thorough treatment of the surface of the radiators and the batteries, thin films (even mica plates) are pierced under high loads.

Tests were carried out in which the thermal resistance and strength of thin films (mica, teflon, vinyl chloride wetted with oil, silicone varnishes) were investigated. The following method gave good results. A mica plate, 20–30 μ thick, was inserted between the radiators and the thermobattery after wetting it on both sides with a silicone varnish containing a suspension of aluminium powder. The radiators were then drawn together with the aid of bolts screwed into ebonite plates. Measurements showed that with this construction $\Delta T_B''$ did not exceed 0.5°, and $\Delta T_C''$ did not exceed 1–2°. The lowest thermal resistance was exhibited by films prepared from FG–9 silicone varnish containing 6% aluminium powder. The films were deposited on the surface, and dried for two hours in a thermostat in which the temperature was gradually raised from 50° to 200°C.

Detrimental thermal resistances across insulating layers between two stages may be avoided by the simultaneous sintering of two-stage thermoelements.

As has been mentioned earlier, the first (lower) stage should have a refrigerating capacity of

$$Q_1 = Q_2 \left(1 + \frac{1}{\epsilon_2}\right).$$

At $\epsilon_1 = \epsilon_2 = \epsilon$ we find

$$W_1 = \frac{Q_1}{\epsilon}$$

and

$$W_2 = \frac{Q_2}{\epsilon},$$

and therefore

$$\frac{W_1}{W_2} = \frac{l_2}{l_1}\bigg|_{S=\text{const}}$$

It is thus possible to vary the ratio of the capacities of the two stages by using branches of different length, which makes it possible to carry out simultaneous sintering of a two-stage thermoelement.

The construction of such a battery is shown in fig. 47.

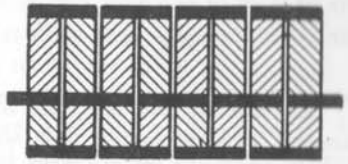

Fig. 47

Fig. 48 shows the design of a battery in which the detrimental resistances across the insulating layers between the battery and the radiator attached to it are eliminated. The junction electrodes also perform the function of heat transfer radiators.

In the preparation of such a battery it is necessary to take into account the electrical resistance of the electrode-radiators, which should not constitute more than 2–3% of the resistance of each thermoelement.

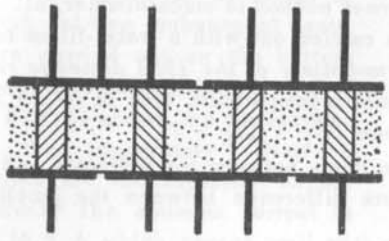

Fig. 48

Calculations show that the design of the external radiator as shown in fig. 46 is unsatisfactory and it should be modified so as to increase the area of the surface on which the fins are mounted by at least 5 times as compared with that for the first prototype refrigerator. A variation of such a design is shown in fig. 49. The base 1 of the external radiator 2

represents a solid aluminium plate, a tank filled with a liquid, or a tank in which heat exchange is achieved by evaporation and condensation of some liquid. The base of the tank is in contact with the hot junctions of the thermobattery 4, whilst an internal radiator 3 is pressed against the cold junctions.

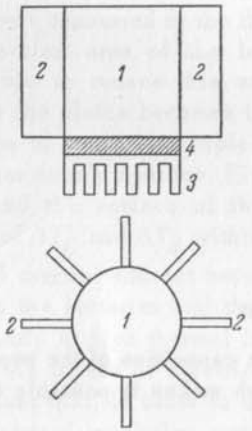

Fig. 49

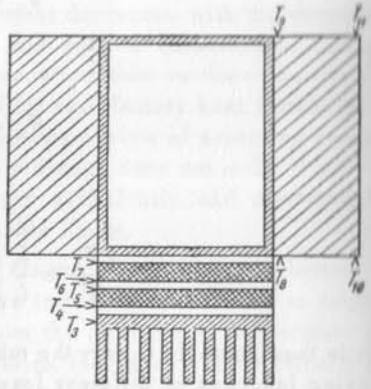

Fig. 50

The second and the third of these alternatives were tried out. In the second alternative the tank was filled with water and in the third with saturated steam. In the last case the tank containing a small amount of water (approx. 100 cc) was evacuated. Under these conditions a high rate of heat transfer was ensured owing to the fact that the water "boiled" at the bottom of the tank and condensed at its side walls.

It was found that under operating conditions the temperature drop across the tank filled with water was only slightly higher than in the tank filled with steam. Since the former method is much simpler, all subsequent tests on refrigerators were carried out with a water-filled tank.

Design calculations for the thermobattery of the 1953 domestic refrigerator. Domestic refrigerators require a temperature drop of $\Delta T_A \approx 25°$. Conforming with previous calculations $\Delta T_C = \Delta T_B = 5°$.

Thus, neglecting the temperature drops between the radiators and the thermocouple block, the temperature difference between the junctions should be

$$\Delta T_0 = 25° + 5° + 5° = 35°.$$

The materials from which the thermobattery was constructed had the following characteristics: $a = 150$ μV/deg, $\sigma = 2000$ ohm$^{-1} \times$ cm^{-1}, $\kappa = 9 \times 10^{-3}$ cal/cm $\times$ sec $\times$ deg, $z = 1.23 \times 10^{-3}$ deg^{-1}; assuming $\Delta T = 35°$ we find from equation (19) that $\epsilon_0 = 14\%$, which cannot be regarded as satisfactory and indicates the need for employing two stages. Assuming $\Delta T_1 = \Delta T_2 = 17.5°$ we find for the individual stages $\epsilon_1 = \epsilon_2 = 75\%$ and for both stages $\epsilon = \dfrac{\epsilon_1}{2 + \dfrac{1}{\epsilon_1}} \approx 22\%$. Assuming the refrigerating capacity of the thermobattery to be equal to $Q_0 = 5$ W, we find that the total power required by the thermobattery is $W = Q_0/\epsilon = 23$ W; for the higher stage $W_1 = Q_0/\epsilon_1 = 7$ W and for the lower stage $W_2 = W - W_1 = 16$ W. The voltage drop across each thermoelement will be $v_0 = 0.03$ V (see equation (18)).

Assuming the power supply voltage $V = 1.4$ V and the thermoelement length $l = 2$ cm, we find from equation (70a) that the number of thermoelements $N = 46$ (for the higher stage $N_1 = 14$ and for the lower stage $N_2 = 32$), the cross-section area of the arms $S_1 = S_2 = 1$ cm^2, and the operating current $I = W/V = 16$ A.

This concludes the calculations for the thermobattery. From design considerations the number of thermoelements was modified to $N_1 = 15$ and $N_2 = 28$. Fig. 50 shows the assembled cooling unit schematically, and the positions of the thermocouples during tests (see table 2).

Tests on the refrigerator. Following an agreement on the co-operation of the Institute for Semiconductors of the Academy of Sciences of the U.S.S.R. and the Leningrad Technological Institute for the Refrigeration Industry, the latter constructed a 10 litre cabinet designed to include the above-described battery. Heat transfer by conduction in this cabinet under operating conditions was accurately measured by the workers of the Refrigeration Institute and found to be equal to 0.053 cal/deg; subsequent tests were carried out on the battery mounted in this cabinet.

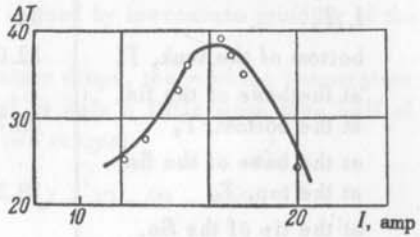

Fig. 51

Fig. 51 shows the dependence of the temperature difference across the thermobattery on the current. The optimum current is $I = 16.5$ A which agrees well with the calculated value $I_0 = 16$ A. The temperature difference across the thermobattery was found to be somewhat larger than the calculated value ($\Delta T_0 = 39°$ as compared with the calculated value $\Delta T_0 = 35°$). However, such differences between the

experimental and the calculated values were quite understandable since the initial data were determined with insufficient accuracy.

It is seen from the plot in fig. 51 that a two-stage battery is much more sensitive towards departures of the current from the optimum value than a single stage battery. This can be attributed to the fact that when the current changes the heat balance between the stages is upset: if the current increases, the upper stage generates more heat than the lower one can absorb and, therefore, the temperature difference across the lower stage drops appreciably.

TABLE 2

Time of operation of the cabinet, hrs	1	2	3	4	5	6
Current, A	16	16	16	16	16	16
Voltage, V	1.6	1.6	1.6	1.6	1.6	1.6
Temperature, °C						
room, T_1	24.6	25	25.7	26	26.7	27
inside the cabinet, T_2	10.8	6.3	6.0	3.6	3.9	4
cold junctions of stage II, T_3, T_4	4.5	3.4	0.8	0.3	0.2	0
hot junctions of stage II, T_5	27	25.8	27.8	27.5	28.1	27.7
cold junctions of stage I, T_6	26	25.9	27.2	26.9	27.5	26.8
hot junctions of stage I, T_7	34	36.7	37.3	38	38.6	39.0
bottom of the tank, T_7'	32.0	34.4	35.1	35.4	36.6	36.2
at the base of the fin, at the bottom, T_8	28.7	31.8	32.5	32.9	34.2	34.4
at the base of the fin, at the top, T_9	28.3	30.0	31.8	32.2	33.5	33.7
at the tip of the fin, at the bottom, T_{10}	27.5	29.6	31.2	32.0	32.7	33.3
at the tip of the fin, at the top, T_{11}	28.1	29.8	31.8	32.2	33.5	33.7
$\Delta T_w = T_1 - T_2$	13.8	18.7	20.7	22.4	22.6	23
$\Delta T_0 = T_7 - T_3$	29.5	33.3	36.5	37.7	38.8	39

Table 2 shows the results of tests on the cabinet made with the optimum current over a six hour period. The table does not show the temperatures of the cold junctions and the base of the internal radiator separately, since these were both found to be equal to the temperature T_3 within the accuracy of the measurements. This means that $\Delta T_B'' = 0$. As is seen from the table, the cabinet virtually reaches a steady state four hours after switching on. The temperature in the cabinet drops to +4°C at a room temperature of +27°C.

For comparison, we are giving data relating to the domestic refrigerator manufactured by the Gazoapparat Works of the Ministry of the Meat Industry of the Russian S.F.S.R. This refrigerator (model XIII-1A) provides a temperature drop of the air inside the cabinet to +8°C 4 hours after switching on, when the temperature of the surroundings is +30°C. The coefficient of performance is $\epsilon \approx 18\%$.

Let us calculate the coefficient of performance of the thermoelectric refrigerator described above. As has been mentioned earlier, the heat transfer by conduction into the cabinet is 0.053 cal/deg. Therefore, for a temperature difference of 23°, the heat flow into the cabinet amounts to $Q_0 = 0.053 \times 23 = 1.22$ cal = 5.1 W. The coefficient of performance is thus

$$\epsilon = \frac{Q_0}{W} = \frac{5.1}{1.6 \times 16} = 20\%.$$

Our calculations yielded the value $\epsilon = 22\%$.

The data in table 2 show that there was a large number of detrimental temperature drops at the interfaces within the thermobattery, partly due to design faults. The temperature differences over the fins $T_8 - T_{10}$ and $T_8 - T_9$ were partly due to lack of care in the design; the temperature difference $T_7 - T_8$ was due to faulty soldering of the fins; the temperature differences $T_5 - T_6$ and $T_7 - T_7'$ were caused by inaccurate grinding of the contact surfaces.

Owing to these detrimental temperature drops, the working temperature difference ΔT_w was found to be equal to only a little more than half of the total temperature drop across the two stages:

$$\Delta T_0' = (T_7 - T_6) + (T_5 - T_4) = 12 + 28 = 40°.$$

A reduction of the sum of the detrimental temperature drops $\Delta T_0 - \Delta T_w$ would have led to an increase of the value of the coefficient of performance to 30%.

Further increase of the coefficient of performance would require an improvement of the thermoelectric properties of the thermocouple arms, i.e. a higher value of z.

Latest thermoelectric refrigerators. The tests on the 1953 thermoelectric refrigerator showed that even with the materials available at that time it was quite feasible to construct a refrigerator with a refrigerated chamber of large volume.

In 1954 work started (also in conjunction with the Leningrad Technological Institute for the Refrigeration Industry) on the construction of a thermoelectric refrigerator with similar technical and economical characteristics to those of existing absorption refrigerators. The refrigerator consisted of a wooden cabinet with a 55 litre capacity refrigerated chamber. The thickness of insulation of the cabinet walls, outside the region where the thermobattery was housed, was equal to 120 mm.

The quality of the cooling thermoelements at that time was improved, which permitted the dissipation of heat from the hot junctions of the thermobattery by natural air convection using a system of radiators. In these refrigerators use was made of PbTe–PbSe alloys (negative branch) and an alloy, the principal constituents of which were tellurium and antimony (positive branch).

Specimens were prepared by the methods of powder metallurgy (sintering at a temperature of 400°C and a pressure of 4–6 tons/cm²). Die-casting and directional crystallisation can also be used successfully for the preparation of thermoelements.

The quality of the thermoelements was controlled by measuring α and σ (by a null method).

There was no necessity in practice to measure the thermal conductivity κ, since the thermal conductivity of the crystalline lattice of the substances employed in the construction of the thermocouples varied very little from one batch to another.

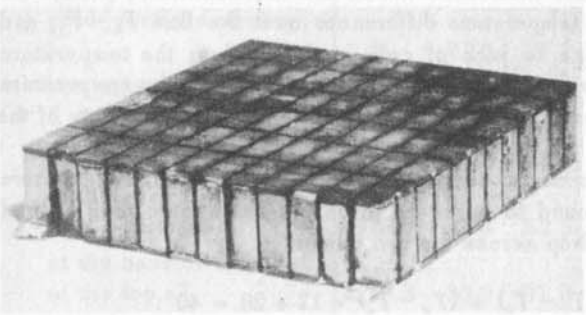

Fig. 52

The specimens were tinned with a special alloy (80% Bi–20% Sn) at a temperature of 200°C, following which, copper plate electrodes were soldered to the specimens. It was very important to eliminate any electrical contact resistance between the electrode and the specimen. The contact resistances were measured by a null method (using alternating current).

The batteries were assembled by connecting positive and negative specimens, separated by layers of electrical insulation, in series.

The construction of such a battery is shown in fig. 52. The testing of the completed batteries consisted of the measurement of ΔT_{max} in vacuo.

The tests showed that the thermobatteries prepared for the refrigerators gave an average maximum temperature drop of 47°C (from +40°C to −7°C). It should be noted that the latest thermoelements, prepared at the Institute for Semiconductors of the Academy of Sciences of the U.S.S.R. from new alloys, give a much greater temperature drop (approximately 70°C) for the same hot junction temperature.

Tests were also carried out on a single-stage and a two-stage battery subjected to a heat load in vacuo. The heat load was applied from a plane electrical heater pressed against the cold junction of the battery but separated from it by a layer of mica.

These tests made it possible to assess the coefficient of performance of the battery, determined as a ratio of the power supplied to the heater W_f to the power consumed by the battery W_b:

$$\epsilon = \frac{W_f}{W_b}$$

for various currents I flowing through the battery.

The radiators fitted to the hot junction were made of copper and mounted in a row on the top parts of the rear and side walls. The design of the radiators ensured a temperature difference between them and the surroundings of not more than 4–5°. The internal cooling radiators were made of aluminium and arranged in a similar row on the upper part of the back wall of the refrigerated chamber. The surface area of the cooling radiators was 1.4 m² and of the heat dissipating radiators was 3.8 m².

The appearance of the cabinet is shown in fig. 53 and its cross-section in fig. 54.

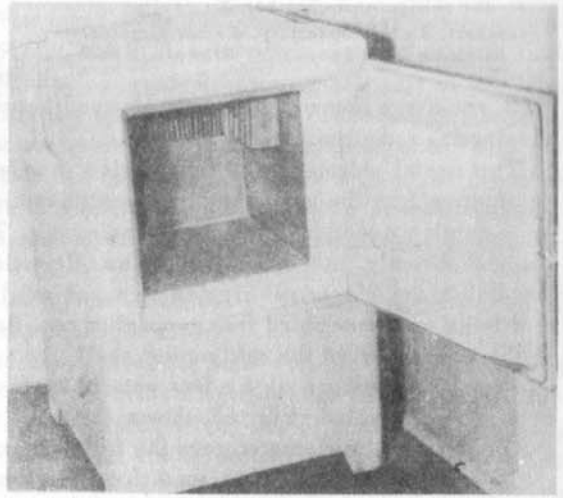

Fig. 53

Four sets of two-stage thermobatteries with a total refrigerating capacity of Q_0 = 20 kcal/hr were constructed for the refrigerator. Tests on the refrigerator gave the following results. With a d.c. power consumption of 40 W, a temperature

of −2°C was set up at the centre of the refrigerated chamber and with a power consumption of 30 W the temperature was +2°C. The temperature of the surroundings was +19°C. Steady conditions were set up in the refrigerator after 4–5 hours. Tests on the cabinet showed a real possibility of constructing a thermoelectric refrigerator on a commercia' scale with a more economical operation than that of absorption refrigerators.

A semi-commercial model of a thermoelectric refrigerator was constructed at the beginning of 1956, in conjunction with No. 2 Stamping Works of the Directorate of Local Industry of Leningrad. The design was based on the cabinet of the 'Leningrad' absorption refrigerator. The cooling units consisted of the thermobatteries used in the earlier model. The radiators fitted to the hot junctions were made of aluminium and mounted on the rear wall of the refrigerator. The internal radiators, also of aluminium, occupied the greater part of the back wall of the refrigerated chamber. The cooling unit as a whole consisted of four sets of two-stage thermobatteries.

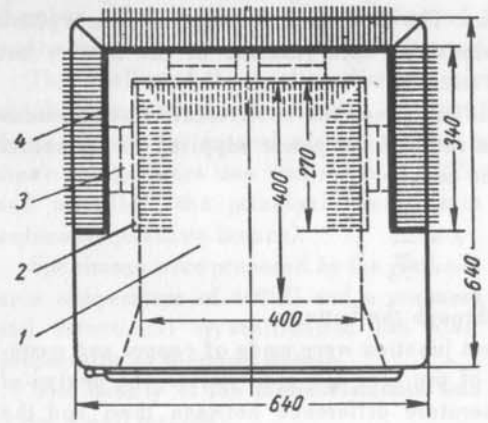

Fig. 54. Diagram of a refrigerator (as seen from above).

1 - the refrigerator chamber, *2* - cooling radiator, *3* - thermobattery, *4* - hot radiator.

Each two-stage thermobattery was clamped between the cooling and heat-dissipating radiators.

The useful volume of the refrigerated chamber was 40 litres. The heat dissipation from the hot radiators was attained, as in the previous model, by natural convection of the surrounding air. The refrigerator could be plugged directly into the 127 V mains. Rectification of the current and smoothing out of current ripples was achieved with the aid of a small rectifying unit assembled from germanium rectifiers. This unit was placed in the bottom part of the refrigerator shell.

Fig. 55 shows one of the four sets of thermoelements from which the unit was assembled. Fig. 56 shows the back wall of the refrigerator.

Tests on the refrigerator gave the following results:

1) under static operating conditions the temperature at the centre of the refrigerated chamber was equal to 0°, in the lower part of the chamber

−2°, and at the cooling radiators −5°C (at a temperature of the surroundings of 20–22°C);

2) the power consumption (d.c.) of the refrigerator when starting up was 75 W and for steady operation was 55 W;

3) the power drawn from the a.c. mains under steady conditions was 75 W; this power could, however, have been reduced to 65–70 W by using better quality transformers in the rectifying unit.

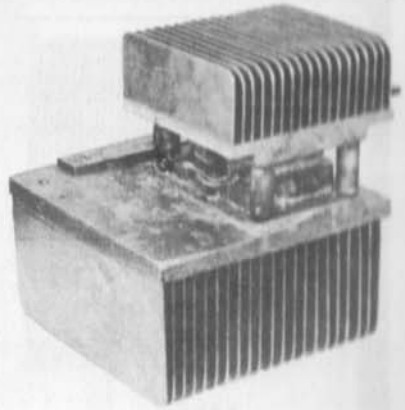

Fig. 55

3.2 Other applications of thermoelectric cooling. As has been mentioned earlier, the first thermoelectric refrigerators were less economical than compression refrigerators, the coefficient of performance of this order could be obtained with thermoelectric refrigerators with the values of z raised to 2.5×10^{-3} to 3×10^{-3} using two-stage cooling, and to 3×10^{-3} using single-stage cooling. Very recently requisite conditions have been created for good quality domestic refrigerators. Refrigerators tested in TU-104 passenger jet aeroplanes were found to give satisfactory service. Similar refrigerators are being developed for the railway transport.

However, even at the present time, there is an ever increasing number of fields of application in which semiconductor thermoelements have undisputed advantages over other cooling systems. We have in mind cases when it is necessary to cool small objects representing a thermal load of a few watts. Even the smallest contemporary cooling unit of any type will weigh much more than the cooled object and consume not less than 20–30 W of electrical power, whereas a cooling thermoelement with the same refrigerating capacity may weigh as little as 5–10 g and consume less than 1 W. Important factors here are the absence of rotating parts, such as are used in compression refrigerators, low inertia, and practically unlimited service life.

We shall consider now a few examples of possible applications of cooling thermoelements and thermobatteries.

The use of cooling thermoelements in meteorology. The measurement of air humidity is important in meteorological observations and in the control of numerous technological processes. One of the instruments most widely used for this purpose is the condensation hygrometer which relies on the measurement of the dew point for the determination of the relative humidity.

To determine the dew point it is necessary to have a surface, the temperature of which can be gradually reduced until water vapour begins to condense on it, knowing the temperature of the surface at this instant and the temperature of the surrounding air one can determine the humidity.

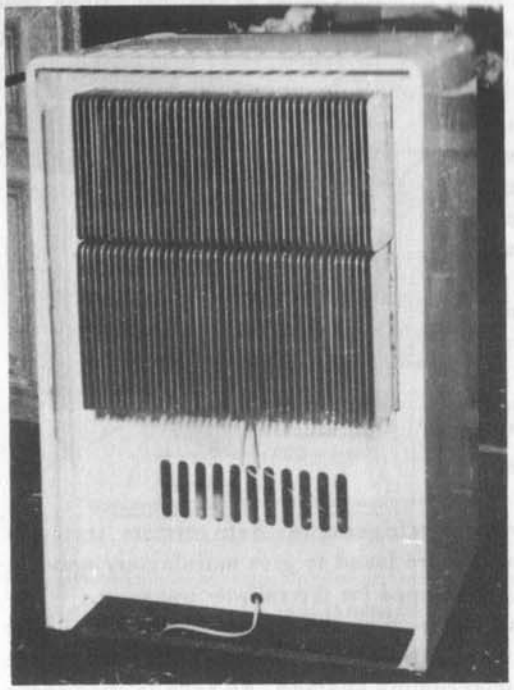

Fig. 56

Until now the working surfaces in various types of hygrometers have been cooled with solid carbon dioxide, a mixture of ice with salt, liquid nitrogen, etc., or by the vaporisation of special liquids (ethers, etc.). This is very inconvenient since it is not always possible, by any means, to employ these substances under field conditions, in polar expeditions, etc.

As a result of collaboration between the Institute for Semiconductors and the Voeikov Principal Geophysical Laboratory, prototypes of an instrument for determining the dew point have now been constructed which employ a semiconductor thermoelement, fed by d.c. from a minute accumulator, as the cooling unit. The cold junction of the thermoelement is provided with a condensation mirror. A beam of light is projected from a small bulb onto the mirror and reflected from it into a special photosensitive relay. When the water vapour begins to condense on the mirror, the reflection coefficient of the mirror changes abruptly, the intensity of the reflected beam of light drops and this actuates the photosensitive relay which changes the direction of the current flowing through the thermoelement. The heat which is now generated at the junction housing the mirror rapidly vaporises the moisture, the intensity of the reflected light again increases and the relay again reverses the direction of the current. With a suitable selection of parameters the entire process takes only a few seconds. Fig. 57 shows a model of such a hygrometer.

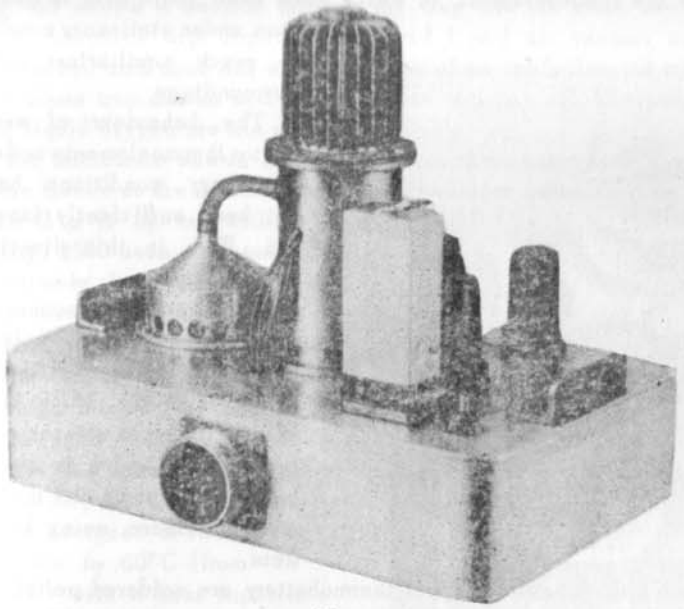

Fig. 57

It should be noted that the inertia of the semiconductor thermoelement may be reduced simply by a reduction of its length, permitting the use of such instruments for meteorological observations from an aeroplane. Another method of reducing the time required for attaining the necessary temperature drop consists of operating the thermoelement under pulsed current conditions. In this case the current pulses substantially exceed the optimum current. The reduction of the time for achieving ΔT_{max} across the thermoelement is due to the fact that the Peltier effect (proportional to the first power of the current) is a surface phenomenon and has a very low inertia, whereas the process of transfer of the Joule heat, generated in the volume of the thermoelement, to the cold junction is characterised by a much higher inertia.

Fig. 58

This last method can only be used, however, when a pulsed temperature drop is required; the pulses should be fed at sufficiently large intervals to allow the thermoelement, in which much more Joule heat is generated than under stationary conditions, to reach equilibrium with the surroundings.

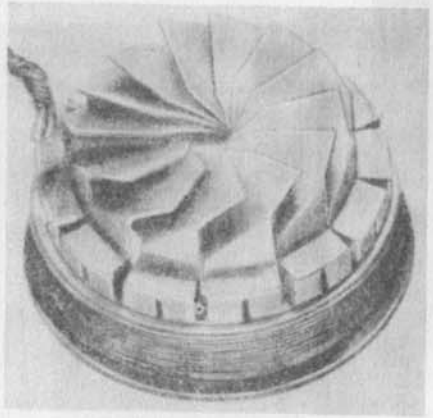

Fig. 59

The behaviour of semiconductor thermoelements under non-stationary conditions has not yet been sufficiently investigated. Work in this direction is continuing.

An oil trap for vacuum pumps developed by E. A. Kolenko at the Institute for Semiconductors is shown in fig. 58. It consists of a cylindrical attachment with two flanges which is connected between the pump and the evacuated enclosure, using lead gaskets.

To the cold junctions of the thermobattery are soldered polished condensing baffles, whilst the hot junctions are in contact with the outer wall (fig. 59). The outer wall is surrounded by a water-cooled jacket. The thirteen baffles are mounted at an angle so that the migrating oil vapour molecules are subjected to multiple collisions. The thermoelectric battery reduces the temperature of the plates to approximately –30°C at a temperature of the surroundings of +20°C.

The thermoelectric battery consumes 10–12 amp at a voltage of 0.6–0.8 V; its power consumption is therefore of the order of 10 W. In the absence of a

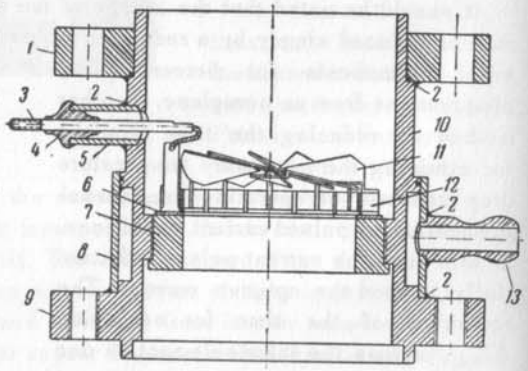

Fig. 60. Section through the trap.

1 and *9* - flanges; *2* - soldered joint; *3* - current terminal; *4* - glass insulator; *5* - Kovar cup; *6* - oxidised aluminium ring; *7* - copper ring; *8* - water jacket; *10* - shell; *11* - cooling baffles; *12* - thermoelectric battery; *13* - cooling water inlet.

* E. A. Kolenko, *Pribory i Tekh. Eksper.*, 1957, No. 3, p. 112.

d.c. source, the trap may be fed by a.c. through a standard selenium rectifier.

Fig. 60 shows a section through the trap and its main components.

When compared with liquid oxygen and liquid air vacuum traps, the thermoelectric unit does not entail the risk of an explosion, as may occur when a glass trap cracks and oxygen mixes with the oil. Moreover, liquid air and liquid oxygen are not always available.

In the microtome shown in fig. 61 a few thermoelements are used to keep the tissue at the optimum cutting temperature permitting sections as thin as 2 μ to be cut without difficulty. 2500 such microtomes have already been distributed.

Low temperature cooling. In 1954 tests were carried out on low temperature cooling with a three-stage thermopile. Thermoelements used for the construction of the thermopile had $z = 1.3 \times 10^{-3}$ deg^{-1}. The thermopile was designed to reduce the temperature by 60°C (from +20° to –40°C) with a heat input to the third stage at –40°C equal to 1 W. The temperature drop obtained from each stage was calculated so that $\epsilon_1 = \epsilon_2 = \epsilon_3 \approx 33\%$.

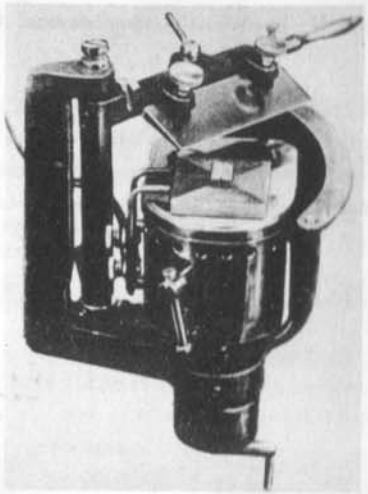

Fig. 61

In this case according to equation (63) $Q_h = 4Q_c$ and therefore $W_1 : W_2 : W_3 \approx 4$.

Table 3 contains data for the calculations for the thermopile.

Column 3 shows ΔT_{max} for the three stages for the specified temperature range, calculated from equation (16). To facilitate the design and also to create some spare cooling capacity, the number of thermoelements in the second and first stages was somewhat increased and amounted to 18 and 72 thermoelements respectively.

As may be seen from table 3, the successive stages had steeply decreasing surface areas. To ensure the requisite heat transfer from the hot junctions of the third and second stages, 10 mm thick copper plates were placed between the stages of the thermopile. Electrical insulation

together with good thermal contact was achieved with the aid of mica sheets. 20 μ thick, wetted with mineral oil. The thermopile stages were

TABLE 3

Stage	ΔT	ΔT_{max}	ϵ, %	Q_c, watt	W, watt	I, amp	V, volts	N, stage	S, cm^2	Weight, gm
I	24°(+20°, – 4°)	42°	32.2	12.4	49.6	16	3.5	64	104	1760
II	21°(– 2°, –23°)	37°	33	3.1	12.4	16	0.79	16	26	440
III	18°(–22°, –40°)	31°	32	1	3.1	16	0.195	4	6.5	110

Note: N - number of thermoelements; Q_c - cooling capacity of the stage.

connected electrically in series in such a manner that the leads joined the cold junction of one stage to the hot junction of the next stage.

Fig. 62 shows the assembled thermopile. As has been mentioned above, the cooling capacity of the third stage at the temperature of –40°C was

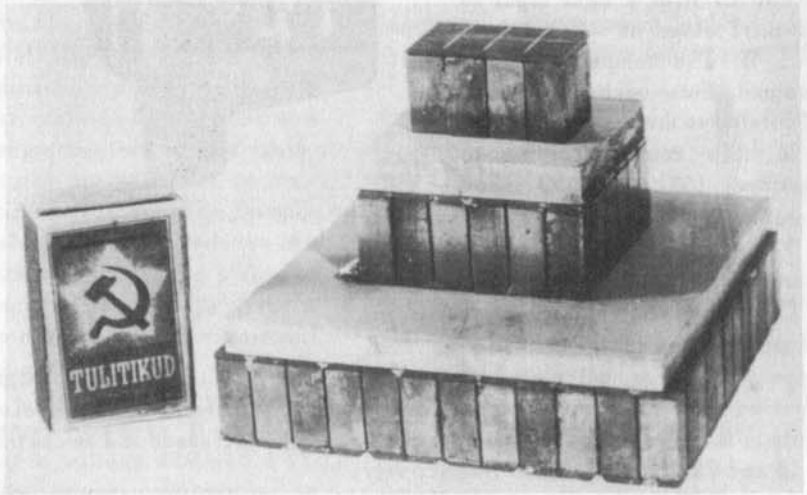

Fig. 62

designed for 1 W only. Such small heat loads can only exist under heat insulation conditions which are close to ideal (i.e. in a high vacuum).

The vacuum apparatus, shown in fig. 63, consisted of a steel base 1 which also served as a radiator dissipating heat generated by the first

stage of the thermopile; the chamber 2 with circulating water for controlling the temperature of the radiator; forevacuum and high vacuum pumps; and a glass bell jar 3. The thermocouples used to measure the temperature of the various portions of the pile were inserted into holes in the flanges 4, and the leads into flanges 5 which were insulated from the base. Good contact between individual stages of the thermopile was achieved with the aid of a special device 6. The very small contact area between the knife edges of the clamping device and the pile (hundredths of a cm^2) made it possible to neglect heat flow to the cold junctions of the third stage.

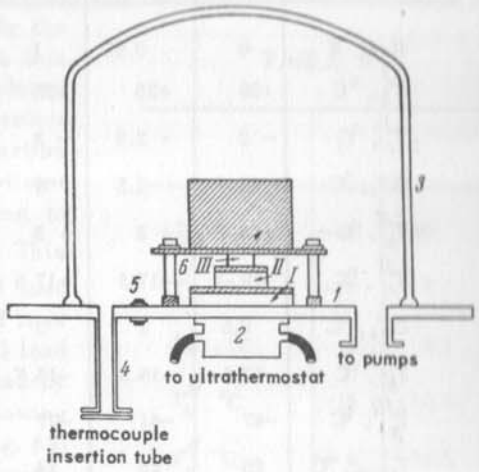

Fig. 63

When it was found necessary to vary the temperature of the radiator by an appreciable amount, container 2 was connected to an ultrathermostat using a circulating liquid cooled with solid carbon dioxide. Copper–constantan measuring thermocouples were connected to the cold and hot junctions of all stages of the thermopile. The effect of a thermal load on the operation of the thermopile was investigated with the aid of a small constantan heater cemented to the cold junctions of the third stage.

Table 4 sums up the results of the measurements of the temperature drops produced by two and three stages of the thermopile, with and without a load, for various temperature intervals.

It will be seen from the table that when the heater was not switched on, the three-stage thermopile produced a temperature drop of 73° (from +26° to –47°C). In this case ΔT of the third stage was 29.5°. ΔT_{max} calculated from equation (16) for the operating conditions of the third stage (at $z = 1.2 \times 10^{-3}$) is equal to 30.6°. This difference seems to be due to a small heat load consisting of the flow of heat along the leads to the heater, the heat absorbed from the radiating surroundings, and the heat conducted by the rarefied air (vacuum of $10^{-3} - 10^{-4}$ mm Hg). Calculations show that the heat load which can be attributed to these factors amounts to 0.1 W.

Table 4 also contains results of tests with thermal loads applied to the thermopile. At loads of 0.55, 1, and 3 W the temperature drop produced by the thermopile was reduced by 7°, 11°, and 29°C respectively.

Columns 5 and 6 show the results obtained with two stages (I and II) of the thermopile in various temperature ranges (cooling from +37°C and from +3°C).

TABLE 4

	1	2	3	4	5	6
Heat, W	0	0.55	1	3	0	0
T_h^I, °C	+26	+25	+25	+33	+37	+ 3
T_c^I, °C	− 2	− 2.5	− 3	+ 6	+ 2.5	−19
ΔT_1, °C	5	5.5	6	4.5	5.5	6
T_h^{II}, °C	+ 3	+ 3	+ 3	+10.5	+ 8.5	−13
T_c^{II}, °C	−18	−17.5	−17.5	− 7.5	−17.5	−39
ΔT_2, °C	0.5	1	2	3	–	–
T_h^{III}, °C	−17.5	−16.5	−15.5	− 4.5	–	–
T_c^{III}, °C	−47	−41	−37	−11	–	–
T_{room}, °C	25	25	24	25	27	26
ΔT_{total}, °C	73	66	62	44	54.5	42
ΔT	72	66	61	36	44.5	–
W_{pile}, W	78	78	75	70	71	68
I_{pile}, A	15.5	15.5	15	14	15	15

Note: ΔT_1 and ΔT_2 are undesirable temperature drops across the insulating layers and plates between stages I and II, and II and III of the thermopile; ΔT_{total} is the difference between room temperature and the temperature of the cold junction of stage III.

It is seen from the table that over the lower temperature range the electric power consumed by the thermopile is somewhat reduced owing to the lower voltage drop across the pile. This is due to the fact that in the material used for the construction of the thermoelement the temperature dependence of the electric conductivity was $\sigma \propto T^{-3/2}$ in the positive arm and $\sigma \propto T^{-5/2}$ in the negative arm. As a result of this the resistance of the pile decreased with the lowering of the temperature.

Two- and three-stage thermopiles were used in experiments consisting of cooling of a cylindrical chamber with a volume of 1300 cm³ having a surface area of 1600 cm². In order to reduce the heat load on the thermopile to a minimum the surface of the chamber was silvered and polished (reflection coefficient approx. 95%). The tests were carried out in a vacuum of the order of 2×10^{-4} to 4×10^{-4} mm Hg. The measuring thermocouple was mounted in the wall of the chamber. Results are reported in table 5.

With a three-stage thermopile the temperature was decreased to 40° below the temperature of the surroundings. As will be seen from table 5 the temperature drop produced by the second and third stages was in this case much smaller than that produced by the first stage and the temperature difference between the hot junction of the first stage and the radiator increased considerably, leading to an increase of T_h^I to +42°C. This demonstrates that the thermal load on the pile was fairly large. If it is again assumed that the thermal load consisted of the heat conducted by the rarefied air, the heat flowing through the clamping rods 6 (fig. 63) and the heat radiated by the surroundings (taking the absorption coefficient of the surface of the chamber to be 0.05), then the calculated total heat load was 2.5 W.

TABLE 5

	1	2
T_h^I, °C	+42	+40
T_c^I, °C	+10	+ 7
ΔT_1, °C	5	3.5
T_h^{II}, °C	+15	+10.5
T_c^{II}, °C	− 6	−16.5
ΔT_2, °C	1	–
T_h^{III}, °C	− 5	– –
T_c^{III}, °C	−17	–
$T_{chamber}$, °C	−15	−16.5
T_{room}, °C	+25	+25
ΔT_{total}, °C	40	41.5

Tests were also carried out on cooling the chamber with the aid of two stages (I and II) of the thermopile. The results were in this case somewhat better (table 5, column 2) mainly as a result of a decrease in the total heat load on the cold junctions of the second stage and the smaller detrimental temperature drops.

Combined cooling. All single-stage refrigerating machines have definite limits of temperature reduction below which further cooling becomes impossible. To achieve lower temperatures use is made of refrigerating machines with two, three, and more stages. The application of semiconductor thermopiles opens up the possibility of constructing combined units in which the first cooling stage is performed by a conventional refrigerating machine and further reduction of the temperature is achieved with the aid of a small size thermopile. In this case the thermopile is mounted in the evaporator of the refrigerating machine.

Such combined units are eminently suitable in cases where the requisite cooling only slightly exceeds the capabilities of a single-stage refrigerating machine. Under these conditions it is in many cases more convenient to use a thermopile than to replace the machine with a bulky two-stage plant.

Several tests on combined cooling were carried out in the Thermoelectric Cooling and Heating Laboratory of the Institute for Semiconductors.

The first stage consisted of the cooling unit of the "ZIS Moskva" electric refrigerator. Cooling to lower temperatures was achieved with the aid of thermopile stages, for which purpose use was made of the stages of the previously described cooling thermopile.

The thermopile was mounted on the bottom wall of the evaporator of the refrigerating unit. Good thermal contact between the hot junction of the thermopile and the base of the evaporator was achieved by covering the base with a low m.pt. alloy (m.pt. = +45°C). The pile was electrically insulated from the base with a layer of mica wetted with mineral oil. A 5 cm thick layer of cotton wool served as thermal insulation between

TABLE 6

	1	2	3	4
T_h^{II}, °C	−24.5	−25	−28	−27
T_c^{II}, °C	−41	−41.5	−45	−43
ΔT_1	0	2.5		
T_h^{III}, °C	−41	−39		
T_c^{III}, °C	−63	−47		
ΔT_2		1.5	2	0
T_h^{IV}, °C		−45.5	−43	−23
T_c^{IV}, °C		−68	−70	−78
ΔT_{pile}, °C	38.5	43	42	51
T_{room}, °C	23	25	24	24
ΔT_{total}, °C	86	93	94	102

Note: ΔT_1 and ΔT_2 are undesirable temperature drops across the insulating layers and plates between the stages of the thermopile; ΔT_{total} is the difference between room temperature and the temperature of the cold junction of the last stage of the thermopile.

the evaporator and the surroundings. When testing the thermopile under no-load conditions, the inside of the evaporator was also packed with cotton wool. A copper container with a volume of 3 litres (surface area of 2.5×10^3 cm²) and a cylindrical chamber with a volume of 0.6 litres served as the low temperature chambers. The thermopile was fed from a d.c. source which was independent of the circuit supplying the power to the compressor-driven refrigerator unit.

The compressor refrigerator unit made it possible to reduce the temperature of the evaporator surface to −30° to −32°C. The results of tests are reported in table 6.

When the compressor unit was used in conjunction with two thermopile stages (II and III) the temperature of the cold junction of the third stage was −63°C at a room temperature of +23°C. With a three-stage thermopile working in conjunction with a compressor unit the temperature of the cold junction of the last stage was −68°C. The last stage consisted of a single thermoelement.

In both the aforementioned cases the stages of the thermopile working under a load gave temperature drops appreciably smaller than the maximum temperature drops. In order to produce still lower temperatures a two-stage thermopile with stages of widely differing power was mounted in the evaporator of the cooling unit. The first stage of the thermopile consisted of 18 thermoelements and the second of a single thermoelement. Under these conditions the loading of the first stage is much smaller, i.e. this stage produces a greater temperature drop.

With a refrigerating unit incorporating such a two-stage thermopile, it was possible to reduce the temperature to −70°C at a room temperature of +24°C (table 6, column 3).

Similar tests were carried out using, for the last stage, a thermoelement with an improved negative arm with z equal to 1.6×10^{-3} to 1.7×10^{-3} deg^{-1} The temperature could then be reduced to −78°C for a room temperature of +24°C, the total temperature drop amounting in this case to 102°C.

Table 7 shows the results of combined cooling of small chambers. Columns 1 and 2 show the data on the cooling of a 3 litre capacity container (with a surface area of 2,500 cm²) with the aid of the first (72 thermoelement) and second (18 thermoelement) stages, respectively. Column 3 gives the data on the cooling of a smaller capacity chamber (0.6 litres) with the aid of the second thermopile stage. Column 4 gives the results of tests on cooling with the aid of both thermopile stages (I and II). The cold junction of the last stage was joined to a copper sheet with a total surface area 900 cm², since the size of the evacuated chamber was such that there was not enough space for mounting the cooling chamber together with a two-stage thermobattery. In this case the thermal

load corresponded to the presence of a chamber with a surface area of 900 cm²; since no heat was generated inside the chambers, the total load depended on the surface area. The temperature at the surface of the sheet was –46.5°C at a room temperature of +25°C. The total temperature drop was 71.5°C.

It is thus possible to reduce the temperatures in chambers of up to a few litres capacity not subjected to thermal loads to –40° to –45°C, using combined cooling with an ordinary refrigerator unit. A modification of the

TABLE 7

	1	2	3	4
T_h^I, °C	–22	–	–	–19.5
T_c^I, °C	–41	–	–	–36
T_h^{II}, °C	–	–25	–24	–35
T_c^{II}, °C	–	–40	–43	–46.5
Chamber				
T_{centre}, °C	–41	–39.5	–42	–46.5
T_{edge}, °C	–40	–38	–41	–46.5
T_{room}, °C	+25	+23	+24	+25
ΔT_{total}, °C	65	61	65	71.5

design of the evaporator, aimed at positioning the main part of the cooling surface in contact with the surface of the hot junction of the thermopile will obviously reduce the hot junction temperature of the thermopile to –30° to –32°C and permit the achievement of still lower temperatures in the chamber.

In principle it is also possible to provide a combination of ordinary and thermoelectric cooling methods with the thermopile serving as the first stage, i.e. with the cold junction cooling the condenser of the refrigerator. In this case the thermopile operates under more favourable

conditions since ΔT_{max} increases with the increase of the temperature of the cold junction and therefore the coefficient of performance of the thermopile for a given temperature drop also increases.

Thermostatic temperature control. The Peltier effect has a reversible character, i.e. when the direction of current flow is changed the cold junction becomes the hot junction, and vice versa. This property permits the use of thermopiles, when necessary, as heating units; from the point of view of power utilisation, up to a certain ΔT_{max}, Peltier heating is preferable to conventional resistance heating. In this case, in addition to the Joule heat generated in the thermopile in the same way as in a conventional heater, heat is also pumped by the Peltier effect from the cold junction to the hot junction. For small temperature differences (10° to 20°C) thermoelectric heating is much more efficient (3 to 4 times) than conventional resistance heating.

One of the important applications of thermopiles will undoubtedly be their use for temperature control.

Semiconductor (principally germanium) devices have found wide application in many branches of radio engineering. They suffer, however, from a very important disadvantage, viz, rapid deterioration of their operating characteristics at temperatures above +50° or +60°C and below –40° or –50°C, which in many cases prevents the conversion to transistor operation of electronic circuits and equipment exposed to overheating.

In 1955, tests were started, with the assistance of Prof. Yu. S. Bykov, on the thermostatic control of small volumes (up to 1 litre) which could house the most vulnerable parts of electronic and other equipment. A pile consisting of 18 thermoelements was used as a temperature stabiliser.

The volume, the temperature of which was stabilised, was the interior of a copper container insulated with a 1 cm thick felt cover. Inside the container was mounted a bimetallic temperature control unit which, through a relay, reversed the current in the thermopile at a temperature inside the chamber of +42°C. The pile operated in this case as a cooler or a heater depending on the direction of current flow. In one arrangement the radiator consisted of an aluminium block (the chassis) with a total surface area of 1500 cm² and a thickness of 1.5 mm, and, in another arrangement, a copper radiator with a surface area of 12,000 cm² was employed.

Tests on controlling the temperature of the chamber with the aid of a pile under still air conditions, using an aluminium chassis as the radiator, gave the following results.

The temperature difference between the hot junction of the thermopile and the inside of the chamber was 42° (+45°, +87°C). It should also be noted that subsequent measurements showed that the temperature inside

the chamber was 3° to 4° higher than at the cold junction of the thermoelement (owing to heat flow from the surroundings through the chamber wall). Thus ΔT for the pile was 45°–47°C. The temperature difference between the inside of the chamber and the surroundings was, under these conditions, only 10° (+45°, +55°C). This was due to the presence of two large detrimental temperature differences:

1) a temperature difference along the chassis (between the area under the hot junction and the edge of the chassis) amounting to 16°–18° and due to the small thickness of the top of the chassis (1.5 mm) and inadequate thermal conductivity of the material from which the chassis was made.

2) a temperature difference between the chassis and the surroundings due to the low thermal conductivity of still air. This temperature difference reached 15°–16°.

To reduce the temperature difference between the chassis and the surroundings measurements were made using a small fan to ventilate the chassis. Under these conditions the temperature difference became much smaller and was only 4° to 4.5°. The temperature difference along the chassis remained, as was expected, practically unaffected. The temperature difference between the inside of the chamber and the surroundings increased to 18° to 19° (+45°, +64°C).

In order to study the possibility of reducing the temperature difference along the chassis tests were carried out on the thermopile–chamber combination after replacing the chassis with a copper radiator of a much larger surface area (12,000 cm²) and a much thicker upper wall (5 mm). The ventilating conditions remained unchanged. In this case the temperature difference along the radiator decreased to 6° to 7° (as compared with 16°–18°). The temperature difference between the radiator and the surroundings decreased to 2.5° to 3° (owing to the larger surface area of the radiator). The temperature difference between the inside of the chamber and the surrounding air increased to 21° to 22° (+45°, +66° to +67°). This relatively small increase of the temperature difference can be attributed to the fact that, for temperature differences of this magnitude, the pile operated under a large thermal load (with the available insulation the heat load for $\Delta T = 15°$ or 20° was 6 to 7 watts). A further increase of the useful temperature difference with a pile having the same power and efficiency can be achieved by improving the insulation or by using a small metallic radiator on the chassis under the pile.

Tests at sub-zero temperatures of the surroundings were carried out by Yu. S. Bykov. In this case the temperature inside the chamber was maintained at +45°C, when the temperature of the surroundings fell to –21°C.

Thus a pile of the investigated type, loaded with an insulated volume of 0.6 litres, can produce a temperature difference between the hot and

cold junctions of up to 45° to 50° and permit the maintenance of the temperature within the chamber at the level of +45°C for ambient temperature variations between the limits of +65° to –21°C.

The problem of reducing the detrimental temperature differences and increasing the useful temperature difference (between the inside of the chamber and the surroundings) can be solved by resort to the following measures:

1) reduction of the temperature drop across the oil-covered mica layer at the cold and hot junctions of the pile, which in our case amounted to 2° to 3° at each contact. By using special varnishes and coatings this temperature drop can be reduced to 1°–1.5°C;

2) reduction of the temperature difference between the chassis and the surroundings to a value of 2° to 3°. This can be achieved by forced convection;

3) reduction of the temperature difference along the chassis to a value of 5° to 6°. This can be achieved by increasing the thickness of the chassis and fitting the chassis with a small radiator immediately below the hot junction of the thermopile;

4) reduction of the heat load on the pile. This can be achieved by improving the insulation.

Work on the solution of these problems will undoubtedly permit the achievement of better results in future investigations.

Tests were also carried out on controlling the temperature of separate semiconductor diodes and transistors with the aid of a single thermoelement. In this case it was found possible either to reduce the temperature of the transistor by 20°–25° or to increase its power by 2–3 times.

A thermostat with a thermoelectric battery consuming 3-4 W may be used to keep the temperature of a thermally insulated chamber with a volume of 100 cm³ constant at 20-30°C under ambient temperature variations from +60 to –60°C.

Such a thermostat has been employed for controlling the temperature of a crystal oscillator employing a transistor.

A block diagram of the apparatus is shown in fig. 64. It consists of a temperature stabiliser 1, thermostatic chamber 2, temperature sensing instrument 3, controller 4, commutator 5, and power supply source 6. The construction of the thermostat is shown diagrammatically in fig. 20. The temperature stabiliser 1 consists of 15 thermoelements connected in series to form a rectangular plate with dimensions of 40×40×13 mm and a cooling surface area of 16 cm². To increase the mechanical strength of

* E. K. Iordanishvili and L. G. Tkalich, *Zhur. Tekh. Fiz.*, 27, No. 6, 1215, 1957.

the battery, the thermoelements are mounted in an ebonite frame. The thermoelements have $z = 1.7 \times 10^{-3}$ deg^{-1}. The calculated optimum current is 3.5 A

The temperature stabiliser (fig. 65) is fixed to one of the walls of the copper working chamber and insulated from it with thin mica leaves wetted with oil. The working chamber 2 contains the oscillator unit 3 and a temperature pick-up 4. The working chamber, together with the thermoelectric battery is mounted in a metallic jacket 5 on top of a copper radiator 6

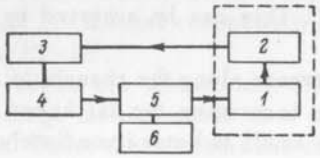

Fig. 64

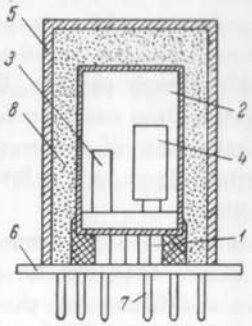

Fig. 65

with fins 7. The space between the working chamber and the jacket is filled with mipora (an expanded plastic material). The total weight of the thermostat is 2 kg and its dimensions are $160 \times 140 \times 110$ mm.

Small thermostats employing thermoelements have also numerous other applications. For example, an automatic 0°C reference point was constructed in which a thermoelement maintains water all the time at a transition point between the liquid and solid phases. Thermostats are also used to distribute the sperm of bulls to collective and state farms for artificial insemination, thus assisting the breeding of high grade cattle. The temperature is maintained at a suitable level so that the sperm remains active for a long period of time.

3.3 Data from foreign literature. There has so far been very little information in the foreign literature giving results of investigations on results of investigations on thermoelectric cooling.

In 1953 there appeared a review article in the journal "Kältetechnik" (German Federal Republic) outlining the results of an investigation by German scientists in this field.* The author of the paper reached the conclusion that the maximum temperature drop which could be obtained with the aid of thermoelements did not then exceed 26°C. In 1954 British scientists reported that they were able to achieve a temperature drop of 37°C.**

* E. Justi, *Kältetechnik*, No. 6, 130, 1953.

** H. J. Goldsmid and R. W. Douglas, *British Journ. of Appl. Phys.*, 3, No. 11, 386, 1954.

At the end of 1955 a report was published in the American journal "Product Engineering" that the Radio Corporation of America had constructed a prototype domestic refrigerator based on the Peltier effect. This brief mention was, however, only of an advertising nature and did not contain any information about the materials of the thermoelements or other characteristics of the refrigerator. It was only noted that the heat transfer from the hot junctions was achieved with the aid of circulating water, from which it may be concluded that the efficiency of the thermoelements was low. Judging from the photograph shown in the journal the volume of the working chamber did not exceed 10 litres.*

* More recently, P. F. Shilliday has published an article "The Performance of Composite Peltier Junction of Bismuth Telluride" (*Journ. Appl. Phys.*, 28, 1035, 1957) describing the work done at the Battelle Memorial Institute. (Editor's note)

CONCLUSIONS

When current-quality materials are used in the construction of thermoelements in thermobatteries for cooling volumes of tens of litres, thermoelectric refrigerators are more economical than absorption units but are as yet inferior to compression units.

It is, however, well known that the coefficient of performance of a compression refrigerator decreases with the decrease of its capacity. Therefore, when it is necessary to design a refrigerator for cooling a chamber of only a few litres capacity, thermoelectric cooling with the existing thermoelements is already preferable, from the power consumption viewpoint, to cooling with compression units; it also has certain other advantages, such as the absence of moving parts, freedom from corrosion, etc.

There is no doubt that, for controlling the temperature of small units, thermoelectric cooling has no competition from existing refrigerators of the conventional types.

This book has described results obtained with thermoelements developed in the period 1952–1955 at the Institute for Semiconductors of the Academy of Sciences of the U.S.S.R.

We now have at our disposal thermoelements with much better performances and there is every reason to believe that the efficiency of thermoelectric refrigerators will, in the immediate future, exceed that of compression-type refrigerating plants and that the fields of application of thermoelectric cooling will become much wider.

INDEX